# Design and Development of High Performance Polymer Light Emitting Diode for Solid State Lighting

A Thesis Submitted to
Indian Institute of Technology Guwahati
in Partial Fulfilment for the Degree of
Doctor of Philosophy


By

**Dipjyoti Das**
Centre for Nanotechnology
Indian Institute of Technology Guwahati
Guwahati-781039, Assam, India

September, 2017

**INDIAN INSTITUTE OF TECHNOLOGY GUWAHATI**

**Centre for Nanotechnology**

## STATEMENT

I do hereby declare that the matter embodied in this thesis entitled "**Design and Development of High Performance Polymer Light Emitting Diode for Solid State Lighting**" is the result of investigations carried out by me at Indian Institute of Technology Guwahati, India under the supervision of Professor Parameswar Krishnan Iyer.

This work has not been submitted elsewhere for the award of any degree.

September, 2017
Guwahati

**Dipjyoti Das**
Centre for Nanotechnology
IIT Guwahati
Guwahati-781039
Assam, India

**INDIAN INSTITUTE OF TECHNOLOGY GUWAHATI**

**Centre for Nanotechnology**

## CERTIFICATE

This is to certify that the thesis entitled "**Design and Development of High Performance Polymer Light Emitting Diode for Solid State Lighting**", submitted by Dipjyoti Das, a PhD student of Centre for Nanotechnology, Indian Institute of Technology Guwahati, Guwahati in partial fulfilment of the degree of Doctor of Philosophy is a record of his own research work carried out by him. He has carried out his investigations for the last five years on the subject matter of the thesis under my guidance at Indian Institute of Technology Guwahati, Guwahati. The matter embodied in the thesis has not been submitted for the award of any other degree by him or by anybody else.

September, 2017
Guwahati

**Prof. Parameswar Krishnan Iyer**
Thesis Supervisor
Centre for Nanotechnology
IIT Guwahati
Guwahati-781039
Assam, India

Dedicated To

....My Beloved Brother

Baba Da

# Acknowledgement

***"Starting something can be easy; it is finishing that is the highest hurdle"***

The journey of doctoral study is always a difficult and challenging task. Throughout this long journey, I have gained a lot by learning to persevere despite hardship. I would never have successfully completed this thesis without the assistance of numerous people who I am indebted to. Their direction, advice, support and contributions have proved invaluable along the way.

First and foremost, I would like to express my special appreciation and thanks to my Supervisor Professor Parameswar Krishnan Iyer, who has been a tremendous mentor for me. I appreciate all his contributions of time, ideas, and funding to make my Ph.D. experience productive and stimulating. I am also thankful to him for the excellent example he has provided as a successful research scientist and professor. The joy and enthusiasm he has for his research was contagious and motivational for me, even during the tough times in my Ph.D. pursuit. A very special gratitude goes to him for not only encouraging my research and for allowing me to grow as a research scientist but also for supporting me emotionally whenever I needed him. Thank you very much Sir, your advices on my research, my career as well as on my personal life have always been priceless.

I offer my sincere thanks to my doctoral committee members, Professor Harshal B. Nemade, Professor Arun Chattopadhyay and Professor Roy P. Paily for their insightful comments and encouragement, and also for the hard question which incented me to widen my research from various perspectives.

I am also grateful to Professor M. Qureshi, Professor A. S. Achalkumar and Professor Aditya Narayan Panda, IIT Guwahati, Professor G. U. Kulkarni, JNCASR Bangalore and Professor K. R. Surati, SVBP University, Gujrat. It was fantastic to have the opportunity to work with them through various collaborations and their valuable suggestions and concise comments has always been a source of inspiration to me.

I have been privileged to attend many International conferences during my PhD tenure where I got the opportunity to meet and interact with the prominent scientists across the globe. I would like to express my sincere thanks to Professor Seunghyup Yoo,

KAIST, South Korea, Professor Shyam S. Pandey, KIT, Japan and Professor C. Jagadish, ANU, Australia and Dr. Vipul Shah, IIT Gandhinagar for their motivations and valuable suggestions when I met them in ICMAT 2017, Singapore.

I am thankful to all members of Central Library, Central Instruments facility and Centre for nanotechnology IIT Guwahati for providing me a research friendly atmosphere with up to date research facilities. I also thank Indian Institute of Technology Guwahati for providing me the fellowship and such a good accommodation in this beautiful campus. A special thanks to Kaustubh Acharya, Dr. Pranjoli Das, Indrajit Talukdar, Paranjyoti Dutta, Madhurjya Borah, Dr. Dolly Gogoi and Dr. Keso Singh for their help and co-operation to complete my work.

*"A good friend is like a four-leave clover; hard to find and lucky to have".* I have been fortunate to be surrounded myself by some amazing friends Ashish, Anand, Shyam, Nilanjan, Purushottam, Gopi, Ujjwol, Namami, Larionette and Nystha who have made my PhD journey a memorable one. Thank you all for your support and encouragement. I am also thankful to my sisters Anamika and Rajlekha for their constant inspiration during the course of my PhD. Special thanks are also due to Swapnali mam, Kishor, Pankaj bhai, Subrat, Basant and all other group members of Badminton Freaks for the beautiful evenings and keeping me healthy and physically fit.

It is my pleasure to acknowledge the help provided by my seniors and juniors in IIT Guwahati, especially Nayan Mani Da, Ramesh Da, Jitu bhai, Subbarao sir, Radha bhaiya, Bheem bhaiya, Suresh bhaiya, Anamika Kalita, Sayan, Rahul, Ravindra, Niranjan, Adil, Rameshji, Ritesh and all other lab members from our device and synthesis group. I am also thankful to Jayraj bhai from NUS singapore, and my friends Keval, Atul from SVBP University and Saurabh, Sunil from IIT Delhi for their help and support.

*"The love of a family is life's greatest blessings".* In this precious moment of my life, I would like to express my deep sense of gratitude to my parents Junu Das and Geeta Das, Maa Aikon Barman, Pita Late Bhagiram Barman for their love, blessings and constant encouragement throughout my life. I would like to thank my sister Mainu ba, Bhindeu Satyajit and Jitumoni, brother Gourab, Dhan da, nephews Rakesh, Manjit, Barnil and Barnav and my niece Dhrup and Trishita for their love and best wishes.

Finally, I want to offer my sincere gratitude to my elder brother Dr. Bijoy Barman (baba da) whose constant support and immense sacrifice for me in time of distress helped me overcoming many obstacles in my life. My dear brother, it is only for you that I could

withstand and face the real hurdles of life boldly. You have been always inspiring, supporting and teaching me to understand the true value of human life. It is only for you that I could stand firmly on my own ground. I would like to attribute all my successful efforts to you. I am very happy to have such loving and caring brother in you. Please keep showering your love and blessings upon me in the days to come. Thank you once again.

***Dipjyoti Das***
Centre for Nanotechnology
IIT Guwahati

# Synopsis

Artificial lighting plays a vital role in our day to day life extending our usable time beyond sunrise and sunset. Almost 20% of the total electricity used for indoor applications globally is consumed by the artificial lighting. Till date, the most common lighting sources are incandescent bulb and the compact fluorescent lamps. An incandescent bulb is still unmatched in terms of its color quality as it possesses a CRI value of 95-100 and its production cost. However, approximately 95% of the consumed energy is not converted into light but into heat and it is hard to think of any other technology still in use today which exhibits such a poor efficiency. The efficiency of fluorescent tubes is very high compared to incandescent light. But they suffer from the disadvantage of poor color quality and since it contains mercury, they are not eco-friendly. A highly energy efficient, large area and eco-friendly lighting solution is therefore the demand of the hour. In the past decades, a new research field has emerged referred to as solid-state lighting (SSL). In SSL, semiconductors are used as active element to fabricate light emitting diode and light is produced by the principle of electroluminescence. The first LED emitting visible light was demonstrated in 1962 and since then the technology has evolved rapidly. Only in 1993 the first practical blue emitting LED was demonstrated by Shuji Nakamura, paving the way for the development of white emitting LEDs. Thanks to its high efficiency and long lifespans inorganic LEDs is dominating the current lighting market is presently reached cost parity with traditional lighting elements.

Recently, a relatively new lighting technology has evolved and has the potential to rule the lighting market and add new dimension to it. Invented in 1987, it is termed as organic light-emitting diodes (OLEDs) as the key functional materials that these diodes are based on, are primarily composed of organic (carbon-based) materials. They offer similar energy-saving potential to that of their inorganic counterpart but offer numerous advantages. Unlike LEDs, which are concentrated point sources of bright light, OLEDs are mainly thin film devices and are therefore a more diffuse light source. Since organic semiconductors have a disordered structure, OLEDs are therefore relatively easy to fabricate and can be made in almost any shape. They can be fabricated on flexible substrates, can be transparent and even can be designed to emit light in both ways. OLEDs therefore offer enormous design possibilities and pave a way to create artistic applications

with light. Furthermore, since organic materials are broadband emitters, OLEDs hold the promise to exhibit a very good color rendering index (CRI) and can produce white light close to daylight, which is not the case for cheap inorganic LEDs.

Despite all these possibilities, OLED technology is less mature than LED technology; however rapid advancement in this field has been made in the past few decades and with a few key breakthroughs it is expected to reach its ultimate potential. OLED is therefore a prime focus of the researchers in the field of organic electronics.

Therefore, considering the demand of recent day's technology, in this thesis, different approaches towards design and development of high performance polymer light emitting diodes have been explored. The thesis content was divided in five chapters.

## Chapter 1: Introduction

This chapter starts with the motivation behind the present thesis and gives a brief overview of organic electronics and its application in the field of semiconductor devices. The importance of OLED, its working principle, device characterization parameter that are used to evaluate an OLED, different approaches towards generation of white light in OLED have also been discussed herein along with a brief overview of the current OLED research. This chapter also includes the details of the fabrication procedure of an OLED and the characterization techniques that are used to evaluate the performance of an OLED.

## Chapter 2: Efficient Blue and White Polymer Light Emitting Diodes Based on a Well Charge Balanced, Core Modified Polyfluorene Derivative

Conjugated polyfluorene (PF) has been widely studied both as the emitting material in blue PLEDs as well as the host material in blended systems for realizing white light. Polyfluorenes are well-known emissive materials for blue PLEDs and serve well for light emission and charge transfer due to their high luminescence efficiency, thermal stability, good processability and excellent film forming properties. Unfortunately, they suffer from poor electron transport as compared to hole transport due to the presence of high density electron traps within the polymer. In order to achieve high efficiency, it is, however, necessary to obtain a balanced charge transport behavior and confinement of electrons and holes inside the active layer. Herein, fabrication of efficient blue and white polymer light-

emitting diodes (PLEDs) using a well charge balanced, core modified polyfluorene derivative, poly[2,7-(9,90-dioctylfluorene)-co-N-phenyl-1,8-naphthalimide (99:01)] (PFONPN01), is presented. The excellent film forming properties as observed from the morphological study and the enhanced electron transport properties due to the inclusion of the NPN unit in the PFO main chain resulted in improved device properties. Bright blue light was observed from single layer PLEDs with PFONPN01 as an emissive layer (EML) as well as from double layer PLEDs using tris-(8-hydroxyquinoline) aluminum ($Alq_3$) as an electron transporting layer (ETL) and LiF/Al as a cathode. The effect of ETL thickness on the device performance was studied by varying the $Alq_3$ thickness (5 nm, 10 nm and 20 nm) and the device with an ETL thickness of 20 nm was found to exhibit the maximum brightness value of 11 662 cd $m^{-2}$ with a maximum luminous efficiency of 4.87 cd $A^{-1}$. Further, by using this highly electroluminescent blue PFONPN01 as a host and a narrow band gap, yellow emitting small molecule, dithiophene benzothiadiazole (DBT), as a guest at three different concentrations (0.2%, 0.4% and 0.6%), WPLEDs with the ITO/PEDOT:PSS/emissive layer/$Alq_3$(20 nm)/LiF/Al configuration were fabricated and maximum brightness values of 8025 cd $m^{-2}$, 9565 cd $m^{-2}$ and 10 180 cd $m^{-2}$ were achieved respectively. 0.4% DBT in PFONPN01 was found to give white light with Commission International de l'Echairage (CIE) coordinates of (0.31, 0.38), a maximum luminous efficiency of 6.54 cd $A^{-1}$ and a color rendering index (CRI) value of 70.

## Chapter 3: White polymer light emitting diodes based on PVK: the effect of the electron injection barrier on transport properties, electroluminescence and controlling the electroplex formation

PVK is a widely used polymer, that has an excellent film forming property and emits in the blue region. It has been widely used as an emissive layer in blue emitting PLEDs and to generate white light by using the electroplex emission. Yet, the effect of electron injection barrier and the electron transport property of PVK on the charge transport, brightness and electroplex formation in PVK based PLEDs have not been widely studied. In this chapter, the effects of the electron injection barrier on the charge transport, brightness and the electroluminescence (EL) properties of polymer light emitting diodes (PLEDs) with poly(9-vinylcarbazole) (PVK) as an emissive layer have been presented. By using Al and LiF/Al as the cathode in single layer PLEDs and diverse electron transporting

layers (ETLs) such as 2,9-dimethyl-4,7-diphenyl-1,10-phenanthroline (BCP), 4,7-diphenyl-1,10-phenanthroline (BPhen) and 2,20,200-(1,3,5-benzinetriyl)-tris(1-phenyl-1-H-benzimidazole) (TPBi) in the case of multilayer PLEDs, the charge transport, brightness, color tuning and the EL properties of the devices were drastically modified. The energy barrier for electrons affects the electron current flowing through the device, thereby affecting the operating voltage and the brightness of the PLEDs. The PLEDs with TPBi as the ETL possess the lowest injection barrier and give the maximum brightness of 426.24 cd $m^{-2}$. The electron injection barrier is also found to play a major role in defining the EL spectra of the PLEDs. A larger injection barrier gives rise to electroplex formation in the EML–ETL interface of the PLEDs and an additional peak at 605 nm was observed in the EL spectrum. As a result, a near white emission with CIE coordinates of (0.30, 0.30) and (0.25, 0.23) at 20 V was obtained from devices with BCP and BPhen as ETLs. Furthermore, PVK doped with 2-phenyl-5-(4-biphenylyl)-1,3,4-oxadiazole (PBD) at 10, 20 and 30 wt% ratios modified the electron transport nature of PVK and had a remarkable influence on the aforesaid properties, especially on the electroplex formation.

## Chapter 4: Highly efficient green phosphorescent organic light emitting diode based on $Ir(mppy)_3$ : effect of annealing temperature and mixed host

Due to its ability to harvest both triplet and singlet excitons, phosphorescent OLEDs (phOLEDs) generally superior device performance. To date, the most efficient phOLEDs are fabricated using thermal deposition method in a finite vacuum chamber, making cost-effective manufacture and large area electronics impossible. To make this novel terminal electronics available for general applications the cost needed to be decreased, and thus new processing techniques were demanded. In this regard, solution processes, such as ink-jet printing and spin coating, can offer the advantage of cost-effective manufacturing of large area devices and solution processed phOLEDs can have the potential to be printed in different designs and shapes thereby allowing enormous design possibilities and pave a way to create artistic applications with light. But the performances of the phOLEDs fabricated by the solution processing techniques are still relatively low compared to their thermally deposited counterparts. The efficiency of phOLEDs mainly depends on the efficient charge injection from the electrodes at a low drive voltage, good charge balance

and high solid-state quantum yield of the emissive layer along with the confinement of the injected charge carriers within the emitting layers. It is therefore of utmost importance to carefully study the effect of processing conditions such as thermal treatment of the emissive layer as they greatly influence the morphology of the films and their interfaces with the adjacent layers thereby influencing the electrical properties such as charge injection and charge transport in the device. Herein, highly efficient, solution processed green phosphorescent organic light emitting diode (phOLED) based on $Ir(mppy)_3$ with single and mixed host namely PVK (Poly(9-vinylcarbazole)), PVK: PBD (2-(4-Biphenylyl)-5-(4-tert-butylphenyl)-1,3,4-oxadiazole), PVK: PBD: TPD (N, N′-Bis(3-methylphenyl)-N, N′-diphenylbenzidine) have been reported. Addition of electron and hole transporting layer in appropriate ratio is found to improve the charge balance at the EML that results in improved device performance. The different host combinations have further been annealed at 80 $^{o}$C, 100 $^{o}$C, 120 $^{o}$C and 140 $^{o}$C and the effect of annealing temperature on the morphological, optical and electrical properties of the phOLEDs have been elucidated. At higher annealing temperature EML is found to form a compact structure with higher RMS roughness that leads to a strong interfacial adhesion and better charge injection. As a result, the device performance is found to increase with increasing annealing temperature and best result was observed for the devices annealed at 140 $^{o}$C. Among all, PVK: PBD: TPD host based devices annealed at 140 $^{o}$C is found to give best result with the maximum brightness of 17273 cd $m^{-2}$ and a maximum luminous efficiency of 61.21 cd $A^{-1}$.

## Chapter 5: Solution processed WPLEDs with good color stability and high color rendering index via a phosphor-sensitized system

In this chapter, efficient, solution processed white polymer light emitting diodes (WPLEDs) with good color stability and high color rendering index (CRI) via a phosphor-sensitized system using blue phosphorescent dye Bis[2-(4,6-difluorophenyl)pyridinato-C2,N](picolinato)iridium(III) (FIrpic) as emitter and sensitizer, and the fluorescent dye Rubrene and 4-(dicyanomethylene)-2-t-butyl-6-(1,1,7,7-tetramethyljulolidyl-9-enyl)-4H-pyran (DCJTB) as yellow and orange/red emitter respectively have been presented. Two different fluorophores, Rubrene and DCJTB, were chosen due to their different emission zone and different charge trapping ability. WPLEDs, in which FIrpic with Rubrene or DCJTB is doped at different feed ratios into poly (N-vinylcarbazole) (PVK) host, were

fabricated and the effect of their concentration on the current density v/s voltage (JV) characteristics and the electroluminescence (EL) spectra were studied. WPLEDs made with FIrpic : Rubrene (10:1) and FIrpic : DCJTB (80:1) were found to give CIE coordinates of (0.30, 0.42) and (0.34, 0.40) with CRI value of 58 and 76 at luminous efficiencies of 4.91 cd $A^{-1}$ and 2.79 cd $A^{-1}$ respectively. Finally, FIrpic, Rubrene and DCJTB were doped into PVK to get high quality white light and CIE coordinates of (0.41, 0.43) with a CRI value of 78 at luminous efficiency of 4.73 cd $A^{-1}$ was achieved for FIrpic : Rubrene : DCJTB feed ratio of (100:8:1).

# List of Publications

## Journals Published

1. **Dipjyoti Das,** Peddaboodi Gopikrishna, Ashish Singh, Anamika Dey and Parameswar Krishnan Iyer, "Solution processed WPLEDs with good color stability and high color rendering index via a phosphor-sensitized system" ***Chemistry Select, 2017, 2, 3184-3190.***
2. **Dipjyoti Das,** Peddaboodi Gopikrishna, Rahul Narasimhan, Ashish Singh, Anamika Dey and Parameswar Krishnan Iyer, "White polymer light emitting diodes based on PVK: the effect of the electron injection barrier on transport properties, electroluminescence and controlling the electroplex formation" ***Phys. Chem. Chem. Phys., 2016, 18, 33077-33084.***
3. **Dipjyoti Das**, Peddaboodi Gopikrishna, Ashish Singh, Anamika Dey and Parameswar Krishnan Iyer "Efficient Blue and White Polymer Light Emitting Diodes Based on a Well Charge Balanced, Core Modified Polyfluorene Derivative" ***Phys. Chem. Chem. Phys., 2016,18, 7389-7394.***
4. **Dipjyoti Das,** Peddaboodi Gopikrishna, Ashish Singh, Anamika Dey and Parameswar Krishnan Iyer, "Influence of emissive layer thickness on electrical characteristics of polyfluorene copolymer based polymer light emitting diodes" ***J. Phys. Conf. Ser. 704 012016.***
5. Ravindra Kumar Gupta[§], **Dipjyoti Das[§]**, Monika Gupta, Santanu Kumar Pal, Parameswar Krishnan Iyer and Ammathnadu S. Achalkumar, "Electroluminescent Room Temperature Columnar Liquid Crystals Based on bay-Annulated Perylenetetraesters" ***J. Mater. Chem. C, 2017,5, 1767-1781*** **([§]Equal Contribution).**
6. Peddaboodi Gopikrishna, **Dipjyoti Das**, Parameswar Krishnan Iyer "Synthesis and Characterization of Color Tunable, Highly Electroluminescent Copolymers of Polyfluorene by Incorporating N -phenyl-1,8-Naphthalimide Moiety into Main Chain" ***J. Mater. Chem. C, 2015, 3, 9318—9326.***
7. Peddaboodi Gopikrishna, **Dipjyoti Das**, Parameswar Krishnan Iyer, "Color Tunable Donor-Acceptor Electroluminescent Copolymers: Synthesis, Characterization, Photophysical Properties and PLED Fabrication" ***Chemistry Select, 2017, 2, 7044-7049.***
8. Peddaboodi Gopikrishna, **Dipjyoti Das**, Parameswar Krishnan Iyer, "Saturated and Stable White Electroluminescence from Linear Single Polymer Systems based on Polyfluorene and Mono-Substituted Dibenzofulvene Derivatives" ***J. Phys. Chem C, 2017, 121, 18137-18143.***

9. Anamika Dey, Ashish Singh, **Dipjyoti Das**, Parameswar Krishnan Iyer "High Performance ZnPc Thin Film based Photo-Sensitive Organic Field Effect Transistors: Influence of Multilayer Dielectric Systems and Thin Film Growth Structure" ***ACS Omega, 2017, 2, 1241-1248.***
10. Anamika Dey, Ashish Singh, **Dipjyoti Das,** Parameswar Krishnan Iyer , "Photosensitive Organic Field Effect Transistor: Influence of ZnPc Morphology and Bilayer Dielectrics to Achieve Low Operating Voltage and Low Bias Stress Effect" Phys. ***Chem. Chem. Phys., 2016, 18, 32602-32609.***
11. Ashish Singh, Anamika Dey, **Dipjyoti Das**, Parameswar Krishnan Iyer "Effect of Dual Cathode Buffer Layer on the Charge Carrier Dynamics of rrP3HT:PCBM Based Bulk Heterojunction Solar Cell", ***ACS Appl. Mater. Interfaces 2016, 8, 10904−10910.***
12. Ashish Singh, Anamika Dey, **Dipjyoti Das**, Parameswar Krishnan Iyer "Combined influence of Plasmonic Metal Nanoparticle and Dual Cathode Buffer Layer for Highly Efficient rrP3HT: PCBM Based Bulk Heterojunction Solar Cell", ***J. Mater. Chem. C,* 2017, *5, 6578-6587***.
13. Anamika Dey, Ashish Singh, Anamika Kalita, **Dipjyoti Das**, Parameswar Krishnan Iyer "High Performance, Low Operating Voltage n-Type Organic Field Effect Transistor Based on Inorganic-Organic Bilayer Dielectric System" ***J. Phys. Conf. Ser. 704 012017.***
14. Saurabh S. Soni, Kishan B. Fadadu, Jayraj V. Vaghasiya, Bharat G. Solanki, Keval K. Sonigara, Ashish Singh, **Dipjyoti Das,** Parameswar K. Iyer, "Improved Molecular Architecture of D-π-A Carbazole Dyes: 9% PCE with Cobalt Redox Shuttle in Dye Sensitized Solar Cells" ***J. Mater. Chem. A, 2015, 3, 21664–21671.***

## Journals Under Review/ Communicated

1. **Dipjyoti Das,** Peddaboodi Gopikrishna, Ashish Singh, Anamika Dey and Parameswar Krishnan Iyer, "Highly Efficient Green Phosphorescent Organic Light Emitting Diode Based on $Ir(mppy)_3$ : Effect of Annealing Temperature and Mixed Host".
2. Bhavna Sharma, **Dipjyoti Das**, Parameswar Krishnan Iyer and Josemon Jacob, "Fluorene based cross-conjugated polymers with thiavinylidene linkers for applications in organic light emitting diodes",
3. Murli Gedda, **Dipjyoti Das**, Parameswar K. Iyer and G. U. Kulkarni, "Highly robust metal wire mesh transparent electrodes for indium-free organic light emitting diodes".

## Conference Papers

1. **Dipjyoti Das**, Debojit Hazarika, Ashish Singh, Anamika Dey and Parameswar Krishnan Iyer, "Polymer / Organic light-emitting diode (PLED / OLED) based on new polyfluorene derivatives" ***conference proceeding, International Conference on LED Lighting & Solar Photovoltaic Systems, 2014***
2. Ashish Singh, Anamika Dey, **Dipjyoti Das**, Parameswar Krishnan Iyer "Effect of Substrate Temperature on Twin Donor Layer Organic Solar Cell", ***Conference Proceeding, Under Revision, Material Today Proceeding.***
3. Ashish Singh, Anamika Dey, **Dipjyoti Das**, Parameswar Krishnan Iyer, "Improvement of Charge Carrier Dynamics in P3HT:PC61BM Based Solar Cell in Presence of Organic Cathode Interfacial Layers" ***IEEE Conference Proceeding, Under Revision.***

## Book Chapter

1. Anamika Dey, Ashish Singh, **Dipjyoti Das**, Parameswar Krishnan Iyer, "Organic Semiconductors: A New Future of Nanodevices and Applications" ***Book Chapter, Springer, 2015, 97-128***

# Workshops and Conferences Attended

1. Symposium B: International Conference on Materials and Advanced Technologies, ***Suntec city, Singapore, 18-23 June, 2017.***
2. Symposium Y: International Conference on Materials and Advanced Technologies, ***Suntec city, Singapore, 18-23 June, 2017.***
3. Research Conclave 2017, ***Indian Institute of Technology Guwahati, India, 16-19 March, 2017.***
4. Fourth International Symposium on Semiconductor Materials and Devices (ISSMD4), ***Jadavpur University, West Bengal, India, 8-10 March, 2017.***
5. 3rd National Workshop on NEMS/MEMS and Theranostics Devices (NWNTD-2016) ***Indian Institute of Technology Guwahati, India, 21-23 February, 2017.***
6. 2nd National Workshop on NEMS/MEMS and Theranostics Devices (NWNTD-2016) ***Indian Institute of Technology Guwahati, India, 21-21 February, 2016***.
7. National Workshop on Advanced Probing Techniques in TEM (APTTEM-2016), ***Indian Institute of Technology Guwahati, India, 15-16 February, 2016.***
8. 4th International Conference on Advanced Nanomaterials and Nanotechnology (ICANN 2015), ***Indian Institute of Technology Guwahati, India, 8-11 December, 2015.***
9. Indo-German workshop on renewable energy (organic solar cells) and curriculum innovation in science education, ***Indian Institute of Science, Bangalore, India, 1-2 December, 2015.***
10. Research Conclave 2015, ***Indian Institute of Technology Guwahati, India, 23-26 March, 2015.***
11. International Conference on LED Lighting & Solar Photovoltaic Systems, ***Indian Institute of Technology Kanpur, India, 27-29 March, 2014.***
12. 3rd International Conference on Advanced Nanomaterials and Nanotechnology (ICANN 2013), ***Indian Institute of Technology Guwahati, India, 1-3 December, 2013.***

# Contents

# CHAPTER-1

## Introduction

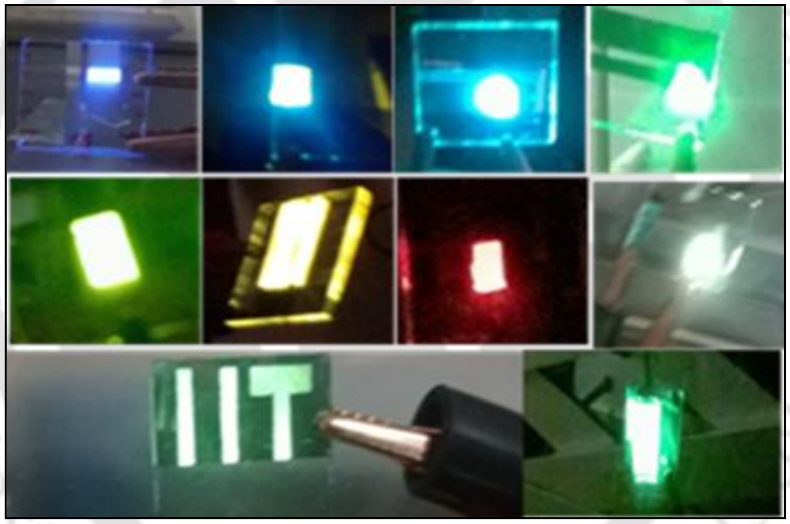

# Introduction

## 1.1 Motivation

In 1880, the discovery of incandescent bulb by Thomas A. Edison began a new era of artificial lighting that brought new light and comfort into people's everyday lives and has freed mankind from the constraints of nature extending our usable time beyond sunrise and sunset. Edison' bulb is based on the principle of thermal radiation where a thin filament is heated till the point of incandescence by passing an electric current through it. An incandescent bulb is still unmatched in terms of its color quality as it possesses a CRI value of 95-100 and its production cost. However, although relatively cheap to fabricate, the incandescent light bulb has a rather poor efficiency. Approximately 95% of the consumed energy is not converted into light[1] but into heat and it is hard to think of any other technology still in use today which exhibits such a poor efficiency.

**Conventional lighting element**

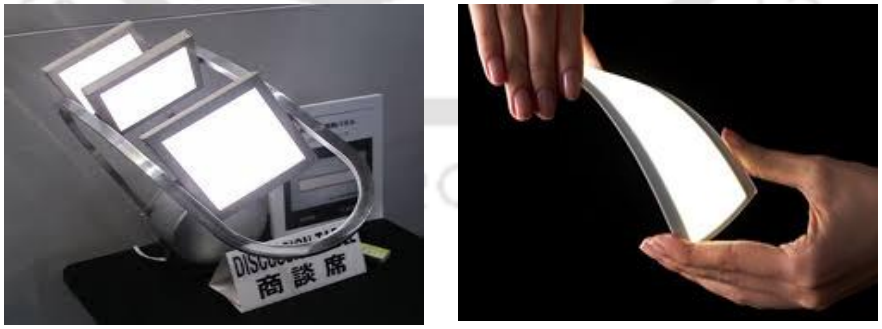


**New generation lighting element**

**Fig. 1.1** Conventional and new generation lighting element (picture source: Internet).

In 1937 General Electric came with an alternate lighting element and demonstrated the first fluorescent tube. The operation mechanism of a fluorescent tube is actually similar

to that of the incandescent bulb. In a fluorescent tube, an electric current is passed through an inert gas containing a small amount of mercury. The electric current excites the mercury which consequently emits ultraviolet light. This is then converted to light in the visible spectrum by phosphors that are coated on the surface of the fluorescent tube. The emission from the phosphors is typically very narrow and accordingly the mixture of phosphors has to be selected with care so that the output spectrum appears as white. The efficiency of fluorescent tubes is very high compared to incandescent light and they are therefore widely adopted in the work place, but due to their size restraints, and the typical low CRI, they are rarely used in residential settings. Also, fluorescent lamps have a very important environmental drawback; the mercury contained in the lamps is very toxic which is released in the environment if it is not properly disposed of.

Considering the low efficiency of incandescent light bulbs, and the poor color quality of the fluorescent lamp, it is evident that there is the potential for a substantial energy saving by switching to a highly energy efficient, large area and eco-friendly lighting solutions. In the past decades, a new research field has emerged referred to as solid-state lighting (SSL). Unlike the conventional incandescent bulb and CFL, in SSL uses a semiconductor light emitting diode, where light is produced directly by the principle of electroluminescence. The first LED emitting visible light was demonstrated in 1962[2], and since then the technology has evolved rapidly. Only in 1993 the first practical blue emitting LED was demonstrated by Shuji Nakamura[3], paving the way for the development of white emitting LEDs. Nowadays, lighting is an extremely large business that consumes about one quarter of the electricity produced annually. Efficient semiconductor LEDs has the potential to replace both fluorescent and incandescent lights as the primary lighting source. They are potentially more efficient and more environmentally benign (no Hg) than these conventional lighting sources. In addition, semiconductor LEDs have unique properties that make them attractive for lighting applications, it is possible to electrically control the spectral properties of the light emitted, and they can be arranged over large areas in various shapes for aesthetic purposes [4]. Thanks to its high efficacy and long lifespans inorganic LEDs is dominating the current lighting market is presently reached cost parity with traditional lighting elements.

Recently, a relatively new lighting technology has evolved and has the potential to rule the lighting market and add new dimension to it. Invented in 1987, it is termed as organic light-emitting diodes (OLEDs) as the key functional materials that these diodes are

based on, are primarily composed of organic (carbon-based) materials[5-8]. They offer similar energy-saving potential to that of their inorganic counterpart but offer numerous advantages. Unlike LEDs, which are concentrated point sources of bright light, OLEDs are mainly thin film devices and are therefore a more diffuse light source. Since organic semiconductors have a disordered structure, OLEDs are therefore relatively easy to fabricate and can be made in almost any shape. They can be fabricated on flexible substrates, can be transparent and even can be designed to emit light in both ways. OLEDs therefore offer enormous design possibilities and pave a way to create artistic applications with light. Furthermore, since organic materials are broadband emitters, OLEDs hold the promise to exhibit a very good color rendering index (CRI) and can produce white light close to daylight, which is not the case for cheap inorganic LEDs.

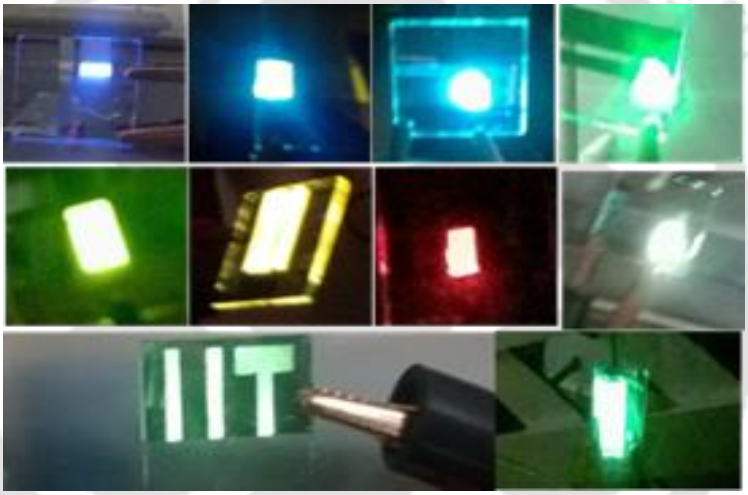


**Fig. 1.2** OLEDs Fabricated at Organic Electronics Laboratory, IIT Guwahati.

Despite all these possibilities, OLED technology is less mature than LED technology; however rapid advancement in this field has been made in the past few decades and with a few key breakthroughs it is expected to reach its ultimate potential. OLED is therefore a prime focus of the researchers in the field of organic electronics.

## 1.2 History of organic electronics

The history of organic electronics is generally assumed to begin in 1977, when Alan J. Heeger, Alan G. MacDiarmid and Hideki Shirakawa of University of Pennsylvania informed "the discovery and development of conductive polymers" by reporting high conductivity in oxidized and iodine-doped polyacetylene[9] for which they received the

Nobel prize in Chemistry in the year 2000[10]. However, a careful evaluation of the scientific literature suggests that research towards the development of so called "conductive polymers" had started way back in 1862, when Henry Letheby of the College of London Hospital obtained a partly conductive material by anodic oxidation of aniline in sulfuric acid[11]. The outcomes of Letheby's experiments were ground breaking as prior to these experiments, all polymers were considered to be intrinsically insulating. Surprisingly, no further or in-depth analysis were carried out based on these important achievements probably due to the limitations associated with the analytical techniques of that era[12].
Almost a century later, in 1950s, it was revealed that polycyclic aromatic compounds can exhibit semi-conducting nature by forming charge-transfer complex salts with halogens. Particularly, a conductivity of 0.12 S/cm was obtained in perylene-iodine complex in the year 1954[13].

It was first discovered by Kallmann and Pope[14,15] that organic materials that are in insulators in general can become semiconducting when charge carriers are injected into them from electrode(s). Based on the simulation work carried out by Akamatu et al.[16], they observed a current flow through an anthracene crystal when holes are injected from a positively biased electrolyte containing iodine. Soon it was realized that the work-function of the electrode is the fundamental parameter that controls injection and the electrolyte used to inject charge carrier was replaced by solid metallic or semiconducting contact of suitable work function. In 1965, Sano et al.[17] observed electroluminescence in organic crystals when they inject electrons and holes from two different electrodes due to their radiative recombination.

Another important breakthrough in the field of organic electronics came when Yu et al. [18] described the linear, polymeric structure of the chemical products along with a possible mechanism to explain the conductivity of the polymer. Soon after this publication, it became routine for the scientists to characterize polymers and other organic materials from an electrical point of view, performing resistance and conductivity measurements[12].
Research in the field of conductive polymers continued and in 1974 Mc Ginness and co-workers of University of Texas realized a dynamic switch based on chemically synthesized melanin doped with iodine[19]. This switch prototype is now displayed at the "Smithsonian Chips" collection of the American Museum of History and is usually considered the first example of organic electronic device[20,21].

It was eventually in 1977, the fundamental discovery by Shirakawa and co- workers of the relatively high electrical conductivity in doped thin films of polyacetylene paved the way for the development of a wide range of organic polyconjugate materials as semiconductors for several technological applications.

Organic semiconductors are now studied widely as active elements in various optoelectronic devices such as organic light emitting diodes (OLEDs), organic solar cells (OSCs), organic thin film transistors (OTFT), electrochemical transistors (ECTs) and recently in biosensing applications.

## 1.3 Organic semiconductors

Organic materials are the basis of organic electronics and in general are primarily composed of carbon. They exhibit semiconducting properties when there is alternating double- and single-bonds in the material and are termed as conjugated hydrocarbons. When the molecular weight of such hydrocarbons is less they are known as small molecule and when they are made up of a repeated base unit or monomer and possess large molecular weight, they are known as polymers.

The carbon atom with an atomic number of six has four valence electrons and an electronic configuration of $1S^2 2S^2 2P^2$. Therefore, when a carbon atom involves in molecular bond formation, depending on the bond, its atomic orbitals are combined either through $SP^2$ or $SP^3$ hybridization. While non-conductive polymers have saturated ($SP^3$ hybridized) carbon atoms along the backbone of their molecular chains, the backbones of organic conjugated polymers mainly consist of $SP^2$ hybridized atoms. In these materials 2S, $2P_x$ and $2P_y$ orbitals of carbon are combined through $SP^2$ hybridization and lie on a single plane with the $2P_z$ orbital perpendicular to this plane.

The overlap of $SP^2$ orbitals of adjacent, carbon atoms creates very strong Sigma (σ) bond. These bonds are highly localized between the atomic nuclei and may form the backbone of a polymer chain. The energy differences between the low energy (σ) state and the excited (σ *) state is quite large and well beyond the visible spectral range. Thus, the electronic properties related with this bond are that of an insulating material.

The fourth orbital ($2P_z$) that does not take part in this hybridization and is perpendicular to the σ bond, however, are symmetric between adjacent atoms and their coupling creates π-bond. Electrons in this bond can create a system of delocalized π-electrons, which can result in interesting and useful optical and electronic properties. Based

on the interference pattern (constructive or destructive) the coupling of two degenerate $2P_z$ orbitals of adjacent carbon atoms generates two new energetically different orbitals called bonding ($\pi$) which is lower in energy compare to original $2P_z$ orbital and anti-bonding ($\pi^*$) which is higher in energy compared to the isolated $2P_z$ orbital. Because of the lower energy of the bonding ($\pi$) orbital both of the $2P_z$ electrons will occupy this orbital, leaving the anti-bonding ($\pi^*$) orbital empty of electrons.

Expanding this scenario into a ring or long chain of carbon atoms, the MOs become two semi-continuous bands of bonding and antibonding orbitals, forming the analog to an inorganic semiconductor's valance and conduction bands, respectively. According to the Pauli Exclusion Principle, each energy state can be occupied by two electrons (spin up and spin down). Therefore, in the ground state, only the bottom half of the energy levels are filled, as shown in Fig. 1.3.

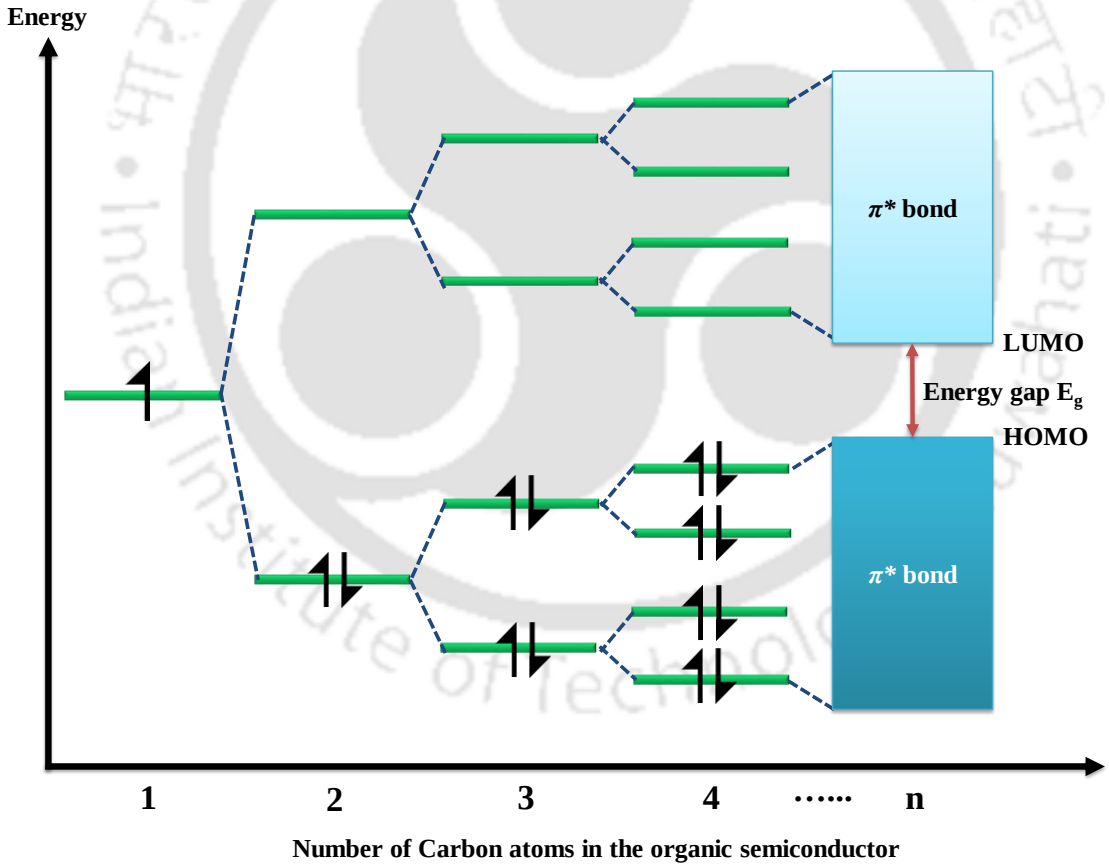


**Fig. 1.3** Energy level splitting and band formation in conjugated molecules.

The filled energy levels are capped with the highest occupied molecular orbital (HOMO) and the empty levels begin at the lowest unoccupied molecular orbital (LUMO).

The gap of unavailable energy states, called the energy gap or the band gap, has energy of Eg 1.5-3.5 eV in most organic materials, covering the entire visible range. Due to this relatively small energy gap, π-conjugated systems can behave as semiconductor and display all the essential optoelectronic properties including light emission, absorption, charge generation and transport etc. Organic semiconductors do not have free electrons as we understand in the conduction in metals but instead have electrons that are shared in a conjugated system. The charge transport is dominated by hopping between electron orbitals.

## 1.4 Charge transport in organic semiconductors

The basic understanding of charge transport phenomena is of vital importance as the performance of most of the modern day optoelectronic devices such as field effect transistors, solar cells and light emitting diodes depends strongly on the motion of charges through the active layer of the device. The charge transport through a solid is mainly defined by its electronic structures. Therefore, to understand the charge transport in organic semiconductor we need to first consider the electronic structure of the organic semiconductors. As discussed earlier, organic semiconductors are primarily composed of carbon atoms. The backbone of the OSCs is formed by the very strong sigma bonds that arise due to the $SP^2$ hybridization of carbon atoms yielding a bonding (σ) and an antibonding (σ*) molecular orbitals. The remaining $P_z$ orbital of adjacent carbon atoms forms the π-bond and generates two new energetically different orbitals (π) and (π*).

The bonding orbitals are of less energy as compared to that of antibonding molecular orbitals. Therefore, in ground state, all bonding orbitals up to the highest occupied molecular orbital, the HOMO, are filled and the antibonding orbitals from the lowest unoccupied molecular orbital (LUMO) onwards are empty. Neutral excited states in an organic molecule is formed when an electron absorbs energy, mainly in the form of light and is promoted from HOMO to LUMO resulting in an additional electron in the antibonding orbital or a hole in the bonding orbital. In organic semiconductors, the binding energy due to the columbic attraction between the above fore said electron and hole is quite large (0.5 eV to 1.0 eV) due to its low dielectric constant. In order to charge transfer to take place in organic semiconductors, there must be a charge on the molecule which can be achieved either by adding an electron into the LUMO of the molecule or by extracting an electron, or in other words creating a hole in its HOMO. The molecule in such case is said

to be in charge excited state. These neutral excited states or charge excited states (or electronic excitations) are responsible for the luminescent and charge transport properties of the organic semiconductors. The excess charge in molecule can be generated either by injection or removal of an electron at a metal-organic interface, through oxidation or reduction or by means of dissociation of a neutral excited state of a molecule by transferring an electron to a nearby molecule. However, the addition or removal of an electron from a molecule alters the relative positions of the molecular orbitals with respect to the vacuum level and also the spatial distribution of the electrons in the molecule thereby changing its molecular geometry. The charge along with the geometric distortion of the molecule is termed as polaron and is a characteristic of organic molecule due to its low dielectric constant. Polarons create intermediate energy states between HOMO and LUMO and can be either positive or negative depending on the charge carrier.

Irrespective of the charge on the molecule, upon absorbing light or photon energy, an electron gets promoted from a lower energy molecular orbital to a higher energy molecular orbital. The different possible optical transitions of the differently charged molecule are shown in Fig. 1.4.

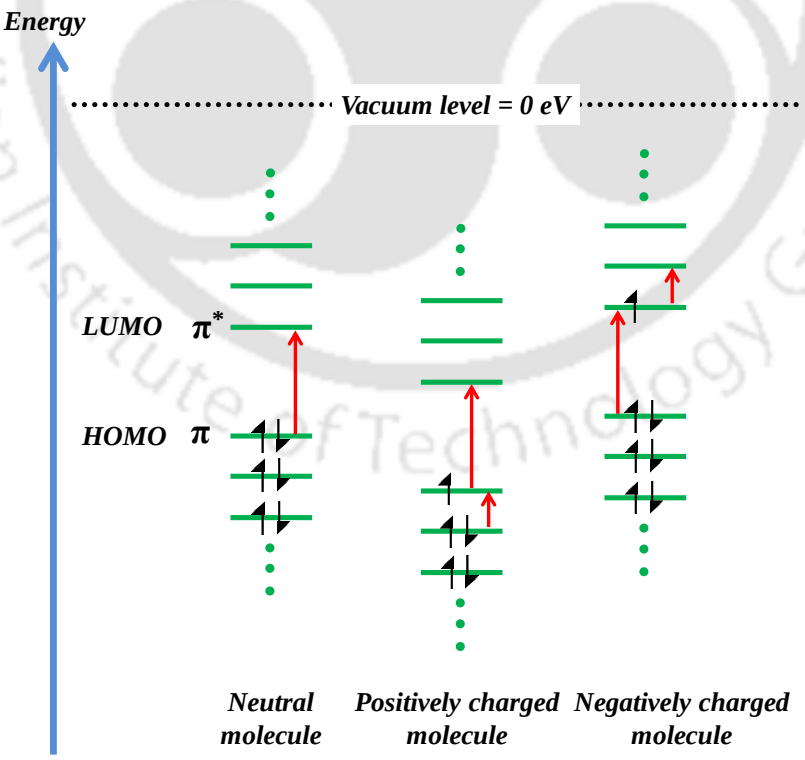


**Fig. 1.4** The different possible optical transitions (red arrow) of the differently charged molecule.

Thus, like in the case of neutral molecule, absorption may cause a transition into different vibrational levels even in case of charged molecule and results in a vibrational structure in the polaron absorption spectra. In solid state, the shift in the energy level with respect to the vacuum level of a molecule is correlated with the change in the polarization in their surroundings. However, in amorphous form (in case of thin film), the polarization in their surroundings varies spatially in Gaussian distribution of excited state energies[22] with a variance σ that is characteristic for the energetic disorder. Such disorder is absent in a molecular crystal.

In case of inorganic semiconductor, strong covalent bonding between the atomic orbitals results in a strong electronic interaction between them and wide bands are formed (bandwidth= few eV). Therefore, charge carrier can travel at high mobilities through these bands. However, since in case of organic semiconductor, there are only the weak van der Waals bonds between adjacent molecules, electronic interaction between them is significantly less resulting in a much narrow band with bandwidth below 500 meV[23]. So, band transport in organic semiconductor can only be observed in case of very pure molecular crystals at low temperature[24-27]. At higher temperatures, coherence between adjacent sites is destroyed by the intra- and intermolecular vibrations. In such cases, the charge carrier is scattered with a mean free path that approaches the distance between adjacent sites. As a result, band transport is no longer possible and charge carriers move by hopping[28].

## 1.5 Luminescence in organic semiconductors

The world of luminescence is a world of beautiful colors. Luminescence is the emission of electromagnetic radiation in the form of ultraviolet, visible or infrared photons from an electronically excited species by the relaxation of an electron from an excited state to the ground state. In Eilhardt Wiedemann's words "luminescence refers to all those phenomena of light which are not solely conditioned by the rise in temperature". It therefore occurs at room temperature and also termed as cold light as opposed to incandescence where light is emitted when an object is heated to a high temperature. It is well established that when an electron of any atom or molecule absorbs energy from any external excitation source, it becomes excited and jumps from ground state to the higher energy excited state. However, as the excited state electron is not stable, it returns to the ground state and in the

process release energy. When the additional energy released by the excited state electron is released in the form of light, it is termed as luminescence. Materials that can generate luminescence are in general termed as phosphors. A phosphor can emit light in the different region of the wavelength range, viz. ultraviolet, visible or infrared region, depending upon the difference between the energy levels of its excited state and the ground state energy levels or in other words its band gap. The luminescence efficiency of a phosphor depends solely on its ability to transform the released excitation energy into light. Luminescent materials can be of different kinds. It can be a small molecule, polymer, organometallic compound, organic or inorganic crystal or any other amorphous material. However, organic luminescent materials are usually of strong interest owing to their application in organic light emitting devices and offer several distinguishing features as compared to their inorganic counterparts:

1. The energy band gap of an organic semiconductor is mainly defined by the conjugation length of the molecule. Molecules with larger conjugation length have small bend gap whereas molecules with small conjugation length have larger band gap. Thus, depending on the conjugation length, organic molecule can produce blue or red light. It also offers the unique feature of color tenability unlike its inorganic analogue.
2. The luminescence of an organic molecule is solely associated with the excited state of the molecule and not with the defects or impurities of the host lattice as in the case of inorganic materials.
3. Due to the low dielectric constant, the coulombic attraction between the oppositely charged electron and hole is more in case of the organic molecules. Therefore, the exciton radius of the organic molecule is less facilitating the emission of photons.

Depending on the source used to excite the ground state electron of a molecule, luminescence can be classified into several categories[29] as shown in the Table 1.1.

Among different luminescence processes, photoluminescence and electroluminescence are of particular importance owing to their prominence in the field of organic light emitting devices.

**Table 1.1** Various types of luminescence processes and their mode of excitation.

| Type of Luminescence | Mode of excitation |
|---|---|
| Photoluminescence | Absorption of Photons or light |
| Radioluminescence | Bombardment with radioactive particles and photons like α, β or γ rays/ ionizing radiation |
| Cathodoluminescence | Irradiation of high energy electron beam or cathode rays |
| Electroluminescence | Passage of electric current or by electric field |
| Thermoluminescence | Heating |
| Chemiluminescence | Chemical or electrochemical reaction concerning an oxidation-reduction process |
| Bioluminescence | Biochemical process |
| Mechanoluminescence | Mechanical energy such as frictional or electrostatic forces, pressure etc. |
| Sonoluminescene | Ultrasound waves |

## 1.6 Mechanism of luminescence

In order for luminescence to occur, the first and foremost thing is that the molecule should be in excited state which is obtained by the promotion of an electron from the ground state to an excited state. The excited electron leaves a vacancy in the ground state which is termed as hole. As oppositely charged, the electron and hole undergoes coulombic attraction between them and forms a quasi-particle termed as exciton and the energy that binds the electron-hole pair together is termed as binding energy. The exciton binding energy varies depending on whether the material is organic or inorganic. Unlike their inorganic counterpart, excitons formed in an organic semiconductor is usually are located on one molecule due to the weak intermolecular van-der-Waals interaction. As a result, organic molecule possesses large binding energy in the order of >500 meV as compare to that of inorganic material (<0.1 eV). Since the excitons formed in organic semiconductor are highly localized in the molecule or the polymer unit, it is also called Frenkel exciton to differentiate it from weakly bound excitons in inorganic semiconductors (Mott-Wannier excitons) which are highly delocalized throughout the lattice.

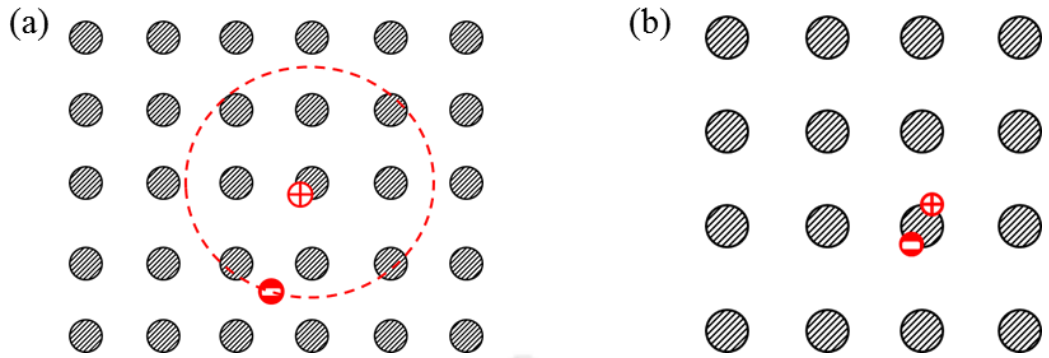


**Fig. 1.5** Mott-Wannier excitons (a) and Frenkel exciton (b).

These exciton states are further divided into two different types based on the quantum mechanical selection rule into singlet and triplet states. Depending on the spin orientation of the excited electron, a singlet or a triplet can form when one electron is excited to a higher energy level. In an excited singlet state, the electron is promoted in the same spin orientation as it was in the ground state (paired). In a triplet excited stated, the electron that is promoted has the same spin orientation (parallel) to the other unpaired electron.

Fig.1.6 shows the Jablonski diagram. A Jablonski diagram is the typical representation of the probable electronic states of a molecule and possible processes through which molecules enter and leave the excited state: photon absorption, internal conversion, fluorescence, intersystem crossing, phosphorescence, delayed fluorescence and triplet–triplet transitions. The singlet electronic states are denoted $S_0$, $S_1$, $S_2$, . . . and the triplet states are denoted as $T_1$, $T_2$, and are represented by bold horizontal lines. Each electronic energy states are associated with multiple vibrational levels and are represented by thin horizontal lines. However, due to the large number of possible vibrational energy levels only a portion of them are shown in the diagram.

The first transition in most Jablonski diagrams is the absorption of a photon of certain wavelength that brings a molecule from one of the vibrational level of $S_0$ to one of the vibrational level of $S_1$, $S_2$…. Since at room temperature the majority of molecules laid in the 0-vibrational level of $S_0$, the absorption process is shown to excite a molecule from this level in the diagram. Absorbance is a very fast process and usually occurs within $10^{-15}$ seconds. Once the molecule is excited by the process of absorption, there are number of possible de-excitation process that can take place.

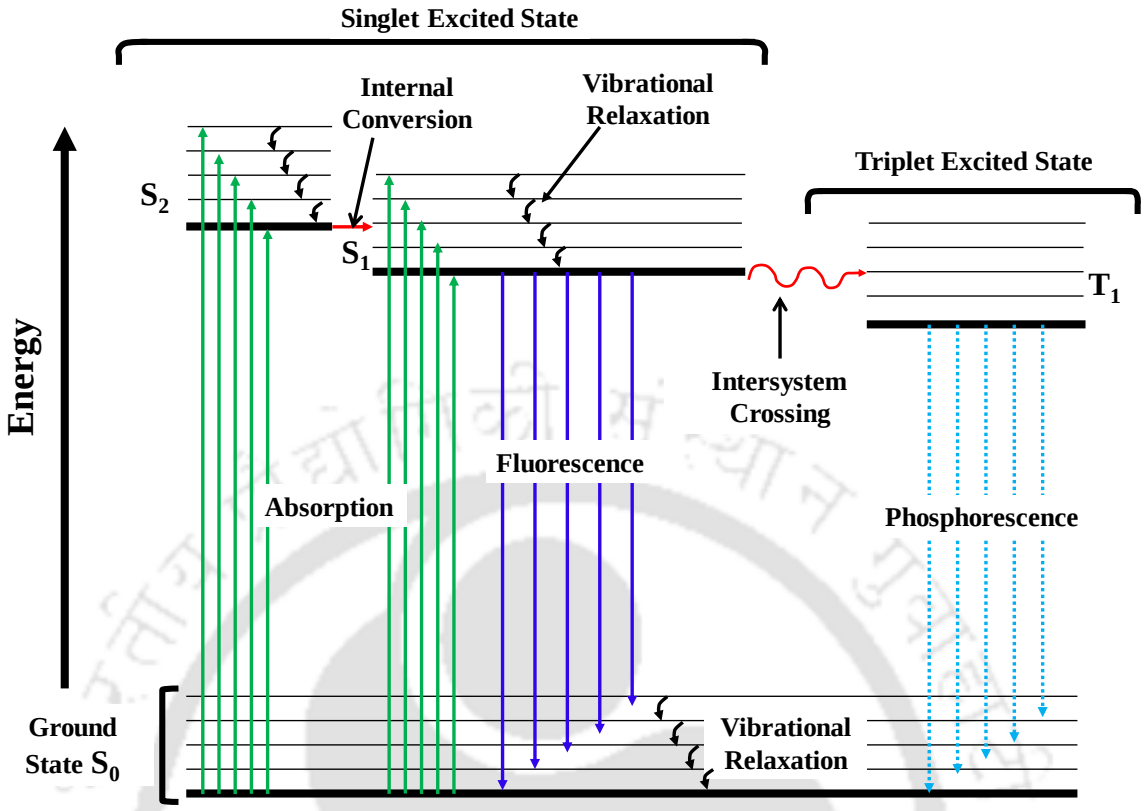


**Fig. 1.6** Jablonski diagram.

The first de-excitation process is vibrational relaxation and internal conversion. It is a non-radiative process. This process is also very fast and occurs immediately following absorbance between $10^{-14}$ and $10^{-11}$ seconds. When a molecule is excited to an energy level higher than the lowest vibrational level of the first electronic state, vibrational relaxation (and internal conversion if the singlet excited state is higher than $S_1$) leads the excited molecule towards the 0-vibrational level of the $S_1$ singlet state. From $S_1$, internal conversion to $S_0$ is possible but is less efficient than conversion from $S_2$ to $S_1$, because of the much larger energy gap between $S_1$ and $S_0$).

The second possible de-excitation process by which an excited molecule can come back to ground state is by means of emitting a photon. This is called as fluorescence. Fluorescence emission generally occurs due to the transition between the first excited state $S_1$ to the ground state $S_0$. Fluorescence is a slow process on the order of $10^{-9}$ to $10^{-7}$ seconds A third possible de-excitation process from $S_1$ is intersystem crossing where an electron changes its spin multiplicity and moves from excited singlet state $S_1$ towards the excited triplet state $T_1$. It is a non-radiative process and occurs within a time scale of $10^{-8}$ to $10^{-3}$

seconds. The crossing of an electron from singlet to triplet state is forbidden in principle due to their different spin multiplicity. However, it can be possible if the spin orbit coupling between the orbital magnetic moment and the spin magnetic moment is large enough.

The fourth possible de-excitation pathway is the transition between the excited triplet state $T_1$ to the ground state $S_0$. This is termed as phosphorescence. Usually this is a forbidden process and can only be observed with materials with heavy atoms that possess high spin orbit coupling. In most of the cases the non-radiative de-excitation from the triplet state $T_1$, is predominant over radiative de-excitation called phosphorescence. Phosphorescence is thus very low with a time scale of $10^{-4}$ to $10^{-1}$ seconds.

Delayed Fluorescence is another possible de-excitation processes through which a molecule can come back to ground state. This can be either thermally activated or due to the triplet-triplet annihilation. In case of thermally activated delayed fluorescence reverse intersystem crossing can happen from $T_1$ to $S_1$ if there is a very small energy difference between them provided that the lifetime of the molecule in the triplet excited state is long enough. This process is thermally activated and therefore the fluorescence increases with the increase in temperature. On the other hand, if the concentration of molecule at the triplet excited state is more, there can be a collision between two molecules in the $T_1$ state. As a result, one of the molecules can gain enough energy to go to the higher triplet excited state and then return to the $S_1$ state, thus leading to a delayed fluorescence emission.

## 1.7 Organic luminescent materials

Organic luminescent materials form the active layer of an OLED and plays an important role in defining the efficiency, emission color and the stability of the device. The luminescent material used as the active layer in OLED should possess good thin film forming property, good luminescence quantum yield, good charge transport property and excellent thermal stability. The design and the characterization of these materials are therefore of utmost importance for fabricating an efficient OLED. The first practical OLED was demonstrated by C. W Tang et al[30] in the year 1987 using $Alq_3$ as the emissive layer. After three years, in 1990, J. H. Burroughes et al[31] demonstrated that poly(p-Phenylene vinylene), prepared by the way of a solution processable precursor, can be used as the active element in a large-area light emitting diode and combination of good structural properties of this polymer, its ease of fabrication, and light emission in the green yellow part of the spectrum with reasonably high efficiency, suggest that the polymer can be used for the

development of large-area light emitting displays. Since then the OLED research community has been divided into two groups, each favouring a specific fabrication method and class of materials resulting from that choice. The highest efficiencies of OLEDs so far have been achieved with small molecule based OLEDs are fabricated via evaporation under high vacuum. On the other hand, in polymer light-emitting diodes (PLEDs, the active layer consists of a semiconducting polymer. These materials cannot be evaporated, but instead they can be tuned to be soluble, which enables solution processing techniques.

### 1.7.1 Small organic materials

In general, small organic materials are organic molecules that possess low molecular weight. They include organometallic chelates, fluorescent and phosphorescent dyes.

**i) Organometallic chelates**

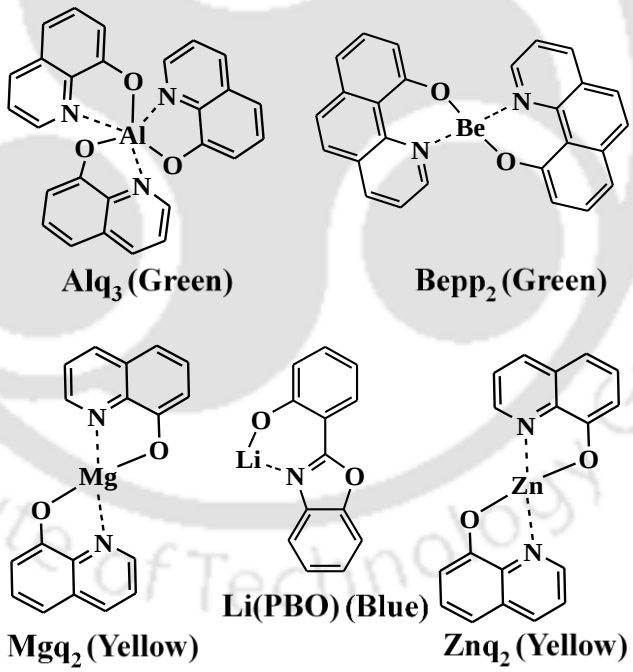


**Fig. 1.7** Some of the commonly used organometallic chelates.

In metal chelates, light is obtained due to the ligand centred π-π* transitions. The d-d* transition can however interfere with the luminescence of such ligands. Therefore, the choice of the metal ions for these class of organic materials are limited to those metals that either do not contain d- electrons or have filled d- shell. $Li^{3+}$, $Be^{3+}$, $Mg^{2+}$, $Zn^{2+}$, $Al^{3+}$ and

$B^{3+}$ are some of the most common metal ions used for this purpose. Tris(8-hydroxyquinoline) aluminium ($ALq_3$) is by far the most commonly used metal chelate in OLED applications and is one of the most efficient luminescent material. Some of the commonly used organometallic chelates are shown in Fig. 1.7.

**ii) Fluorescent dyes**

Fluorescent dyes are the most commonly used emissive materials in small molecule based OLEDs and emit light by the radiative decay of the singlet excited states. The large availability of the fluorescent dyes makes them an interesting choice for OLED application and till date numerous dyes have been utilized as emissive materials. Some of the widely used fluorescent dyes are shown in Fig. 1.8. Since no emission is obtained from the triplet excited states, the efficiency of devices with these dyes are limited to 25%.

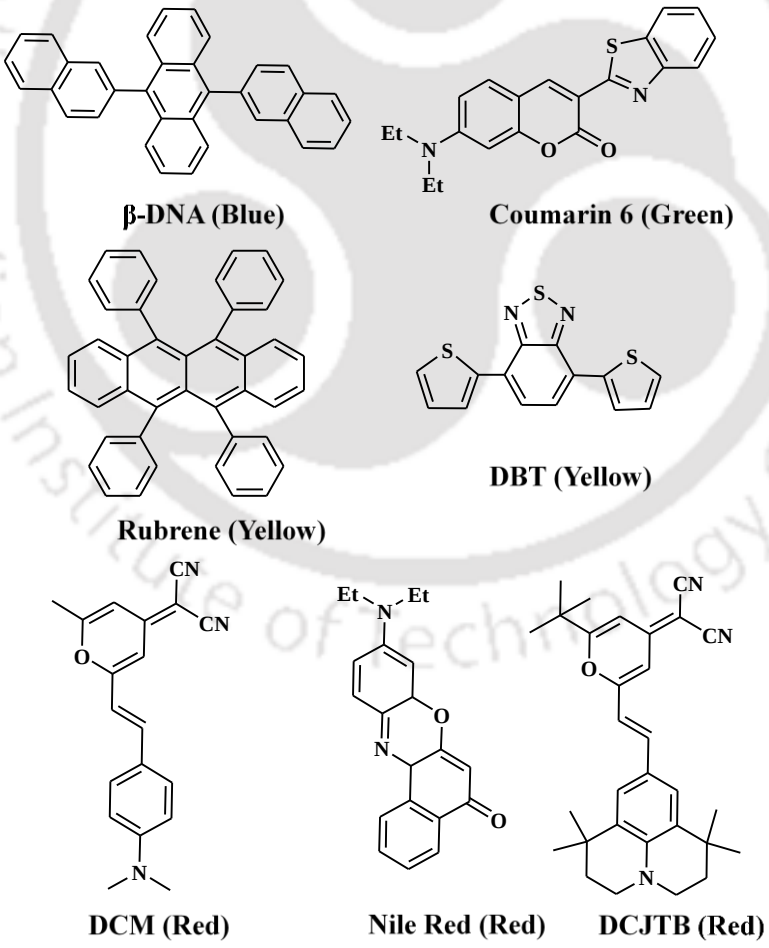


**Fig. 1.8** Some of the commonly used fluorescent dyes.

**iii) Phosphorescent dyes**

Phosphorescent dyes are generally triplet light emitter and utilizes both singlet and triplet excited states to produce light. The presence of heavy metal ions such as iridium, platinum etc in these emitters induces strong spin orbit coupling that eliminates the spin forbidden nature of the triplet states and allows them to decay radiatively. Due to the utilization of singlet as well triplet excited states, these materials possess very high efficiency and the efficiency of devices with these dyes can be 100%. However, confining of the triplet excitons in the emissive layer is a major challenge in this type of devices. Some of the commonly used phosphorescent dyes are shown in Fig. 1.9.

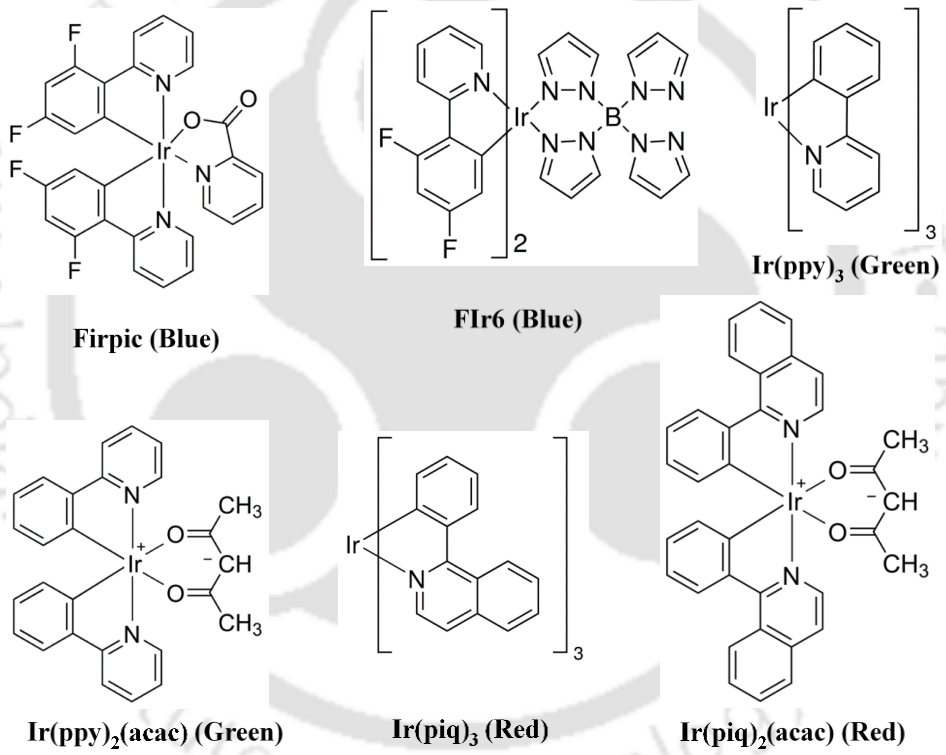


**Fig. 1.9** Some of the commonly used phosphorescent dyes.

### 1.7.2 Polymers

Polymers are also used as emissive materials in OLEDs and possess several advantages over small molecules. They have higher glass transition temperature, better thermal stability, excellent film forming property and due to their longer conjugation length, they can be processed by low cost techniques such as spin coating, inkjet printing etc. The most commonly used polymers in OLED application are the π conjugated polymers. Another significant advantage of polymer emissive material is that their color

tunability and also their charge transport property can be modified by incorporating suitable electron donating or accepting moieties in either side chain or main chain. Some of the widely used polymer emissive materials are shown in Fig. 1.10.

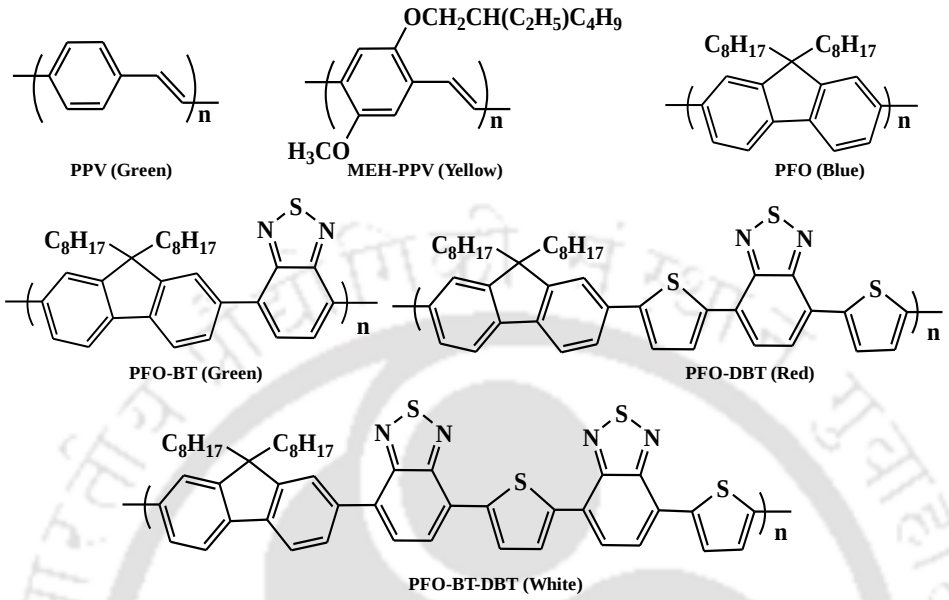


**Fig. 1.10** Some of the commonly used polymers.

## 1.8 Organic light emitting diodes (OLEDs)

An organic light emitting diode (OLED) consists of either one or more semiconducting organic layers sandwiched between two electrodes. The light is generated in the emissive layer by the principle of electroluminescence and in order to light escape from the device, at least one of the electrode should be transparent. A simplified device structure of an OLED is shown in Fig. 1.11.

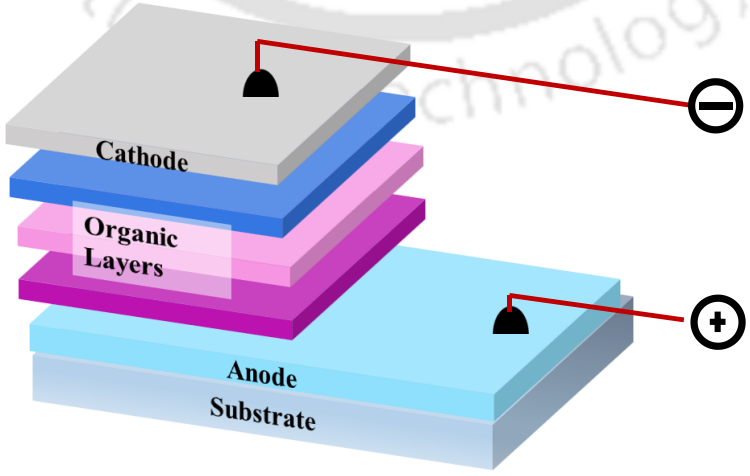


**Fig. 1.11** Simplified device structure of an OLED.

When a voltage is applied across the OLED such that the anode is positive with respect to the cathode a current of electrons starts to flow through the device from cathode to anode. Thus, the cathode gives electrons to the emissive layer and the anode withdraw electrons from the emissive layer; in other words, the anode gives electron holes to the emissive layer. Electrostatic forces bring the electrons and the holes towards each other and they recombine. The recombination causes a drop in the energy levels of electrons, accompanied by an emission of radiation whose frequency is in the visible region. The process is shown in the Fig.1.12.

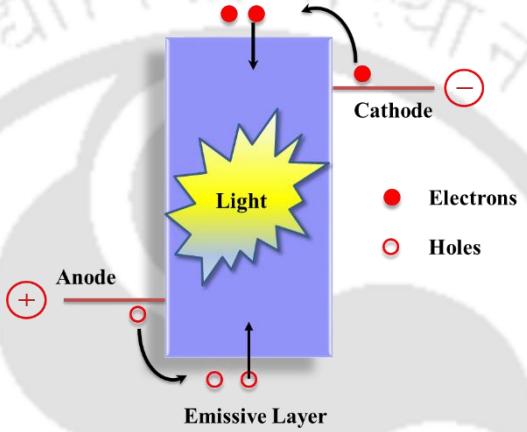


**Fig. 1.12** The process of light generation in OLED.

Depending on the number of organic layer used, OLEDS can be termed as Mono layered, or multilayered devices.

### 1.8.1 Mono layered OLEDs

As the name suggests, a mono layer or single layer OLED consists of the emissive layer sandwiched between the anode and cathode layer.

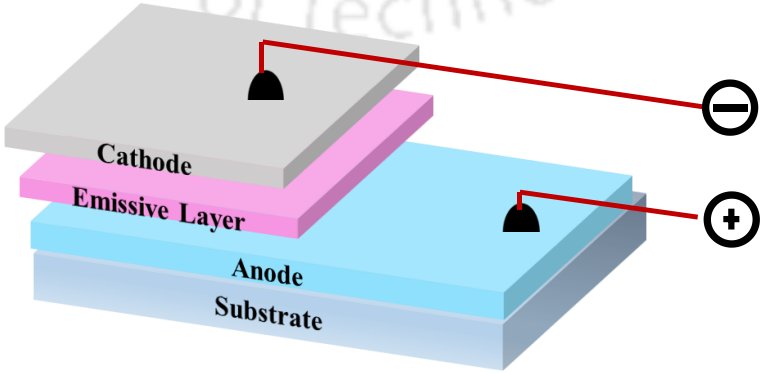


**Fig. 1.13** The basic schematic of a mono layered OLED.

Fig.1.13 shows the basic schematic of a mono layered OLED. Monolayered OLEDs have the simplest structure and offers the advantage of low fabrication cost. However, the mobility offset between the hole and electrons in the organic semiconductor causes exciton quenching either at the anode of cathode and is a major factor that reduces the efficiency of such OLEDs.

### 1.8.2 Multilayered OLEDs

The efficiency of an OLED usually depends on the number of electron hole pairs that is formed in the emissive layer of an OLED and decay radiatively. Therefore, the confinement of electrons and holes injected from the cathode and the anode of the devices into its emissive layer has been the main driving force while designing the structure of an OLED. This has led to the multilayer device structure of OLEDS where apart from the emissive layer, several other layers are incorporated into the device to confine the injected electrons and holes into the emissive layer. Fig.1.14 shows the basic schematic of a multilayered OLED.

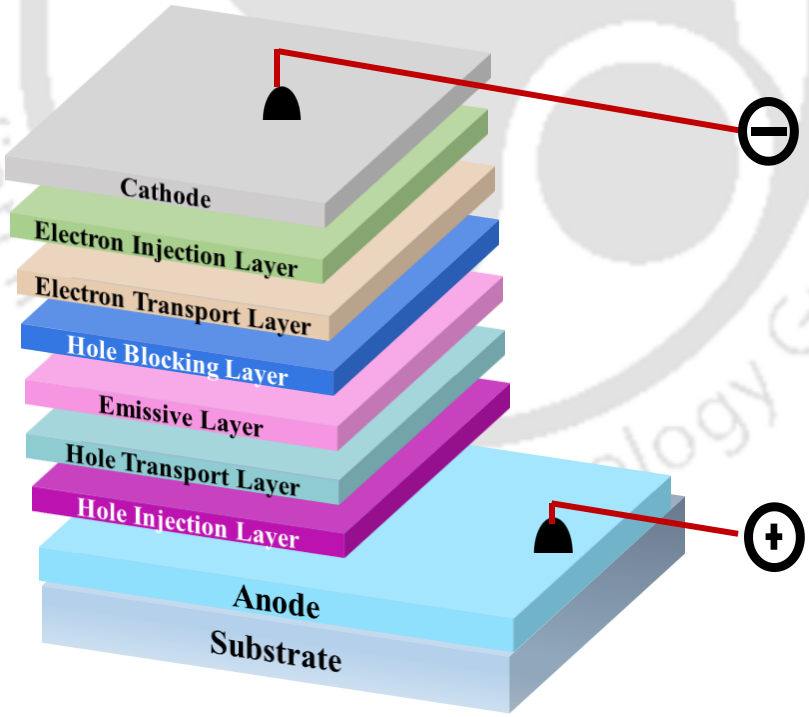


**Fig. 1.14** The basic schematic of a multilayered OLED.

The role of the different layers of a multilayered OLED are described in the following section.

**i) Substrate:** The main role of the substrate is to provide mechanical support to the device. Usually it is a rigid glass substrate or flexible plastic substrate and most likely made upm of transparent materials.

**ii) Anode:** In its most common form, the anode of an OLED should be transparent so that the light generated inside the device due to the exciton decay can escape the device. The primary function of the anode is to inject holes to the organic layers. Usually the material used as anode in OLED should have high work function, good transparency and low electrical resistivity. Indium tin oxide (ITO) is the most commonly used anode in OLED.

**iii) Hole injection layer (HIL):** HIL is inserted between anode and the hole transporting layer (HTL) in order to enhance hole injection from the anode. Strong electron acceptors or p type doped organic molecules are the most common choices for HIL. Some of the commonly used HIL are Copper phthalocyanine (CuPc), m-MTDATA, PEDOT:PSS etc.

**iv) Hole transport layer (HTL):** HTL is used to facilitate hole transport into the emissive layer and the materials used as HTL have high hole mobility and low electron mobility. Sometimes this layer also acts as electron blocker and helps confining the electrons in the emissive layer. Some of the commonly used HTL are PVK, PPV, TPD, a-NPD, TCTA etc.

**v) Emissive layer (EML):** EML is also termed as the active layer of the OLED and defines the color emitted from the device. The materials used as emissive layer should possess high quantum yield and good charge balance.

**vi) Hole blocking layer (HBL):** Hole blocking layer is used to block the hole from flowing towards the cathode and to confine them inside the emissive layer thereby enhancing the recombination and the efficiency. BCP, BPhen, TPBi are some of the widely used hole blocking layer.

**vii) Electron transport layer (ETL):** ETL is used to facilitate electron transport into the emissive layer and the materials used as ETL have high electron mobility and high electron mobility. Usually n-type-doped materials are used in this layer. Alq3 is the most commonly used ETL.

**viii) Electron injection layer (EIL):** EIL is inserted between cathode and the ETL in order to enhance electron injection from the cathode.

**ix) Cathode:** The primary function of the cathode is to inject electrons to the organic layers. Usually the material used as anode in OLED should have low work function and high reflectivity. Some of the widely used cathodes are lithium (Li, 2.90 eV), cesium (Cs, 2.14 eV), calcium (Ca, 2.87 eV), magnesium (Mg, 3.66 eV), aluminum (Al, 4.3 eV) etc.

## 1.9 Approaches to white light generation

White is generally the color produced by the combination of all the colors of the visible spectrum. Usually white light is obtained either by combining blue, green and red emitter together or by combining a blue emitter with an orange emitter (Fig.1.15)

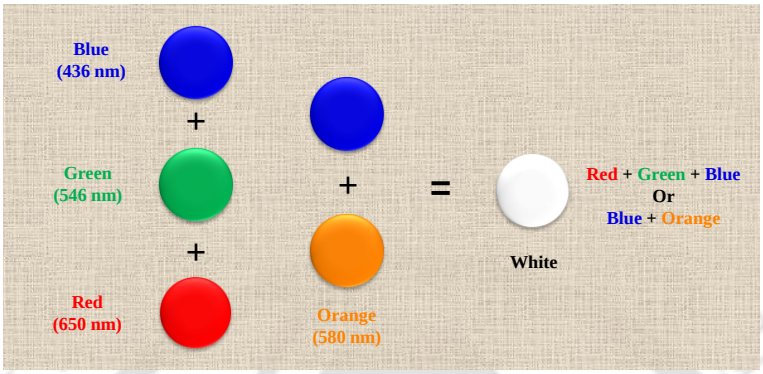


**Fig. 1.15** Approaches to white light generation.

To become an ideal source of white light, OLEDs output spectrum should cover the entire visible range (400-800 nm) and its spectral distribution should match that of the natural sun light. To achieve this, the dominating approach is to combine the electroluminescence obtained from different materials, typically two or three. In evaporated OLEDs, this can be achieved by the fabrication of multilayer devices where each layer emits a specific color. However, in case of WPLEDs, white light is basically generated by single layer of a white-emitting copolymer where the emission of several colors takes place in a single layer. WPLEDs can also be fabricated using multilayer device structure, however, the preparation of multilayer polymer devices is more complicated as multilayer devices are difficult to process from solution and there is always a possibility that the solvent used in wet-processing may harm the underlying layer.

## 1.10 Polymer based white light emitting diode

There are basically four main approach that has been used to date for the generation of white light from a polymer light emitting diode.

### 1.10.1 Doping of Small molecule in polymer films

In this approach, small molecular dyes are dispersed in the polymer and the mixture is used as the active layer of the device as shown in Fig. 1.16.

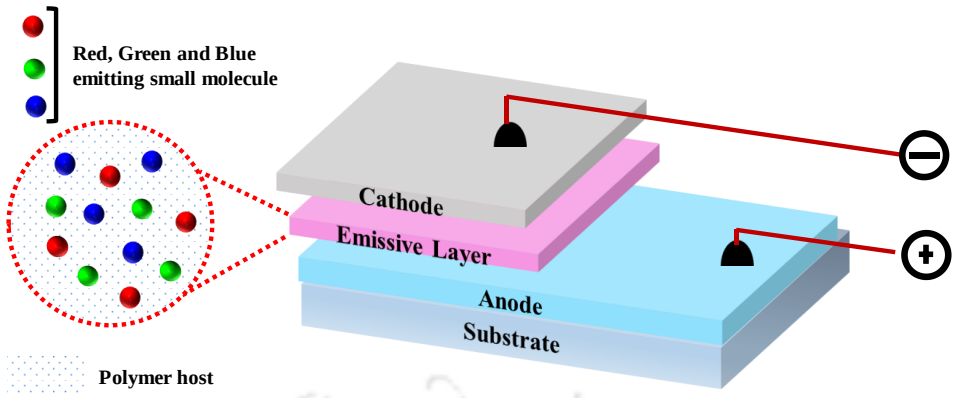


**Fig. 1.16** WPLED using small molecule doped polymer films.

The polymeric materials are used to function solely as the host material and in part as a charge transport material. The emission is however obtained from the small molecular dyes doped into the polymer host.

Using this approach, Kido et al[32], for the first time, succeeded to obtain bright white emission which covers wide range of the visible region. TPB, coumarin 6, and DCM 1 were doped in PVK as emissive layer in their work and TAZ and $Alq_3$ are used to confine the emission center in the emissive layer by blocking the holes from reaching cathode and transporting electrons respectively. White emission was observed from EL cells when operated in a continuous dc mode with ITO at positive polarity.

Following the work reported by Kido et al, significant amount of research was carried out in the following years to develop highly efficient WPLED[33-35]. In 2006, Jinsong Huang et al[36] reported a device structure with improved luminous efficiency by doping a blue polyfluorene host polymer by orange emitting rubrene dye.

In order to improve the device efficiency further, a significant amount of research effort has been spent to develop all-phosphorescent WOLEDs with other polymer hosts, which can fully harvest excitons for emission through the phosphorescent[37-40]. For all-phosphor phosphor doped, solution-processed WOLEDs, PVK is widely used as the host polymer, owing to its high triplet level (ca. 2.5 or 2.9 eV). To date, PVK-based WPLEDs are essentially based on sky-blue FIrpic as the blue component.[39,40] But due to the poor color purity of FIrpic, these types of devices were unable to provide the required CRI value ideal for solid state lighting. To pursue high CRI WOLEDs, a commercial deep-blue phosphor IrIII bis(4',6'-difluorophenylpyridinato) tetrakis(1-pyrazolyl) borate (FIr6) with CIE coordinates of (0.16,0.26) is expected to replace FIrpic as the blue dopant in these

WOLEDs[37,41]. However, due to the relatively low triplet levels of PVK as compared to Fir6 it seems to be impossible to realize efficient PVK-based WPLEDs with FIr6.

Very recently, Zhang et al[42] changed this perspective by reporting an efficient deep-blue and white PhOLEDs with $FIr_6$ as the blue emitter with PVK as the host material. Although PVK possesses a lower triplet level than that of $FIr_6$, it is found that the deep-blue emission of $FIr_6$ is strongly dependent on the triplet exciton confinement in the PVK: $FIr_6$ emissive layer. By incorporating an interfacial layer with a ultra-high triplet level (3.07 eV), such as 3,6-bis(diphenylphosphoryl)-9-[4'-(diphenylphosphoryl) phenyl] carbazole (TPCz), it could effectively cut off the potential loss pathways of the triplet excitons within the PVK/$FIr_6$ EML. The resultant PVK/$FIr_6$-based deep-blue and white solution-processed WOLEDs achieved an unprecedented forward-viewing EQE of 16.1% and a total EQE of 28.0% (38.4 $lmW^{-1}$) at a practical luminance of 1000 $cdm^{-2}$.

### 1.10.2 Polymer blending

This is the most simplified approach as it offers simpler device fabrication than all other approaches. By tailoring the effective conjugation length or chemically anchoring a variety of light-emitting chromophores, light-emitting polymers covering the whole region of visible light were synthesized.[43] White electroluminescent device can thus be prepared by simply blending these efficient single-color polymers into a single active layer as shown in Fig. 1.17. However, the film morphology of the blended polymers should be manipulated properly to control the optoelectronic process of the blended films.

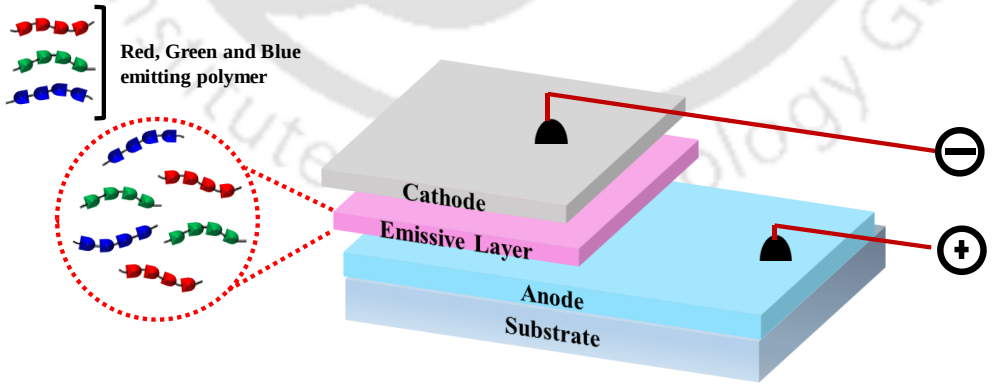


**Fig. 1.17** White light from polymer blending.

The first white polymer OLEDs based on polymer blends were discussed by Tasch et al.[44] By highly diluting a red-emitting polymer poly (perylene-co-diethynyl benzene)

into a blue ladder-type polymer polyparaphenylene with a concentration of 0.05%, white emission is realized. Here the red emitter is excited via exciton energy transfer and charge transfer and trapping. With an addition of 10 wt% PMMA to the mixed layer, CIE coordinates of (0.31, 0.33) were reached with a maximum external quantum efficiency of 1.2%.

Huang, Li et al.[45] reported on a simple two-polymer blend white device with a greatly improved device efficiency. They introduced a $Cs_2CO_3$ interfacial layer between the LEP layer and cathode to enhance the injection of the minority charge carriers. Furthermore, the dopant's (MEH-PPV) energy levels are within the band gap of the host material (PFO), so that the excitation of the dopant can occur via energy transfer and charge trapping, the latter leading to a charge confinement effect.

In 2013, Yu et al[46] synthesized a series of blue (B), green (G), and red (R) 9,9-bis [4-(2 ethylhexyloxy)phenyl] fluorene (PPF)-based polymers containing a dibenzothiophene- S,S dioxide (SO) unit (PPF-SO polymer), with an additional benzothiadiazole (BT) unit (PPF-SO-BT polymer) or a 4,7-di(4-hexylthien-2-yl)benzothiadiazole (DHTBT) unit (PPF-SO-DHTBT polymer). These polymers exhibit high fluorescence yields and good thermal stability. PLEDs using PPF-SO25, PPF-SO15-BT1, and PPF-SO15-DHTBT1 as emissive polymers have maximum efficiencies of 7.0, 17.6, and 6.1 $cdA^{-1}$ with CIE coordinates of (0.15, 0.17), (0.37, 0.56), and (0.62, 0.36), respectively. Blending different ratios of these polymers realized highly efficient WPLEDs. With incorporating an alcohol-soluble poly ({9,9-bis[3'-(N,N dimethylamino)- propyl]-2,7-fluorene}-alt-2,7-(9,9-dioctylfluorene)) (PFN) EIL and a B/G/R blend ratio 100 : 8 :7 by weight, a maximum LE of 9.8 $cdA^{-1}$ and PE of 8.9 $lmW^{-1}$ were reached. The optimized devices have a CCT of 4700 K and an excellent CRI of 90, owing to the wide spectral regions covered with these polymers.

### 1.10.3 Polymer heterolayers

A multilayered device structure, comprising of a hole injection/ transport layer (HIL/HTL), a single or multilayered EML, and an electron injection/transport layer (EIL/ETL) is promising for pursuing high device efficiencies because of the convenient manipulation of the charge balance and exciton formation region as well as the confinement of charges/excitons within the EML for emission. The schematic of a multilayer device is shown below.

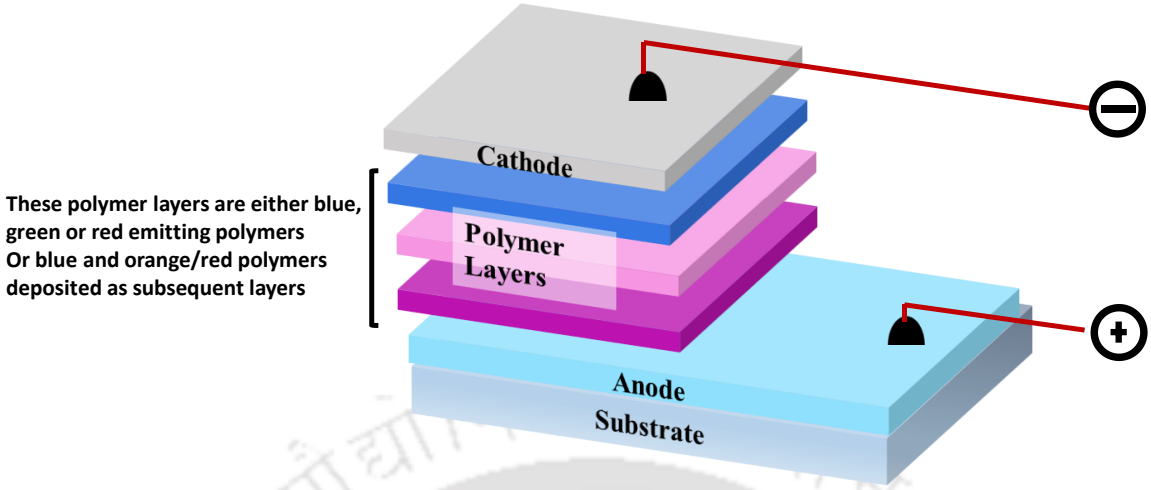


**Fig. 1.18** WPLED using of a multilayer device structure.

On the basis of a multilayered device structure, thermally evaporated OLEDs/WOLEDs have already achieved extremely high device efficiencies. Unfortunately, the multilayered solution- processed OLEDs/WOLEDs generally cannot be prepared owing to intermixing issues between layers during fabrication, which originate from similar solubility in common solvents for commonly used optoelectronic materials. As a result, solution-processed OLEDs/ WOLEDs are typically based on single active layer structures, in which all materials, including host, dopant, and charge-transport moieties, are blended together, as introduced in Approach 2. Excitingly, some efforts have been made to breakthrough such limits.[47,48] To solve the intermixing problems during sequential coating, "orthogonal" solvents or cross-linking methodology have been developed, and high-performance multilayered solution-processed WOLEDs have been obtained.

Gong et al. [49] showed that high performance, multilayer, white light emitting PLED can be fabricated by using a blend of luminescent semiconducting polymers and organometallic complexes as the emission layer, and water soluble (or ethanol soluble) polymers and/or small molecules as the hole injection/transport layer (HIL/HTL) and the electron injection/transport layer (EIL/ETL).

Kohnen et al.[50] reported on a fully wet-processed bilayer polymer system consisting of two fluorescent emitters with complementary emission colors (a PPV derivative for yellow and a polyfluorene for blue). In their work, the yellow-emitting PPV derivative (SY) was thermally cross-linked. An optimized device emits white light with CIE coordinates

(0.323, 0.345) very close to standard white light (0.33, 0.33). The maximum efficiency of the device is 6.1cdA$^{-1}$.

### 1.10.4 Single polymer system

An alternative but very promising concept for generation of while light is by using a white single polymer (WSP). The key idea here is to realize a single copolymer, in which the polymer host is chemically linked with red, green, and red chromophores for three-color white emission or linked with blue and orange chromophores for two-color white emission.

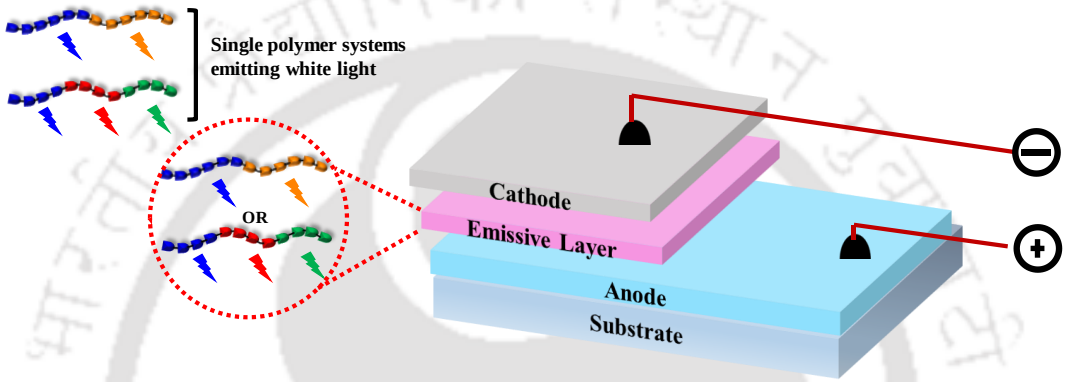


**Fig. 1.19** Single polymer based WPLED.

In this approach, white light is generated by intra- and intermolecular energy transfer from host moieties to chromophores. The WSP route is unique, since it simplifies the fabrication procedures and also enhances the reproducibility of the device. Furthermore, unlike common WOLEDs, the intrinsic phase separation risk of multi components of the blends, and thus, device and spectral instability under long-term operation, are removed for WSP-based WOLEDs.

WSP can be designed by two processes. In the first process, the main polymer (host) and all chromophores form the copolymer main chain in a stoichiometric manner, where conjugation occurs. In second approach, the chromophores are attached to the polymer main chain as side groups, where the conjugation is lost. In the latter approach, the chromophores can be seen as isolated molecules dispersed in a host polymer.

Tu et al.[51] reported on an efficient white light emitting polymer by admixing moieties of an orange fluorophore (1,8-naphthalimide) into the blue PFO main polymer. Used as a single EML device, a chromphore concentration of 0.05% in the PFO main chain yields a device efficiency of 5.3 cdA$^{-1}$ and 2.8 lmW$^{-1}$ at 6 V [CIE (0.26, 0.36)]

Later, Luo et al[52] proposes a novel strategy to realize white electroluminescence simultaneously with three primary color emissions from a single conjugated copolymer with a backbone consisting of poly(9,9-dioctylfluorene) (PFO), 2,1,3- benzothiadiazole (BT), and 4,7-bis(2-thienyl)-2,1,3-benzothiadiazole (DBT) as the blue-, green-, and red-light-emitting units, respectively. A maximum efficiency of 3.43 $cdA^{-1}$ with a CIE coordinate of (0.34,0.33) was obtained by using the PFO-R010-G018 polymer as the emissive layer.

Recently, Zhang et al[53] reported on a highly efficient single-component polymer system containing three chromophores that are covalently attached to the polymer backbone. With a correlated color temperature of approximately 4500 K [CIE coordinates (0.37, 0.42)], the best device reaches 6.2% EQE and a luminous efficacy of 10.4 $lmW^{-1}$ measured at $500Cdm^{-2}$.

## 1.11 Techniques used to fabricate OLEDs

OLED is a thin film device that consists of thin films of metals and organic semiconductors. Some of the most common techniques used to deposit organic or metal thin film in an OLED are described in this section.

### 1.11.1 Thermal evaporation

Thermal evaporation is widely used to deposit thin films of small organic molecules and the metals. It is one of the simplest of the Physical Vapor Deposition (PVD) techniques. In this technique material to be deposited is first placed on a suitable source and then the source is heated in a vacuum chamber until its surface atoms of the material to be deposited have sufficient energy to leave the surface. Once they have sufficient energy, they traverse through the chamber and deposited on the substrate placed on the top as shown in Fig. In order to avoid collision between the atoms and air molecules, the chamber is usually maintained at high vacuum. In this technique, resistive boat or coil is used as source for metal deposition and alumina crucible or Knudsen cells are used as source for organic molecule deposition.

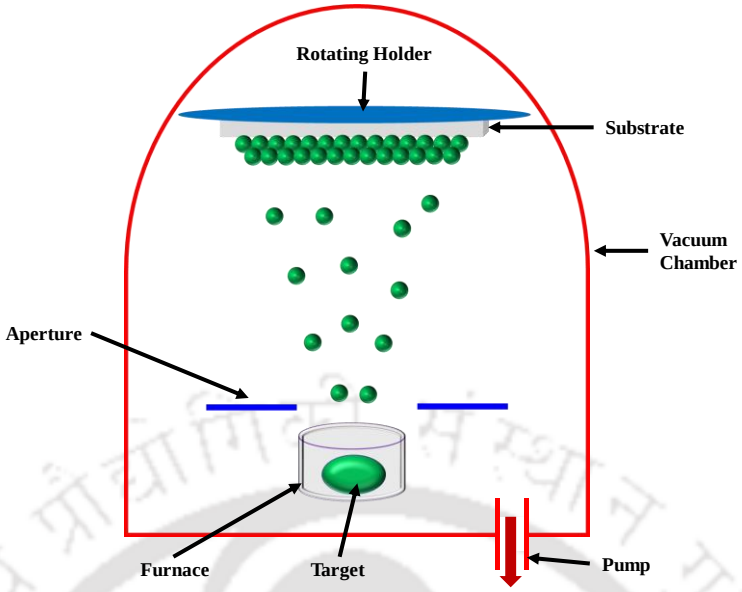


**Fig. 1.20** Thermal evaporation technique.

### 1.11.2 Inkjet printing

Inkjet printing is used to form thin films of polymeric material. In this technique, solution of polymeric material to be coated is used as ink and is dispensed on the substrate to be coated through inkjet nozzles. The film thus formed in then dried to remove the residual solvents. This technique is useful for large area coating.

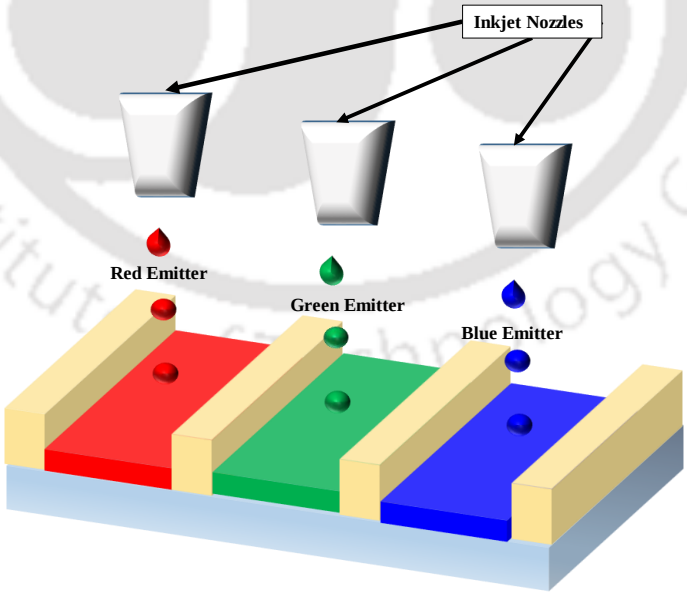


**Fig. 1.21** Inkjet printing technique.

### 1.11.3 Dip coating

Dip coating is another method used to deposit thin films of organic semiconductor. In this method, the substrate on which the film is to be deposited is dipped into the material solution and allowed for coating. After the formation of the film the substrate is withdrawn and dried for the removal of solvent. It is a very simple and easy of film deposition. However, it is hard to obtain a uniformly thick film over the whole substrate using this technique.

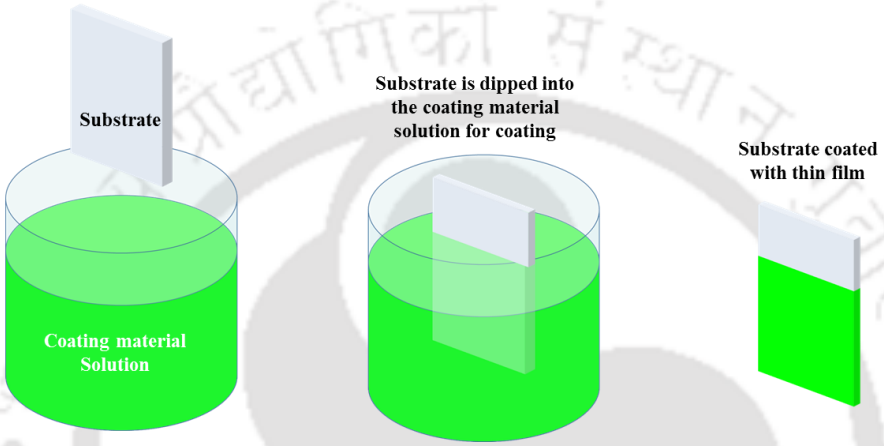


**Fig. 1.22** Dip coating technique.

### 1.11.4 Spin coating

Spin coating is one of the most common techniques used to deposit organic thin films. It is an easy and quick process and produces uniform and smooth films within a thickness range of a few nanometer to a few micrometers.

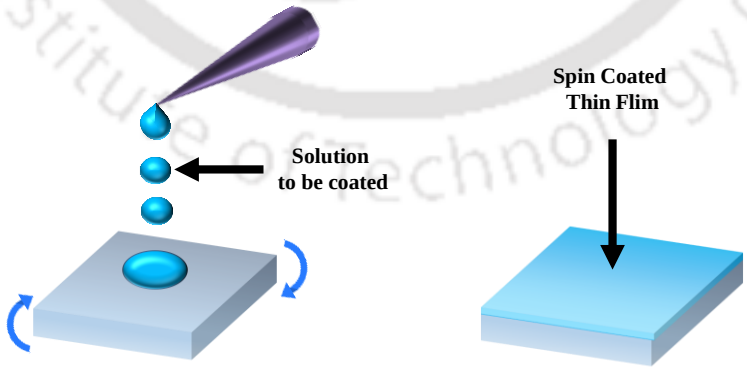


**Fig. 1.23** Spin coating technique.

In this process, the material to be coated is first made soluble in a solvent. A small puddle of that solution is then dropped onto the center of the substrate on which the thin

film is to be deposited and the substrate is spun at a high speed. As a result, under the influence of centripetal acceleration, the solution spread over the whole surface and eventually off the edge of the substrate leaving a thin film on the surface. The solution concentration, its viscosity, surface tension between the solution and the substrate, rotating speed plays vital role in defining the thickness and the properties of the as deposited thin films.

## 1.12 OLED fabrication process

ITO coated glass substrate were used as anode material in all the OLEDs. The ITO coated glass substrates with sheet resistance 25 ohm/cm were patterned using scotch tape to give the desired device area. After masking, to remove the ITO coating from the unmasked glass substrates, zinc dust was spread over the unmasked area into which a mixture of conc. HCl and $H_2O$ (1:1 ratio) was added dropwise and removed immediately. After patterning, the substrates were cleaned in sequential ultrasonic baths of 2% soap solution, acetone and isopropanol, each for ten minutes at room temperature and then dried under argon gas. The ITO substrate was then treated using UV-ozone treatment for 30 min. After cleaning, different organic layers were deposited either by using thermal evaporation process or by spin coating technique depending on the type of the materials used in the device. Finally, the different interfacial layers along with the cathode materials were deposited by using thermal evaporation technique at a pressure of $10^{-6}$ bar.

## 1.13 Characterization parameters for WPLEDs

The performance of any white light source is determined by the following parameters

**(a) Efficiency*:*** The efficiency of WOLEDs is characterized by its luminous efficiency (LE), quantum efficiency (QE), and power efficiency (PE). Of which, LE and QE are important for material evaluation while PE is important for device evaluation and engineering design.

**Luminous efficiency (LE):** LE is measured in candela per ampere (cd $A^{-1}$) and obtained on the basis of measurement of luminous intensity (in candela, cd), or luminance (L, in candela per meter square cd $m^{-2}$) at a given current density (J). i.e.

$$EQE = \frac{Luminous\ intensity}{Current\ density} cdA^{-1}$$

**Quantum efficiency (QE):** QE of a device is defined as the ratio between generated photons and the injected electron–hole pairs in the device. Of which, photons emitted outside the device are correlated to external quantum efficiency (EQE) while all the photons generated in the device contribute to its internal quantum efficiency (IQE),

$$EQE = \frac{No.of\ photons\ emitted\ outside\ the\ device}{No.of\ e-h\ pair\ injected\ into\ the\ device}$$

$$IQE = \frac{No.of\ photons\ generated\ inside\ the\ device}{No.of\ e-h\ pair\ injected\ into\ the\ device}$$

**Power efficiency (PE):** This is the most important parameter describing the performance of any light source and is typically measured in lumen per watt. Artificial white light sources are usually evaluated in terms of PE, which is defined as the luminous flux output (in lumen) per input power of the device. It is also termed as luminous efficacy.

$$PE = \frac{luminous\ flux\ output\ (in\ lumen)}{input\ power\ to\ the\ device\ (in\ watt)}\ lmW^{-1}$$

***(b)*** **Commission internationale de l'Eclairage or International commission on illumination (CIE):** The CIE coordinates describes how the human eye perceives the emission color of any light using a pair of two numbers (x,y). For pure white light, the CIE coordinates are (0.33, 0.33).

**(c) Correlated color temperature (CCT):** The correlated color temperature of a light source is defined as the temperature [usually measured in Kelvin (K)] at which the heated black-body radiator matches the color of the light source. Higher Kelvin temperatures (5,000 K or more) are said to be "cool" (green–blue) colors whereas lower color temperatures (2,700–3,000 K) are called "warm" (yellow–red) colors. Cool-colored light is considered better for visual tasks and warm-colored light is preferred for living spaces because it is considered more flattering to skin tones and clothing.

**(d) Color rendering index (CRI):** The color rendering index (CRI) is a quantitative measure of the ability of a light source to reveal the colors of various objects faithfully in comparison with an ideal or natural light source. It is represented by a number between 0 and 100. Natural sunlight is assumed to have a CRI value of 100. To be used for indoor lighting, a light source should have a minimum CRI value greater than or equal to 80.

## 1.14 Current progress and future development of OLED

Due to its versatility, low cost of production, and ease of large area fabrication, the past few decades have witnessed organic light-emitting devices (OLEDs) being widely pursued as a potential replacement for their inorganic counterparts (commonly known as LEDs) in flat-panel-display and light-emitting elements. Now-a-days, OLED technology is used in different commercial applications such as displays for mobile phones, portable digital media players, etc. Similarly, OLED based televisions have begun entering the commercial market area. In the field of lighting, OLEDs are one of the most promising new lighting technologies to emerge over the years and has the potential to become a highly energy-efficient, large area and eco-friendly lighting solution and alternative to existing technology.

The efficiency of the WOLEDs designed for solid state lighting has already surpassed that of the traditional incandescent lamp and compact fluorescent lamp and is at par with their inorganic counterparts. Recently, WOLEDs with efficiency as high as 156 lm $W^{-1}$ has been claimed by NEC lighting which was co-developed with Yamagata University's research group led by Kido.[54] Although OLEDs have many advantages, the cost of the OLED-based products is still on the expensive side, and as the organic materials in general have a limited lifetime, the long-term stability of those devices is yet to be tested. However, considering the wide versatility of the organic semiconducting materials available, there is still huge scope for chemists, material scientists, and engineers for further improvement in the performance of organic light-emitting devices.

## 1.15 References


1. C. J. Humphreys, *Mrs. Bull.*, 2008, **33**, 459-470.
2. N. Holonyak and S. F. Bevacqua, *Appl. Phys. Lett.*, 1962, **1**, 82-83
3. S. Nakamura, T. Mukai and M. Senoh, *Appl. Phys. Lett.*, 1994, **64**, 1687-1689.
4. www.lanl.gov/orgs/adtsc/docs/8Yang.
5. J. R. Sheats, H. Antoniadis, M. Hueschen, W. Leonard, J. Miller, R. Moon, D. Roitman and A. Stocking, *Science*, 1996, **273**, 884-888.
6. A. Misra, P. Kumar, M. N. Kamalasanan and S. Chandra, *Semicond. Sci. Tech.*, 2006, **21**, R35-R47.
7. K. T. Kamtekar, A. P. Monkman and M. R. Bryce, *Adv. Mater.*, 2010, **22**, 572-582.
8. M. C. Gather, A. Kohnen and K. Meerholz, *Adv. Mater.*, 2011, **23**, 233-248.
9. H. Shirakawa, E. J. Louis, A. G. Macdiarmid, C. K. Chiang and A. J. Heeger, *J Chem. Soc. Chem. Comm.*, 1977, DOI: 10.1039/C39770000578, 578-580.
10. "Chemistry 2000". Nobelprize.org. Retrieved 2010-03-20.
11. H. Letheby, *J. Chem. Soc.*, 1862, **15**, 16-19.
12. J. C. Scott, Nanostructured Conductive Polymers - Chapter 1: History of conductive polymers, *John Wiley & Sons Ltd*, 2010. ISBN: 978-0-470-74585-4.
13. H. Naarmann, Polymers, Electrically Conducting, *Ullmann's encyclopedia of Industrial Chemistry, Wiley-VCH*, 2002, DOI:10.1002/14356007. a21_429.
14. H. Kallman and M. Pope, *Nature*, 1960, **186**, 31-33.
15. H. Kallman and M. Pope, *J. Chem. Phys.*, 1960, **32**, 300-301.
16. H. Akamatu, H. Inokuchi and Y. Matsunaga, *Bull. Chem. Soc. Jap.*, 1956, **26**, 213-218.
17. M. Sano, M. Pope and H. Kallmann, *J. Chem. Phys.*, 1965, **43**, 2920-2921.
18. L. T. Yu, M. S. Borredon, M. Jozefowicz, G. Belorgey and R. Buvet, *J. Polym. Sci. Pol. Sym.*, 1967, **16**, 2931-2942.
19. J. Mcginness, P. Corry and P. Proctor, *Science*, 1974, **183**, 853-855.
20. D. Micha and I. Burghardt, Quantum Dynamics of Complex Molecular Systems, *Springer*, 2007. ISBN: 978-3-540-34458-2.
21. N. S. Hush, *Annals of the New York Academy of Sciences*, 2003, 1-20.
22. L. Kador, *J. Chem. Phys.*, 1991, **95**, 5574-5581.
23. V. Coropceanu, J. Cornil, D. A. da Silva, Y. Olivier, R. Silbey and J. L. Bredas, *Chem. Rev.*, 2007, **107**, 926-952.

24. W. Warta, R. Stehle and N. Karl, *Appl. Phys. a-Mater.*, 1985, **36**, 163-170.
25. N. Karl, "Madelung O, Schulz M, Weiss H (eds) Semiconductors (Landolt-Boernstein (New Series), Group III)", *Springer*, 2000.
26. N. Karl, "Farchioni R, Grosso G (eds) Organic Electronic Materials", *Springer*, 2001.
27. M. Schwoerer, H. C.Wolf, "Organic Molecular Solids", *Wiley-VCH*, 2007.
28. H. Bässler and A. Köhler, *Top. Curr. Chem.*, 2012, **312**, 1–66.
29. B. Valeur and M. N. B. Santos, "Molecular Fluorescence: Principles and Applications, Second Edition", *Wiley-VCH*, 2012.
30. C. W. Tang and S. A. Vanslyke, *Appl. Phys. Lett.*, 1987, **51**, 913-915.
31. J. H. Burroughes, D. D. C. Bradley, A. R. Brown, R. N. Marks, K. Mackay, R. H. Friend, P. L. Burn and A. B. Holmes, *Nature*, 1990, **347**, 539-541.
32. J. Kido, M. Kimura and K. Nagai, *Science*, 1995, **267**, 1332-1334.
33. G. Li and J. Shinar, *Appl. Phys. Lett.*, 2003, **83**, 5359-5361.
34. C. H. Chuen and Y. T. Tao, *Appl. Phys. Lett.*, 2002, **81**, 4499-4501.
35. X. Gong, S. Wang, D. Moses, G. C. Bazan and A. J. Heeger, *Adv. Mater.*, 2005, **17**, 2053-2058.
36. J. S. Huang, W. J. Hou, J. H. Li, G. Li and Y. Yang, *Appl. Phys. Lett.*, 2006, **89**, 133509.
37. P. E. Burrows, A. B. Padmaperuma, L. S. Sapochak, P. Djurovich and M. E. Thompson, *Appl. Phys. Lett.*, 2006, **88**, 183503.
38. M. S. Liu, Y. H. Niu, J. W. Ka, H. L. Yip, F. Huang, J. D. Luo, T. D. Kim and A. K. Y. Jen, *Macromolecules*, 2008, **41**, 9570-9580.
39. H. B. Wu, J. H. Zou, F. Liu, L. Wang, A. Mikhailovsky, G. C. Bazan, W. Yang and Y. Cao, *Adv. Mater.*, 2008, **20**, 696-702.
40. J. H. Zou, H. Wu, C. S. Lam, C. D. Wang, J. Zhu, C. M. Zhong, S. J. Hu, C. L. Ho, G. J. Zhou, H. B. Wu, W. C. H. Choy, J. B. Peng, Y. Cao and W. Y. Wong, *Adv. Mater.*, 2011, **23**, 2976-2980.
41. J. Li, P. I. Djurovich, B. D. Alleyne, I. Tsyba, N. N. Ho, R. Bau and M. E. Thompson, *Polyhedron*, 2004, **23**, 419-428.
42. B. H. Zhang, L. H. Liu, G. P. Tan, B. Yao, C. L. Ho, S. M. Wang, J. Q. Ding, Z. Y. Xie, W. Y. Wong and L. X. Wang, *J. Mater. Chem. C*, 2013, **1**, 4933-4939.

43. A. C. Grimsdale, K. L. Chan, R. E. Martin, P. G. Jokisz and A. B. Holmes, *Chem. Rev.*, 2009, **109**, 897-1091.
44. S. Tasch, E. J. W. List, O. Ekstrom, W. Graupner, G. Leising, P. Schlichting, U. Rohr, Y. Geerts, U. Scherf and K. Mullen, *Appl. Phys. Lett.*, 1997, **71**, 2883-2885.
45. Hoi
46. L. Yu, J. Liu, S. J. Hu, R. F. He, W. Yang, H. B. Wu, J. B. Peng, R. D. Xia and D. D. C. Bradley, *Adv. Funct. Mater.*, 2013, **23**, 4366-4376.
47. X. D. Niu, C. J. Qin, B. H. Zhang, J. W. Yang, Z. Y. Xie, Y. X. Cheng and L. X. Wang, *Appl. Phys. Lett.*, 2007, **90**. 203513.
48. C. V. Hoven, A. Garcia, G. C. Bazan and T. Q. Nguyen, *Adv. Mater.*, 2008, **20**, 3793-3810.
49. W. L. Ma, P. K. Iyer, X. Gong, B. Liu, D. Moses, G. C. Bazan and A. J. Heeger, *Adv. Mater.*, 2005, **17**, 274-277.
50. A. Kohnen, M. Irion, M. C. Gather, N. Rehmann, P. Zacharias and K. Meerholz, *J. Mater. Chem.*, 2010, **20**, 3301-3306.
51. G. L. Tu, Q. G. Zhou, Y. X. Cheng, L. X. Wang, D. G. Ma, X. B. Jing and F. S. Wang, *Appl. Phys. Lett.*, 2004, **85**, 2172-2174.
52. J. Luo, X. Z. Li, Q. Hou, J. B. Peng, W. Yang and Y. Cao, *Adv. Mater.*, 2007, **19**, 1113-1117.
53. B. H. Zhang, C. J. Qin, J. Q. Ding, L. Chen, Z. Y. Xie, Y. X. Cheng and L. X. Wang, *Adv. Funct. Mater.*, 2010, **20**, 2951-2957.
54. T. Nozawa, NEC announces OLED device with world's highest efficiency, Nikkei Electronics (2013), http://techon.nikkeibp.co.jp/english/NEWS_EN/20130307/269942 /. Accessed 7 Mar 2013.

# CHAPTER-2

## Efficient blue and white polymer light emitting diodes based on a well charge balanced, core modified polyfluorene derivative

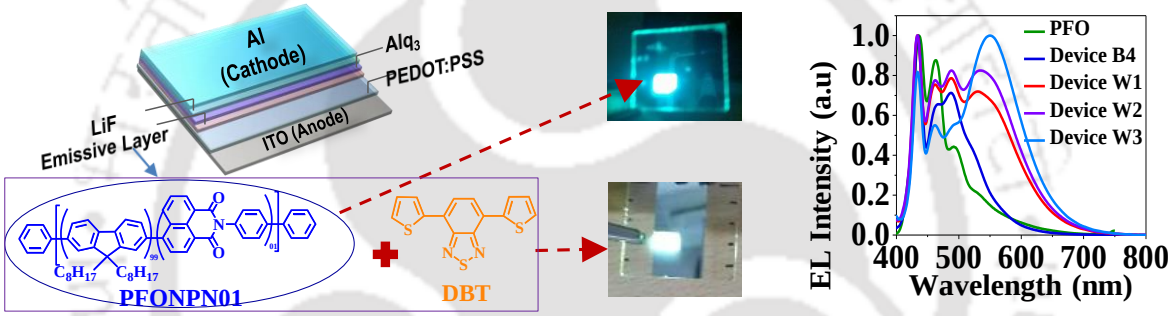


*Phys. Chem. Chem. Phys.,2016,18, 7389-7394*

# Efficient blue and white polymer light emitting diodes based on a well charge balanced, core modified polyfluorene derivative


## ***Abstract***

*"Fabrication of efficient blue and white polymer light-emitting diodes (PLEDs) using a well charge balanced, core modified polyfluorene derivative, poly[2,7-(9,90-dioctylfluorene)-co-N-phenyl-1,8-naphthalimide (99:01)] (PFONPN01), is presented. The excellent film forming properties as observed from the morphological study and the enhanced electron transport properties due to the inclusion of the NPN unit in the PFO main chain resulted in improved device properties. Bright blue light was observed from single layer PLEDs with PFONPN01 as an emissive layer (EML) as well as from double layer PLEDs using tris-(8-hydroxyquinoline) aluminum ($Alq_3$) as an electron transporting layer (ETL) and LiF/Al as a cathode. The effect of ETL thickness on the device performance was studied by varying the $Alq_3$ thickness (5 nm, 10 nm and 20 nm) and the device with an ETL thickness of 20 nm was found to exhibit the maximum brightness value of 11662 cd $m^{-2}$ with a maximum luminous efficiency of 4.87 cd $A^{-1}$. Further, by using this highly electroluminescent blue PFONPN01 as a host and a narrow band gap, yellow emitting small molecule, dithiophene benzothiadiazole (DBT), as a guest at three different concentrations (0.2%, 0.4% and 0.6%), WPLEDs with the ITO/PEDOT:PSS/emissive layer/$Alq_3$(20 nm)/LiF/Al configuration were fabricated and maximum brightness values of 8025 cd $m^{-2}$, 9565 cd $m^{-2}$ and 10180 cd $m^{-2}$ were achieved respectively. 0.4% DBT in PFONPN01 was found to give white light with Commission International de l'Echairage (CIE) coordinates of (0.31, 0.38), a maximum luminous efficiency of 6.54 cd $A^{-1}$ and a color rendering index (CRI) value of 70."*

# *Chapter 2*

## 2.1 Introduction

White organic light-emitting diodes (WOLEDs) are one of the most promising new lighting technologies emerging over the past few decades due to their versatility, low cost of production and ease of large area fabrication, and have potential applications in the field of full color displays and new generation lighting sources, providing a viable alternative to the existing technology.[1–6] To become an ideal source of white light, the output spectrum of OLEDs should cover the entire visible range (400–800 nm) and its spectral distribution should match that of the natural sunlight. To achieve this, the dominating approach is to combine the electroluminescence obtained from different materials, typically two or three. Significant improvement in the field of small molecule based WOLEDs has been made and their efficiencies have already surpassed those of the conventional incandescent and fluorescent lamps. However, small molecules are generally deposited using a vacuum deposition method, thus making them expensive for large area fabrication. On the contrary, due to the advantage of solution processability, polymer thin films can be easily made using less expensive methods such as spin coating and inkjet printing. Recently, several approaches to achieve WPLEDs have been reported, including solution-processed WPLEDs by doping small molecules in polymers,[7,8] polymer–polymer blending,[9,10] multilayer structure by incorporating orthogonal solvent[11] or by using cross linking polymers,[12] WOLEDs or WPLEDs based on the broad emission of exciplexes or excimers,[13] single emissive polymers with red, green and blue chromophores attached to their main backbone[14] or side chain[15] and so on. However, to realize bright white light, efficient blue light emitting materials are of utmost importance. Inspiringly, a significant amount of research has been carried out on the design and development of efficient blue PLEDs that are essential for high-quality displays and lighting sources. In this regard, conjugated polyfluorene (PF) was widely studied both as the emitting material in blue PLEDs as well as the host material in blended systems for realizing white light.[7,8,16] Polyfluorenes are well-known emissive materials for blue PLEDs and serve well for light emission and charge transfer due to their high luminescence efficiency, thermal stability, good processability and excellent film forming properties.[17] Unfortunately, they suffer from poor electron transport as compared to hole transport due to the presence of high density electron traps within thepolymer.[18] In order to achieve high

efficiency, it is, however, necessary to obtain a balanced charge transport behavior and confinement of electrons and holes inside the active layer. Several attempts have been made to improve the electron-transporting properties of polyfluorenes by incorporating electron-withdrawing moieties into the main or side chains of the polymers.[19–27] Recently, highly electroluminescent, well charge balanced polyfluorene copolymers were developed by incorporating the 1,8-naphthalimide (NPN) moiety into the polyfluorene main chain.[28,29] Herein, the fabrication of efficient blue polymer light emitting devices (PLEDs) using PFONPN01 as the active material is discussed. The excellent film forming properties along with the enhanced electron transport properties of PFONPN01 resulted in improved device properties. The device performance of PFONPN01 was then further improved by fabricating multilayer devices using $Alq_3$ as an electron transporting layer (ETL) with various thicknesses (0, 5, 10 and 20 nm) and using LiF/Al as a cathode. A maximum brightness value of 11662 cd $m^{-2}$ and a maximum current efficiency of 4.87 $cdA^{-1}$ were achieved. The high brightness and wide electroluminescence spectra in the blue-green region (400–550 nm) make PFONPN01 a suitable host material for realizing white light and therefore it was further utilized for fabrication of WPLEDs by doping it with a narrow band gap yellow dopant DBT.[30] In order to achieve white light, three different DBT concentrations (0.2%,0.4%and 0.6%) were added into a solution of PFONPN01 in chloroform and stirred for 30 minutes to ensure efficient doping. White light was obtained due to the blue emission from the PFONPN01 host polymer and simultaneous yellow emission originating from the suppressed singlet Förster energy transfer induced by low concentration DBT doping. The solution processed WPLEDs with a highest maximum luminous efficiency of 6.54 cd $A^{-1}$ and Commission International de l'Echairage (CIE) coordinates of (0.31, 0.38) were achieved for 0.4% DBT doped PFONPN01 with a color rendering index (CRI) value of 70.

## 2.2 Experimental

### 2.2.1 Materials and measurements

The π-conjugated poly[2,7-(9,90-dioctylfluorene)-co-N-phenyl-1,8naphthalimide (99:01)] (PFONPN01) and small molecule DBT used as emissive materials and $Alq_3$ used as the electron transport material were synthesized using previously reported methods[28,31,32]

and their structures are given in Fig. 2.1 (a). The other materials such as poly (3,4-ethylendioxythiophene): poly (styrene sulfonate) (PEDOT:PSS), LiF and aluminum (Al) were purchased from Sigma Aldrich. Atomic force microscopy images were taken using an Agilent5500-STM instrument. The UV-visible absorption spectra of DBT and the emission spectra of PFONPN01 were recorded on a Perkin-Elmer Lambda 35 spectrophotometer and on a Varian-Cary Eclipse spectrophotometer respectively.

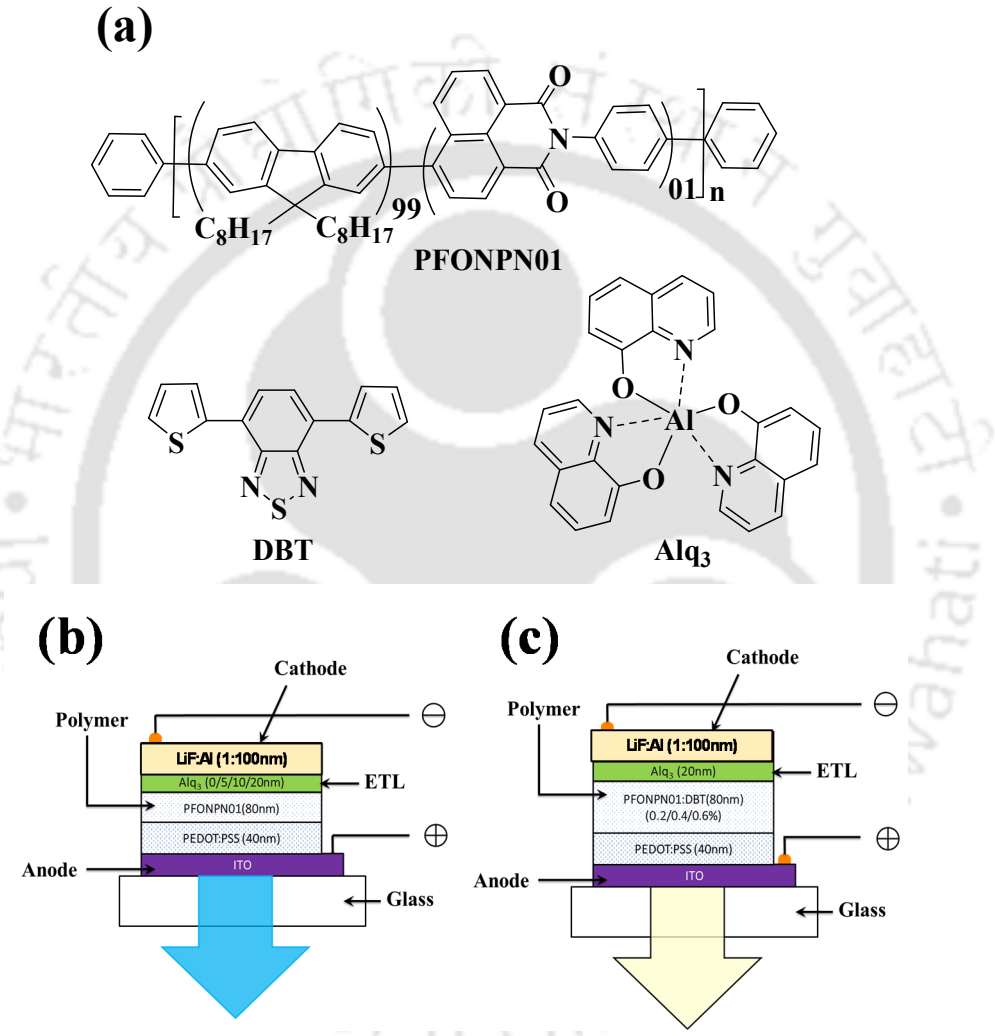


**Fig. 2.1** (a) The chemical structures of the materials used and (b) schematic of the device structure for blue PLEDs (c) schematic of the device structure for WPLEDs.

### 2.2.2 PLED fabrication and characterization

Fig. 2.1 (b) and (c) shows the schematic of the device structures used in this study. The PLED device configuration is composed of a pre-cleaned and pre-patterned indium tin oxide (ITO) as the transparent anode. Prior to device fabrication, the ITO surface was thoroughly cleaned in sequential ultrasonic baths of

2% soap solution, acetone and isopropanol, each for ten minutes at room temperature and then dried under argon gas. The ITO substrate was then treated using UV-ozone treatment for 30 min. After cleaning, a 40 nm thin layer of PEDOT:PSS as a hole injecting layer was spin-coated at 3000 rpm for 60 seconds followed by baking for 15 minute in an argon environment at 130 $^{o}$C. The emissive layer was then spin-coated above the PEDOT:PSS layer from chloroform solution to form a ~ 80 nm thick film. Five different types of emissive layers: pure PFO, PFONPN01, 0.2% DBT doped PFONPN01, 0.4% DBT doped PFONPN01 and 0.6% DBT doped PFONPN01 were studied. The emissive layer was annealed under an ambient atmosphere at 80 $^{o}$C for 30minutes to remove the residual solvent. After annealing, $Alq_3$ was thermally deposited over the emissive layer at a rate of 2 Å $s^{-1}$ for better electron injection. Finally, LiF and aluminium were thermally evaporated at a rate of 0.1Å $s^{-1}$ and 10 Å $s^{-1}$, respectively, at a base pressure of $10^{-6}$ mbar to form the cathode electrode. The active area of the diodes was 12 $mm^{-2}$. The thicknesses of di□erent layers of the PLEDs were measured using a Dektak 150 profilometer. The current density–voltage (J–V) characteristics of the fabricated PLEDs were measured using a Keithley 2400 source meter, whereas the luminance and the electroluminescence spectra were recorded using an LCS-100 integrated sphere. All the devices were fabricated and characterized under an argon atmosphere inside a glove box.

## 2.3 Results and discussion

### 2.3.1 Morphological studies

The performance and lifetime of a PLED are critically dependent on the properties of active materials and quality of their interfaces, and therefore the surface morphology of PFONPN01 polymer thin films was explored using atomic force microscopy (AFM) images. Fig. 2.2 shows the AFM images of the PFONPN01 thin films heated at various temperatures for 30 mins, ranging from 60 $^{o}$C to 100 $^{o}$C (Fig. 2.2 (a)–(c)) and DBT doped PFONPN01 thin films heated at 80 $^{o}$C (Fig. 2.2 (d)), deposited using a spin coating method. The thin films had very smooth and amorphous surfaces, with a root mean square (RMS) roughness of 1.573 nm, 0.550 nm and 0.774 nm for the 60 $^{o}$C, 80 $^{o}$C and 100 $^{o}$C heated films respectively. PFONPN01 was then doped with the DBT molecule and the AFM images of the thin film (heated at 80 $^{o}$C) show no aggregation, which means that DBT is dispersed homogenously in PFONPN01. The DBT doped PFONPN01 thin film shows a

root mean square (RMS) roughness of 0.447 nm. 80 $^{o}$C annealing was selected for device fabrication because at this annealing temperature, the emissive layer film morphology was found to be the best.

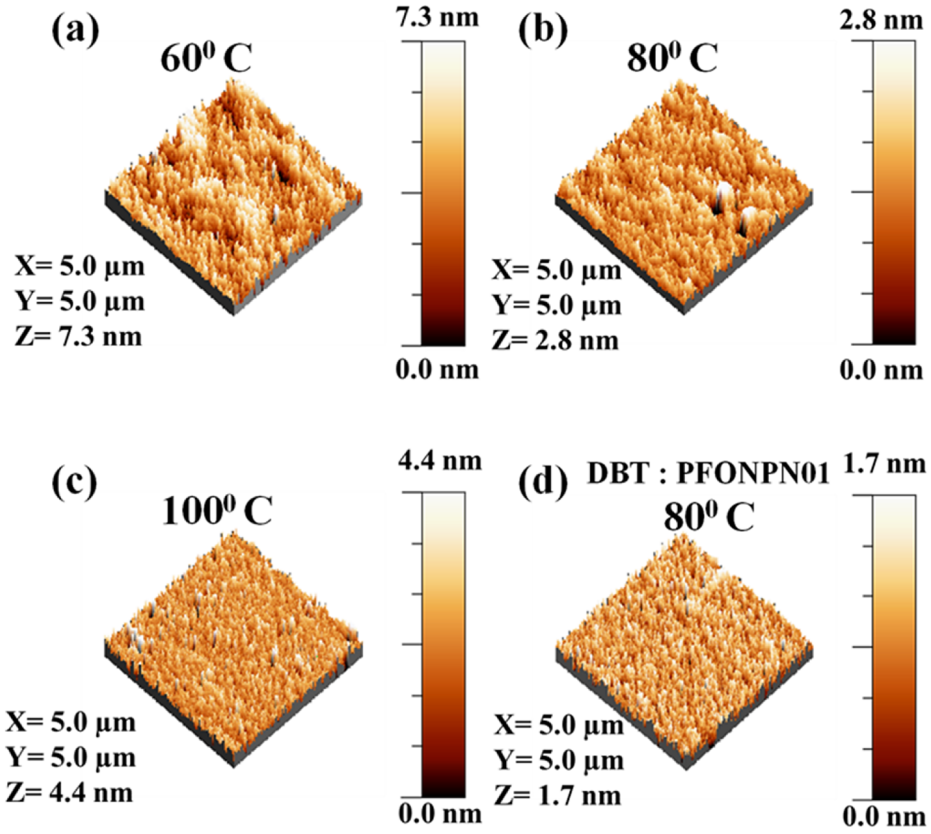


**Fig. 2.2** AFM images of the PFONPN01 thin films heated at various temperatures, (a) 60 °C, (b) 80 °C, (b) 100 °C and (d) DBT doped PFONPN01 thin films heated at 80 °C.

### 2.3.2 Blue PLEDs

The blue emitting host plays a significant role in determining the properties of a host–guest system emitting white light. The efficiency of such a system is highly affected by the electron and hole transporting properties of the polymer host as well as the efficiency of charge injection from the cathode side. Here, single layer PLEDs were fabricated using pure PFO and PFONPN01 as the emissive layer (EML) in the ITO/PEDOT:PSS (40 nm)/ PFONPN01(80 nm)/LiF(1.0 nm)/Al(100 nm) (device B1) configuration. Fig. 2.3 (a) and Fig. 2.3 (b) shows the current density vs. voltage (J–V) and brightness vs. current density (B–J) curves of the single layer devices respectively. From these curves, it was observed that the maximum brightness value of device B1 improves significantly to 5636 cd m$^{-2}$ as compared to 2328 cd m$^{-2}$ of PFO (more than 2 times).

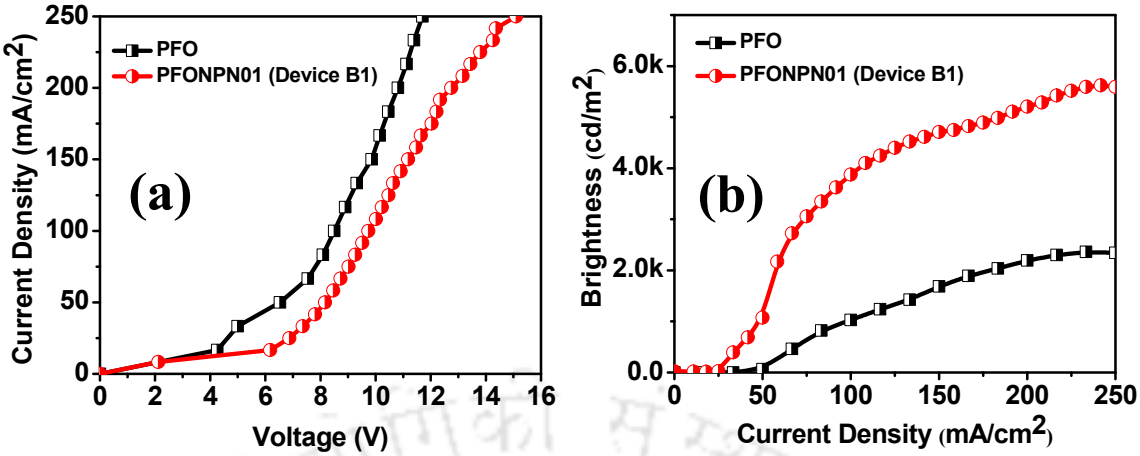


**Fig. 2.3** Current density vs. voltage (J-V) (a) brightness vs. current density (B-J) and (b) curves of the single layer Blue PLEDs.

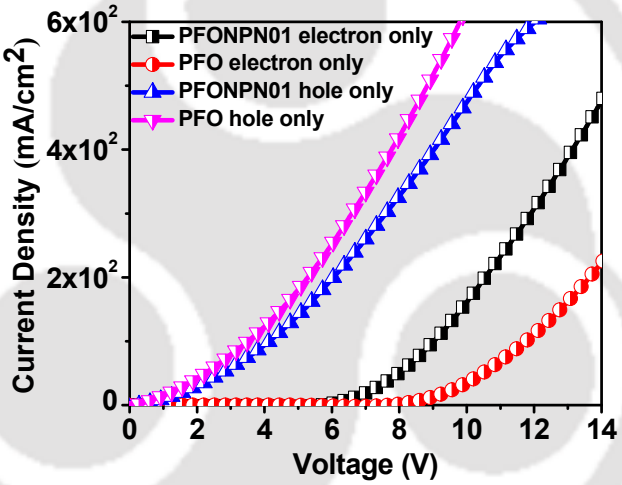


**Fig. 2.4** Current density vs. voltage (J-V) curves of PFO and PFONPN01 based hole only and electron only devices, film thickness = 80 nm.

To understand this improvement in the device properties, an electron dominated device using structure ITO/Al (40 nm)/polymer (80 nm)/LiF(1.0 nm)/Al(100 nm) and an hole dominated device using structure ITO/PEDOT:PSS(40 nm)/ polymer(80 nm)/$MoO_3$(15 nm)/Al(100 nm) for both PFO and PFONPN01 were fabricated and the curves are shown in Fig. 2.4. The hole current in the case of PFONPN01 is found to be little less as compared to that of PFO, however, there has been more than two-fold improvement in electron current in the case of PFONPN01 as compared to that of PFO. Therefore, the high device performance of PFONPN01 as compared to that of PFO can be

attributed to the enhanced electron transport properties of the PFONPN01 copolymer due to the high electron affinity of the NPN moiety.

To further improve the device performance, multilayer PLEDs using $Alq_3$ as the electron transporting layer were fabricated. The thickness of the $Alq_3$ layer was varied for optimum device performance (5 nm, 10 nm and 20 nm for devices B2, B3 and B4 respectively). Fig. 2.5 (a) and Fig. 2.5 (b) shows the current density vs. voltage (J–V) and brightness vs. current density (B–J) curves of the multilayer devices respectively. The luminous efficiency vs. current density (LE–J) curves of all the single as well as multilayer devices are shown in Fig. 2.6 and the key device properties are summarized in Table 2.1. The maximum brightness value and LE of multilayer devices B2, B3 and B4 are found to be 9649 cd $m^{-2}$ and 4.27 cd $A^{-1}$, 11479 cd $m^{-2}$ and 4.63 cd $A^{-1}$ and 11662 cd $m^{-2}$ and 4.87 cd $A^{-1}$ respectively.

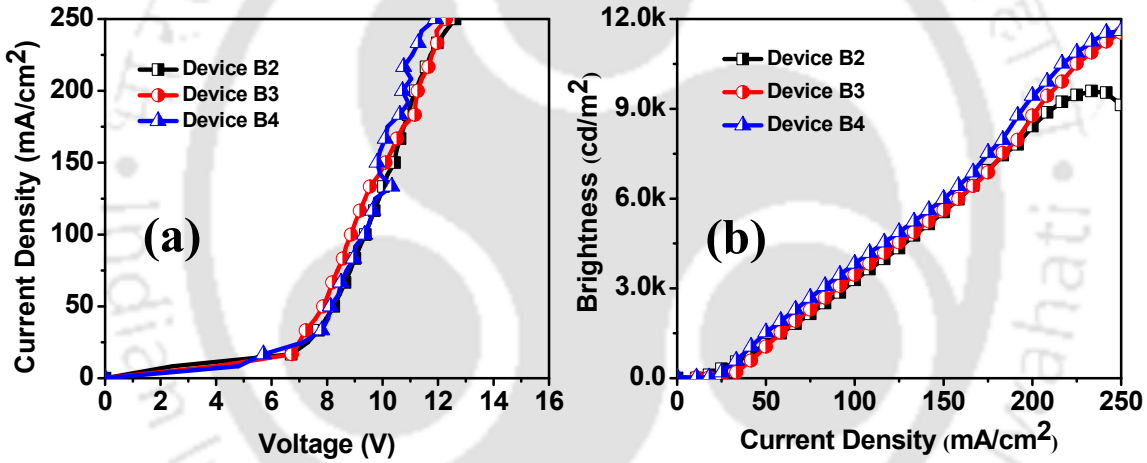


**Fig. 2.5** Current density vs. voltage (J-V) (a) brightness vs. current density (B-J) and (b) curves of the multilayer Blue PLEDs.

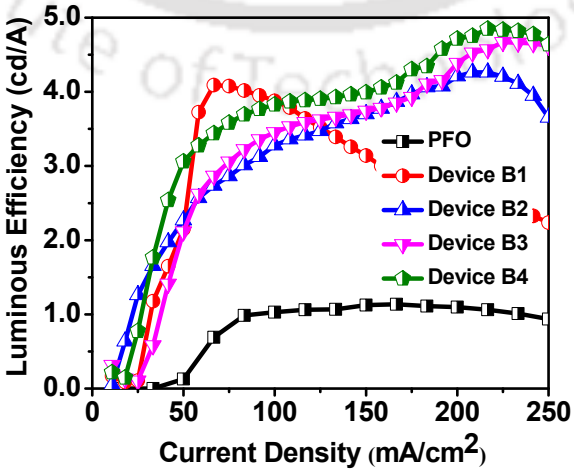


**Fig. 2.6** The luminous efficiency vs. current density (LE–J) curves of blue PLEDs.

**Table 2.1** Key device properties of the fabricated blue PLEDs.

| Device | Onset Voltage (V) | Maximum Brightness B (cd/m$^2$) | Luminous Efficiency LE[a] (cd/A) | Power Efficiency[a] PE (lm/W) | CIE coordinates (x,y) |
|---|---|---|---|---|---|
| **PFO** | 6.4 (6.48, 0.13) | 2328 (2284, 51.87) | 1.13 (1.10, 0.03) | 0.25 (0.22, 0.03) | 0.15, 0.14 |
| **B1** | 7.2 (7.26, 0.05) | 5636 (5599, 29.95) | 4.21 (4.16, 0.06) | 0.94 (0.86, 0.05) | 0.15, 0.22 |
| **B2** | 7.3 (7.42, 0.11) | 9649 (9488, 132.8) | 4.27 (4.17, 0.09) | 0.96 (0.89, 0.04) | 0.16, 0.22 |
| **B3** | 6.8 (6.98, 0.18) | 11479 (10951, 513.3) | 4.63 (4.47, 0.13) | 1.04 (1.00, 0.03) | 0.15,0.23 |
| **B4** | 7.1 (7.18, 0.08) | 11662 (11286, 308.8) | 4.87 (4.78, 0.06) | 1.10 (1.05, 0.03) | 0.16, 0.23 |

[a]Maximum value. Values in the bracket are average value of 10 devices and standard deviation.

From these results, it was observed that the maximum brightness value of devices B2, B3 and B4 is almost two times that of device B1. The increase in this device brightness can be attributed to the addition of $Alq_3$ as the ETL as well as the better electron injection from the $Alq_3$/LiF/Al cathode. The difference in hole mobility between PFONPN01 and $Alq_3$ results in hole accumulation at the EML–ETL interface. As a result, shifting of the recombination zone away from the cathode occurs. Also, the thin layer of LiF, deposited between $Alq_3$ and Al, reacts with Al and forming Li atoms and $AlF_3$ compounds. The Li atoms then donate electrons to $Alq_3$ molecules resulting in the formation of $Alq_3$ anions that effectively increase electron injection by forming good contact with Al cathodes,[33–35] thereby increasing the device brightness. The ETL thickness is also found to affect the device performance by controlling the relative distribution of electrons and holes in the active layer. The brightness value is found to increase with increasing ETL thickness from 5 to 20 nm. Device B4 with an ETL thickness of 20 nm is found to exhibit better properties among all the devices and hence an ETL thickness of 20 nm is used for making WPLEDs.

### 2.3.3 White PLEDs

Fig. 2.7 (a) shows the solid-state photoluminescence (PL) spectra of PFONPN01 and the DBT chromophore used for realizing white light. The emission from PFONPN01 covers the range of 400–550 nm whereas the emission from the DBT molecule covers the range of 500–650 nm of the visible region, thus making them a suitable combination for realizing white light. However, in order to confirm energy transfer from PFONPN01 to the

DBT chromophore, the solid-state UV-visible absorption spectrum of the DBT molecule was also recorded and is shown in Fig. 2.7 (b) along with the PL spectra of PFONPN01. As shown in Fig. 2.7 (b), the absorption spectrum of DBT shows two peaks centred at around 306 nm and 446 nm, whereas the emission spectrum of PFONPN01 shows two peaks centred at around 415 nm and 441 nm. The excellent overlap between the PL spectrum of the PFONPN01 solid film and the absorption spectrum of DBT suggests efficient Förster energy transfer from the PFONPN01 host to the DBT guest. All these spectra were measured by spin casting DBT and PFONPN01 over a glass substrate. The film thickness used was ~ 80 nm.

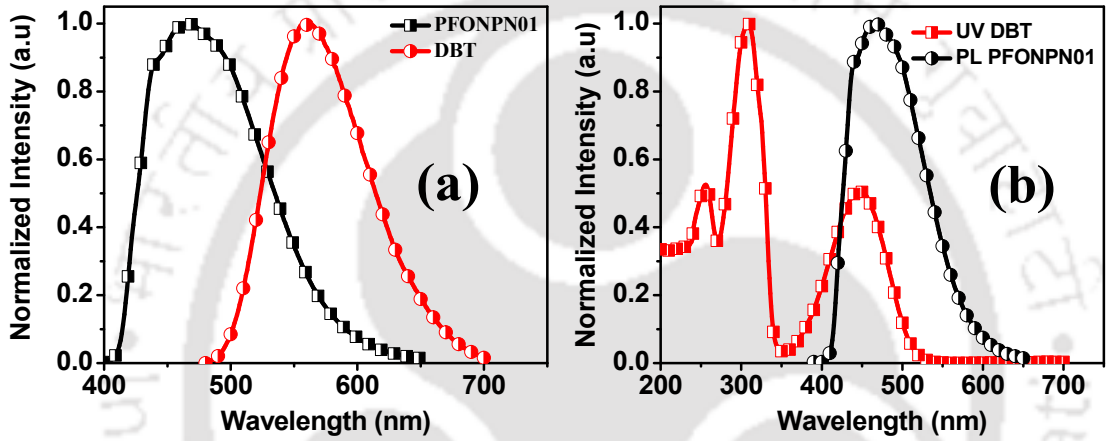


**Fig. 2.7** (a) The solid-state PL spectra of PFONPN01 and DBT and (b) the solid-state UV-visible absorption spectra of DBT and the solid-state PL spectra of PFONPN01 polymer.

In order to achieve white light, PFONPN01 was doped with di□erent DBT concentrations in device W1 (0.2%), in device W2(0.4%) and in device W3(0.6%). Fig. 2.8 (a) and Fig. 2.8 (b) shows the current density vs. voltage (J–V) and brightness vs. current density (B–J) and curves of the fabricated devices. The key properties of all these WPLEDs are listed in Table 2.2. All the devices start emitting light at a voltage of approximately 5 V and are found to be highly bright. Device W3 exhibits a maximum brightness value of 10180 cd $m^{-2}$, whereas devices W1 and W2 possess a maximum brightness value of 8025 cd $m^{-2}$ and 9565 cd $m^{-2}$ respectively. The increase in the respective brightness of the WPLEDs as compared to that of the host material is due to the doping of narrow band gap DBT molecules. The addition of DBT introduces trap energy states inside the emissive

layers that act as a hole trap, resulting in a decrease in the hole mobility and current density.

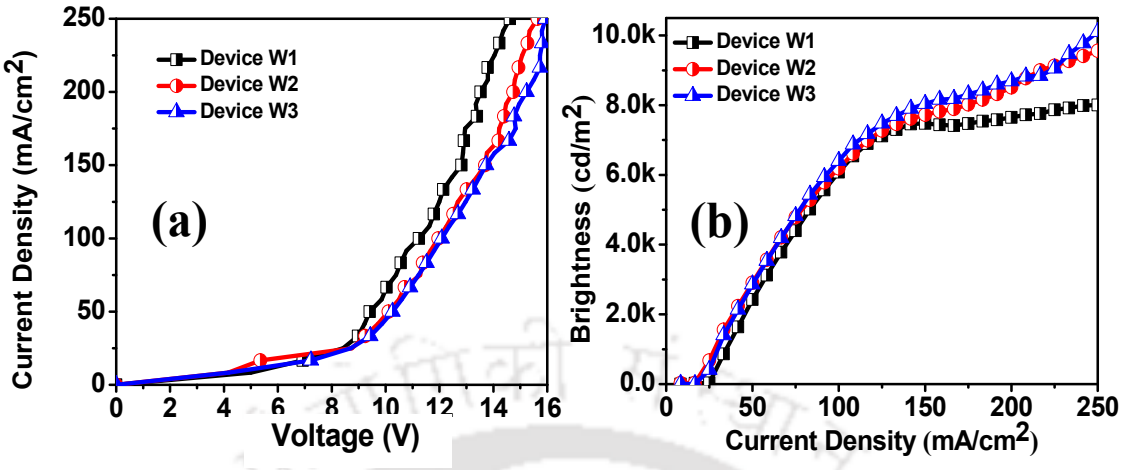


**Fig. 2.8** Current density vs. voltage (J-V) (a) brightness vs. current density (B-J) and (b) curves of the white PLEDs.

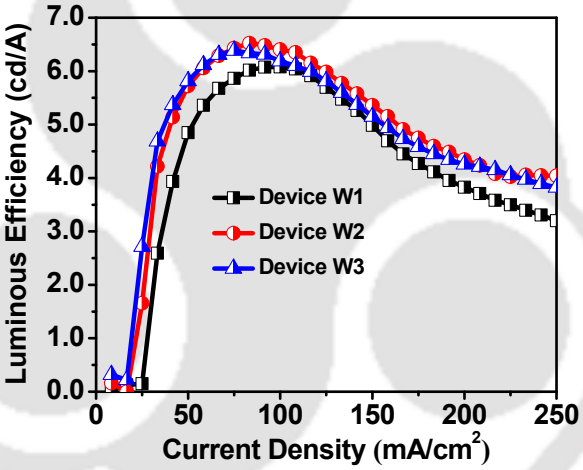


**Fig. 2.9** The luminous efficiency vs. current density (LE–J) curves of WPLEDs.

**Table 2.2** Key device properties of the fabricated white PLEDs.

| Device | Onset Voltage (V) | Maximum Brightness B ($cd/m^2$) | Luminous Efficiency[a] LE (cd/A) | Power Efficiency[a] PE (lm/W) | CIE Coordinate (x,y) at 10V | CRI |
|---|---|---|---|---|---|---|
| **W1** | 8.16 (8.27, 0.09) | 8025 (7814, 176.2) | 6.07 (5.78, 0.36) | 1.73 (1.66, 0.06) | 0.26, 0.32 | 59 |
| **W2** | 8.56 (8.64, 0.06) | 9565 (9205, 237.1) | 6.54 (6.31, 0.21) | 1.87 (1.80, 0.05) | 0.31, 0.38 | 70 |
| **W3** | 8.90 (8.99, 0.07) | 10180 (9910, 213.3) | 6.37 (6.13, 0.20) | 1.81 (1.73, 0.06) | 0.30, 0.40 | 64 |

[a]Maximum value. Values in the bracket are average value of 10 devices and standard deviation.

The luminous efficiency vs. current density (LE–J) curves of all the devices are shown in Fig. 2.9. Device W2 is found to be the most efficient with a maximum luminous efficiency of 6.54 cd $A^{-1}$, whereas devices W1 and W3 have a maximum luminous efficiency of 6.07 cd $A^{-1}$ and 6.37 cd $A^{-1}$ respectively. It was found that the device efficiency remains as high as ~ 3.25 cd $A^{-1}$ with a luminance of over ~8025 cd $m^{-2}$ for device W1, ~ 4.07 cd $A^{-1}$ with a luminance of over ~ 9565 cd $m^{-2}$ for device W2 and ~ 3.85 cd $A^{-1}$ with a luminance of over ~ 10167 cd $m^{-2}$ for device W3 at a current density of 250 mA $cm^{-2}$.

### 2.3.4 Electroluminescence properties

Fig. 2.10 (a) shows the electroluminescence spectra of PFO, devices B4, W1, W2 and W3 taken at 10 V, whereas Fig. 2.10 (b) shows the chromaticity diagram representing the CIE coordinates of the fabricated PLEDs.

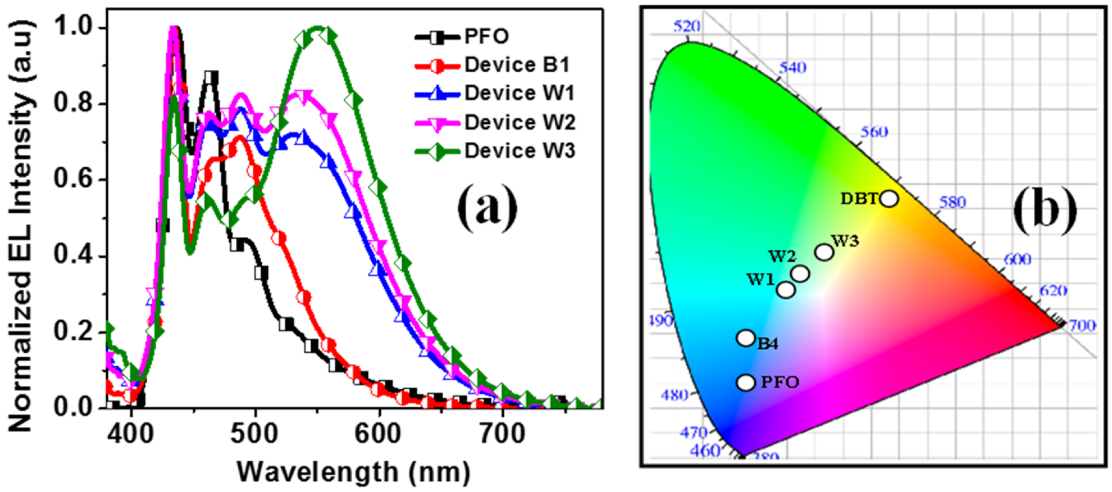


**Fig. 2.10** The electroluminescence spectra of PFO, devices B4, W1, W2 and W3 taken at 10 V (a) and the chromaticity diagram representing the CIE coordinates of the fabricated PLEDs (b).

In EL spectra, we observed three peaks in the case of PFO centered at 436 nm, 463 nm and 493 nm. Another low intensity peak at around 530 nm is also observed which can be due to the excimers, interface species (exciplexes etc.) or keto defects.[36–39] However, in the case of the PFONPN01 copolymer (device B4), the peak intensity at 464 nm gets reduced and the peak at 493 nm gets completely quenched. Instead, we get a peak at 486 nm. Hence, we assume that this peak is the result of the partial energy transfer from the PFO to the NPN unit. The EL spectra of devices W1, W2 and W3 show an additional peak

centered at around 550 nm with CIE coordinates of (0.26, 0.32), (0.31, 0.38) and (0.30, 0.40) respectively. The peak at around 550 nm can be attributed to the emission originating from the DBT molecule due to the Förster type energy transfer from the host matrix PFONPN01 to the dopants. The intensity of this peak is found to be altered with the DBT doping concentration. Device W2 with a 0.4% DBT doped PFONPN01 emissive layer is found to emit white light closest to the pure (0.33, 0.33) with a CIE coordinate of (0.31,0.38).

## 2.4 Conclusions

In summary, efficient blue PLEDs based on a well charge balanced, core modified copolymer of polyfluorene, poly[2,7-(9,90-dioctylfluorene)-co-N-phenyl-1,8-naphthalimide (99:01)] (PFONPN01) were fabricated. Bright blue light was observed from single layer PLED devices with PFONPN01 as an emissive layer (EML) and the maximum brightness value and luminous efficiency were found to increase almost 2 times and 4 times, respectively, as compared to that of pure polyfluorene which can be attributed to the enhanced electron transport resulting from the high electron affinity of the NPN unit. To improve the brightness value, double layer PLED devices were also fabricated using tris-(8-hydroxyquinoline) aluminum ($Alq_3$) as an electron transporting layer (ETL) and LiF/Al as a cathode and the effect of ETL thickness on device performance was optimized by varying the $Alq_3$ thickness (5 nm, 10 nm and 20 nm). PLEDs with an ETL thickness of 20 nm were found to exhibit the highest maximum brightness value of 11662 cd $m^{-2}$ with a maximum luminous effciency of 4.87 cd $A^{-1}$. PFONPN01 was then used as a host and WPLEDs were fabricated using a narrow band gap, yellow emitting small molecule dithiophene benzothiadiazole (DBT) as a guest. White light was obtained due to the blue emission from the PFONPN01 host polymer and simultaneous yellow emission originating from the suppressed singlet Förster energy transfer induced by the low-concentration DBT doping. PFONPN01 was doped with three different concentrations (0.2%, 0.4% and 0.6%) of DBT and maximum brightness values of 8025 cd $m^{-2}$, 9565 cd $m^{-2}$ and 10180 cd $m^{-2}$ were achieved respectively. 0.4% DBT in PFONPN01 was found to give white light closest to the pure with Commission International de l'Echairage (CIE) coordinates of (0.31,0.38), a highest maximum luminous efficiency of 6.54 cd $A^{-1}$ and a color rendering index (CRI) value of 70.

## 2.5 References


1. J. Kido, K. Hongawa, K. Okuyama, and K. Nagai, *Appl. Phys. Lett.,* 1994, **64**, 815-817.
2. B. W. D'Andrade and S. R. Forest, *Adv. Mater.,* 2004, **16**, 1585-1595.
3. M. C. Gather, A. Kohnen, and K. Meerholz, *Adv. Mater.*, 2011, **23**, 233-248.
4. K. T. Kamtekar, A. P. Monkman, and M. R. Bryce, *Adv. Mater.,* 2010, **22**, 572-582.
5. S. Reineke, M. Thomschke, B. Lussem, and K. Leo, *Rev. Mod. Phys.,* 2013, **85**, 1245-1293.
6. Y. L. Chang and Z. H. Lu, *J. of Display Technol.,* 2013, **9**, 459-468.
7. J. H. Kim, P. Herguth, M. S. Kang, A. K-Y. Jen, Y. H. Tseng, and C.-F. Shu, *Appl. Phys. Lett.,* 2004, **85**, 1116-1118.
8. Q. Xu, H. M. Duong, F. Wudl, and Y. Yang, *Appl. Phys. Lett.,* 2004, **85**, 3357-3359.
9. J. S. Huang, G. Li, E. Wu, Q. F. Xu, and Y. Yang, *Adv. Mater.,* 2006, **18**, 114-117.
10. J. F. de Deus, G. C. Faria, E. T. Iamazaki, R. M. Faria, T. D. Z. Atvars, and L. Akcelrud, *Org. Electron.,* 2011, **12**, 1493-1504.
11. X. Gong, S. Wang, D. Moses, G. C. Bazan, and A. J. Heeger, *Adv. Mater.,* 2005, **17**, 2053-2058.
12. A. Kohnen, M. Irion, M. C. Gather, N. Rehmann, P. Zacharias, and K. Meerholz, *J. Mater. Chem.,* 2010, **20**, 3301-3306.
13. M. Mazzeo, D. Pisignano, F. Della Sala, J. Thompson, R. I. R. Blyth, G. Gigli, R. Cingolani, G. Sotgiu, and G. Barbarella, *Appl. Phys. Lett.,* 2003, **82**, 334-336.
14. J. Luo, X. Z. Li, Q. Hou, J. B. Peng, W. Yang, and Y. Cao, *Adv. Mater.,* 2007, **19**, 1113-1117.
15. B. H. Zhang, C. J. Qin, J. Q. Ding, L. Chen, Z. Y. Xie, Y. X. Cheng, and L. X. Wang, *Adv. Funct. Mater.,* 2010, **20**, 2951-2957.
16. J. S.Huang, W. J.Hou, J. H. Li, G. Li, and Y. Yang, *Appl. Phys. Lett*. 2006,**89,** 133509-133509.
17. G. Klarner, J. I. Lee, M. H. Davey, and R. D. Miller, *Adv. Mater.,* 1999, **11**, 115-119.

18. A. Kadashchuk, R. Schmechel, H. von Seggern, U. Scherf, and A. Vakhnin, *J. Appl. Phys.,* 2005, **98**, 024101(1)- 024101(8).
19. J. L. Kim, H. N. Cho, J. K. Kim, and S. I. Hong, *Macromolecules* 1999, **32**, 2065-2067.
20. J. L. Kim, J. K. Kim, H. N. Cho, D. Y. Kim, C. Y. Kim, and S. I. Hong, *Macromolecules* 2000,**33**, 5880-5885.
21. J. L. Kim, J. K. Kim, H. N. Cho, D. Y. Kim, C. Y. Kim, andS. I. Hong, *Synthetic Met.* 2000,**114**, 97-100.
22. A. Donat-Bouillud, I. Levesque, Y. Tao, M. D'Iorio, S. Beaupre, P. Blondin, M. Ranger, J. Bouchard, and M. Leclerc, *Chem. Mater.,* 2000,**12**, 1931-1936.
23. S. Becker, C. Ego, A. C. Grimsdale, E. J. W. List, D. Marsitzky, A. Pogantsch, S. Setayesh, G. Leising, andK. Mullen, *Synthetic Met.* 2001**, 125**, 73-80.
24. X. W. Zhan, Y. Q. Liu, X. Wu, S. Wang, and D. B. Zhu, *Macromolecules* 2002,**35**, 2529-2537.
25. Q. Peng, Z. Y. Lu, Y. Huang, M. G. Xie, D. Xiao, and D. C. Zou, *J. Mater. Chem.,* 2003, **13**, 1570-1574.
26. Q. Peng, Z. Y. Lu, Y. Huang, M. G. Xie, S. H. Han, J. B. Peng, and Y. Cao, *Macromolecules* 2004, **37**, 260-266.
27. X. L. Yang, X. B. Xu, andG. J. Zhou, *J. Mater. Chem. C.* 2015,**3**, 913-944.
28. P. Gopikrishna, D. Das, and P. K. Iyer, *J. Mater. Chem. C*. 2015, **3**, 9318-9326.
29. J. Liu, Q. Zhou, Y. Cheng, Y. Geng, L. Wang, D. Ma, X. Jing and F. Wang, *Adv. Funct. Mater.* 2006, **16**, 957-965.
30. S. Fan, M. Sun, J. Wang, W. Yang, and Y. Cao, *Appl. Phys. Lett*. 2007, **91**, 213502.
31. U. Lemmer, S. Heun, R. F. Mahrt, U. Scherf, M. Hopmeier, U. Siegner, E. O. Gobel, K. Müllen, and H. Bassler, *Chem. Phys. Lett*. 1995, **240**, 373-378.
32. E. J. W. List, R. Guentner, P. S. de Freitas, and U. Scherf, *Adv. Mater*. 2002, **14**, 374-378.
33. Q. Hou, Y. S. Xu, W. Yang, and M. Yuan, J. B. Peng, Y. Cao, *J. Mater. Chem*. 2002, ***12***, 2887-2892.
34. J. Wang, K. D. Oyler, and S. Bernhard *Inorg. Chem*. 2007, **46**, 5700-5706.
35. C. I. Wu, G. R. Lee, and T. W. Pi, *Appl. Phys. Lett.* 2005, **87**, 212108.

36. H. Heil, J. Steiger, S. Karg, M. Gastel, H. Ortner, H.von Seggern, and M. Stossel, *J. Appl. Phys.* 2001, **89**, 420-424.
37. K. Narayan, S. Varadharajaperumal, G. M. Rao, M. M. Varma, and T. Srinivas, *Curr. Appl. Phys.* 2013, **13**, 18-25.
38. U. Scherf, and E. J. W. List, *Adv. Mater.* 2002, **14**, 477-487.
39. A. P. Kulkarni, X. X. Kong, and S. A. Jenekhe, *J. Phys. Chem. B*. 2004, **108**, 8689-8701.

# CHAPTER-3

## White polymer light emitting diodes based on PVK: effect of electron injection barrier on transport property, electroluminescence and controlling the electroplex formation

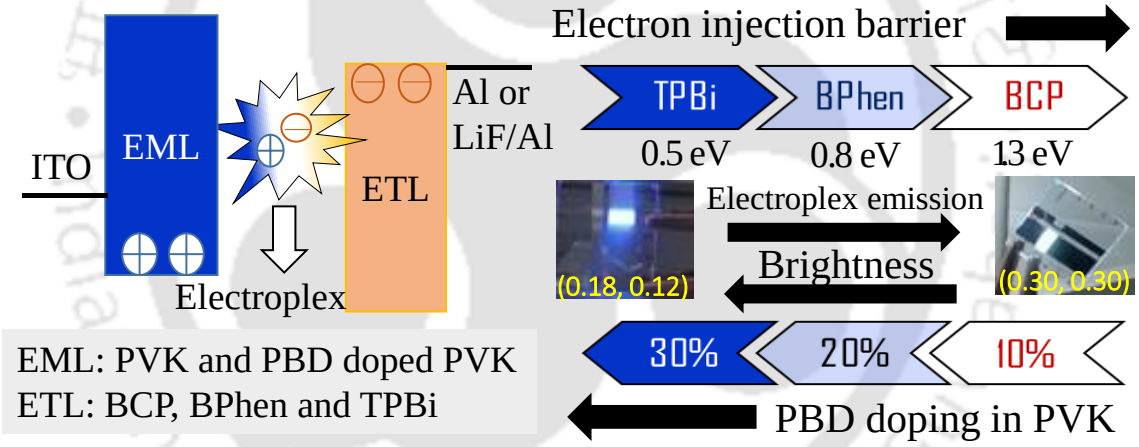


*Phys. Chem. Chem. Phys., 2016, 18, 33077-33084*

# *Chapter 3*

# White polymer light emitting diodes based on PVK: effect of electron injection barrier on transport property, electroluminescence and controlling the electroplex formation


## ***Abstract***

*"The effects of the electron injection barrier on the charge transport, brightness and the electroluminescence (EL) properties of polymer light emitting diodes (PLEDs) with poly(9-vinylcarbazole) (PVK) as an emissive layer have been studied. By using Al and LiF/Al as the cathode in single layer PLEDs and diverse electron transporting layers (ETLs) such as 2,9-dimethyl-4,7-diphenyl-1,10-phenanthroline (BCP), 4,7-diphenyl-1,10phenanthroline (BPhen) and 2,20,200-(1,3,5-benzinetriyl)-tris(1-phenyl-1-H-benzimidazole) (TPBi) in the case of multilayer PLEDs, the charge transport, brightness, color tuning and the EL properties of the devices were drastically modified. The energy barrier for electrons affects the electron current flowing through the device, thereby affecting the operating voltage and the brightness of the PLEDs. The PLEDs with TPBi as the ETL possess the lowest injection barrier and give the maximum brightness of 426.24 cd $m^{-2}$. The electron injection barrier is also found to play a major role in defining the EL spectra of the PLEDs. A larger injection barrier gives rise to electroplex formation in the EML–ETL interface of the PLEDs and an additional peak at ~ 605 nm was observed in the EL spectrum. As a result, a near white emission with CIE coordinates of (0.30, 0.30) and (0.25, 0.23) at 20 V was obtained from devices with BCP and BPhen as ETLs. Furthermore, PVK doped with 2-phenyl-5-(4-biphenylyl)-1,3,4-oxadiazole (PBD) at 10, 20 and 30 wt% ratios modified the electron transport nature of PVK and had a remarkable influence on the aforesaid properties, especially on the electroplex formation."*

# *Chapter 3*

## 3.1 Introduction

The discovery of organic light emitting diode (OLED) using Tris(8-hydroxyquinolinato) aluminum ($Alq_3$) as emissive layer by Tang in 1987[1] established a new era of research in the field of organic electronics. Three years later, it was demonstrated by Burroughs et al. that not only small molecules but polymers can also be used as emissive materials in organic light emitting diode.[2] Since then, polymer light emitting diodes (PLEDs) have been in prime focus. They seize the advantages of having high mechanical flexibility, low production cost and ease of large area fabrication, for which they can have potential applications in the field of display technology and solid state lighting.[3-10] Considerable amount of research has been dedicated in developing new conjugated polymers (CPs) and till date a variety of CPs have been reported as emissive layers in PLEDs to exhibit efficient electroluminescence (EL).[11-14] Numerous studies on organic light-emitting diodes (OLEDs) have been reported that showed very different ELs in contrast to the characteristics emission of the emissive materials.[15-20,] Long-wavelength emission bands have often been observed in the EL spectra of OLEDs, which are mainly due to the emission from the recombination of the holes and electrons residing in two adjacent molecules. If the two molecules are same, it may lead to the formation of excimers or electromers.[21] On the other hand, when the two molecules are different, the recombination may result in the formation of exciplexes or electroplexes.[22-24,] Electroplex is generally used to define the excited species that can be seen only in the EL spectra of a material but is absent in its photoluminescence (PL) spectra. It plays an important role in tuning the emission color of PLEDs and is used to generate white light.[25-29,]

PVK is a widely used polymer,[30-33] that has an excellent film forming property and emits in the blue region. It has been widely used as an emissive layer in blue emitting PLEDs[34,35] and to generate white light by using the electroplex emission.[25,36] Yet, the effect of electron injection barrier and the electron transport property of PVK on the charge transport, brightness and electroplex formation in PVK based PLEDs have not been widely studied.[25,36-39] In this chapter, we have fabricated single as well as multilayer PLEDs using different ETLs possessing different electron injection barrier and carefully studied and discussed its effect on the charge transport, brightness and the EL properties, especially on the electroplex

formation. PVK has a good hole transport ability but a poor electron transport property which is considered as one of its disadvantages. Thus, an electron transport material such as PBD has been doped with PVK in order to enhance its electron transport property. The effect of doping PBD on the overall modification in the charge transport, brightness and EL properties of PVK based PLEDs have also been investigated herein. The intensity of the electroplex emission was found to be controlled by the electron injection barrier and the electron transporting property of PVK as a significant observation in this study.

## 3.2 Experimental

Fig. 3.1 shows the chemical structures of the materials used in this study. All the materials were purchased from Sigma Aldrich and used as received.

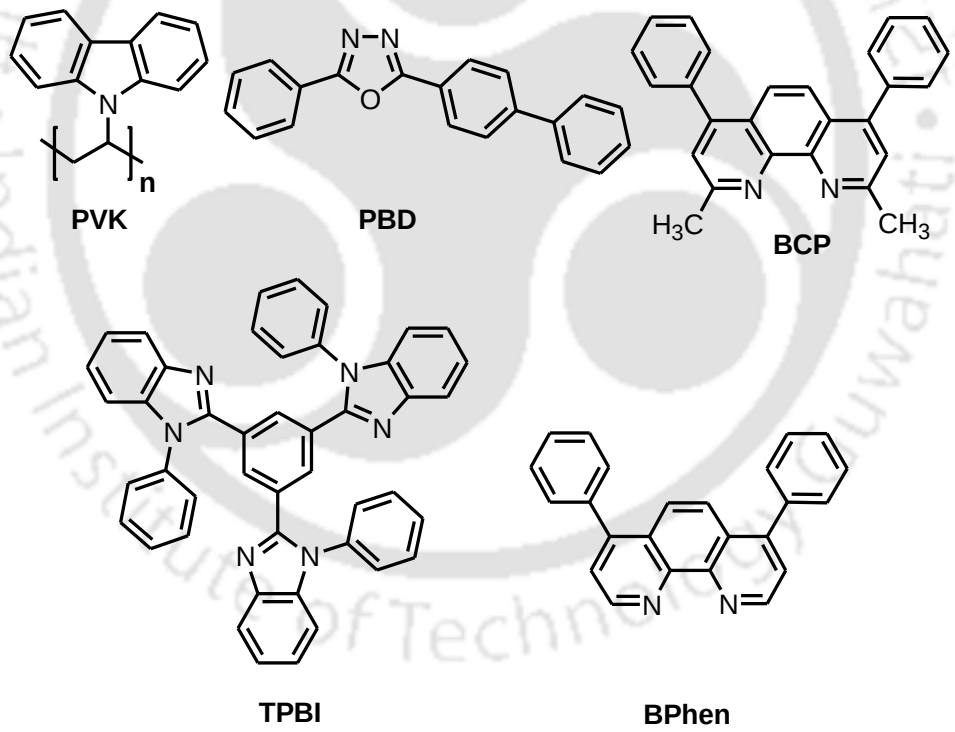


**Fig. 3.1** Chemical structures of PVK, PBD, BCP, TPBi and BPhen.

ITO substrates with a sheet resistance of 20 ohm/cm (Sigma Aldrich) were used as transparent anodes after patterning, using chemical etching technique. The patterned ITO substrates were cleaned thoroughly in sequential ultrasonic baths of soap solution, Millipore water, acetone and isopropanol, each for ten minutes at

room temperature followed by 30 min of UV-Ozone treatment. Both undoped and doped PVK thin films were deposited onto the ITO substrates by spin coating technique from a chlorobenzene solution. In case of doped PVK thin films, separate solution of PVK and PBD were made in chlorobenzene solution and then PBD solution was mixed to the PVK solution to get three different doping concentrations (10%, 20% and 30%). The mixed solutions were then stirred for 30 min to ensure efficient doping. The as prepared thin films were then annealed at 80°C for 30 min to remove the residual solvents. The three different ETL viz. BCP, BPhen and TPBi, interfacial layer LiF and Cathode material Al were thermally evaporated at a base pressure of $10^{-6}$ mbar. The active area of the PLEDs was 24 $mm^2$. The current density–voltage (J–V) characteristics of the PLEDs were measured using a Keithley 2400 source meter, whereas the brightness–voltage (B–V) characteristics and the EL spectra were recorded using Konica Minolta CS 2000 Spectroradiometer. All characterizations were done inside glove box under argon atmosphere.

## 3.3 Results and discussion

### 3.3.1 Morphological studies

The surface morphology of PVK and PBD doped PVK thin films was explored using atomic force microscopy (AFM) images. Fig. 3.2 shows the AFM images of the PVK thin films spin coated from a solution of chloroform (a), chlorobenzene (b), dichlorobenzene (c) and p-xylene (d) respectively and heated at 80 $^oC$ for 30 minutes. The PVK thin films spin coated from chloroform solution was found to be not so good with a root mean square (RMS) roughness of 2.059 nm. Also, the films were found to suffer from the pinhole problem. The PVK thin films spin coated from chlorobenzene, dichlorobenzene and p-xylene solution were found to have smooth surfaces with a RMS roughness of 0.569 nm, 0.789 nm and 0.991 nm respectively. Since PVK thin films spin coated from chlorobenzene was found to possess minimum RMS roughness, chlorobenzene was used as the solvents for the deposition of the PVK and PBD doped PVK emissive layer in this study. Fig. 3.3 shows the AFM images of PVK (a), 10% PBD doped PVK (b), 20% PBD doped PVK (c) and 30% PBD doped PVK (d) thin films spin coated from chlorobenzene solution respectively and heated at 80 $^oC$ for 30 minutes.

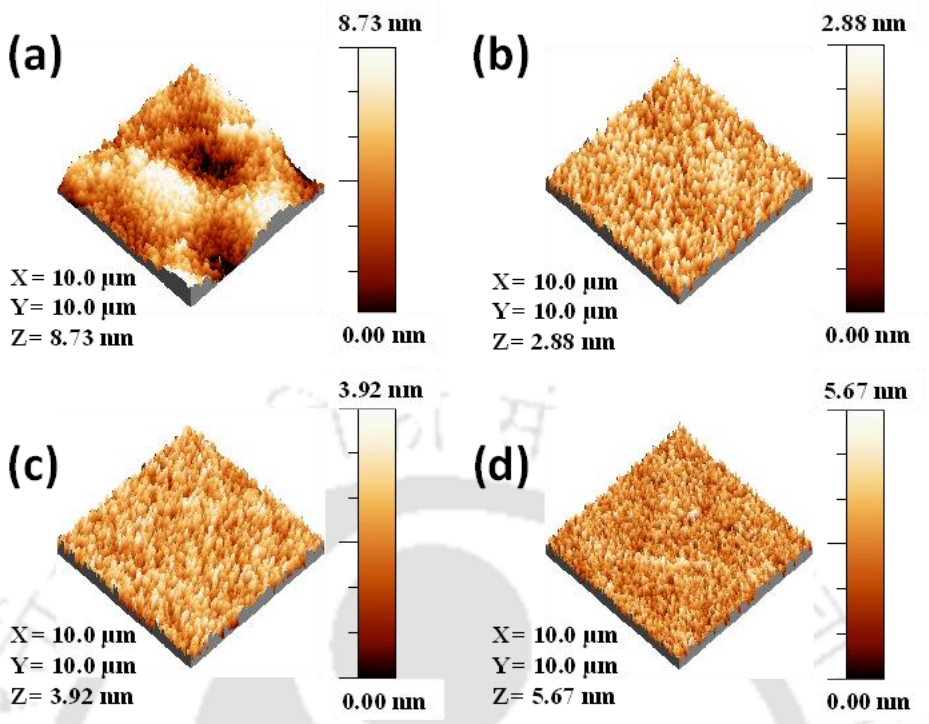


**Fig. 3.2** AFM images of the PVK thin films spin coated from a solution of chloroform (a), chlorobenzene (b), dichlorobenzene (c) and p-xylene (d), heated at 80 °C.

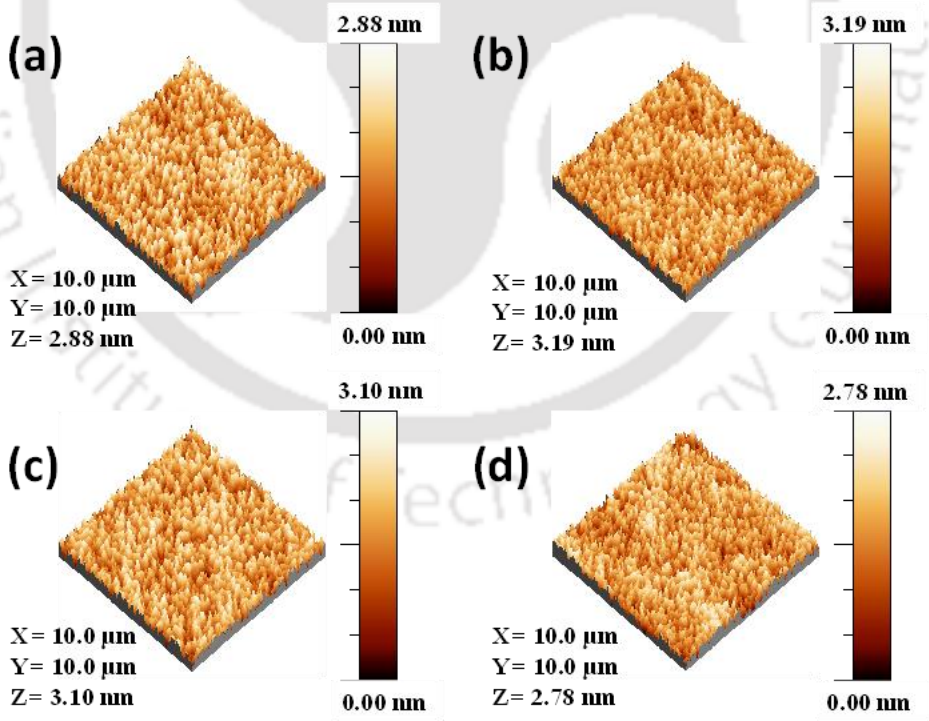


**Fig. 3.3** AFM images of PVK (a), 10% PBD doped PVK (b), 20% PBD doped PVK (c) and 30% PBD doped PVK (d) thin films spin coated from chlorobenzene solution.

It was observed that the doping of PBD further smoothens the surface of the thin films and the RMS roughness of the PVK, 10% PBD doped PVK, 20% PBD doped PVK and 30% PBD doped PVK thin films was found to be 0.569 nm, 0.551 nm, 0.547 nm and 0.531 nm respectively.

**3.3.2 Device studies**

A series of single as well as multilayer PLEDs with pristine Poly(9-vinylcarbazole) (PVK) and PVK doped with an electron transporting material 2-Phenyl-5-(4-biphenylyl)-1,3,4-oxadiazole (PBD), as emissive layer has been fabricated. Different electron transporting layers (ETL) such as 2,9-Dimethyl-4,7-diphenyl-1,10-phenanthroline (BCP), 4,7-Diphenyl-1,10-phenanthroline (BPhen) and 2,2′,2"-(1,3,5-Benzinetriyl)-tris(1-phenyl-1-H-benzimidazole) (TPBi) are used in case of multilayer configuration and the key device properties are listed in Table 3.1.

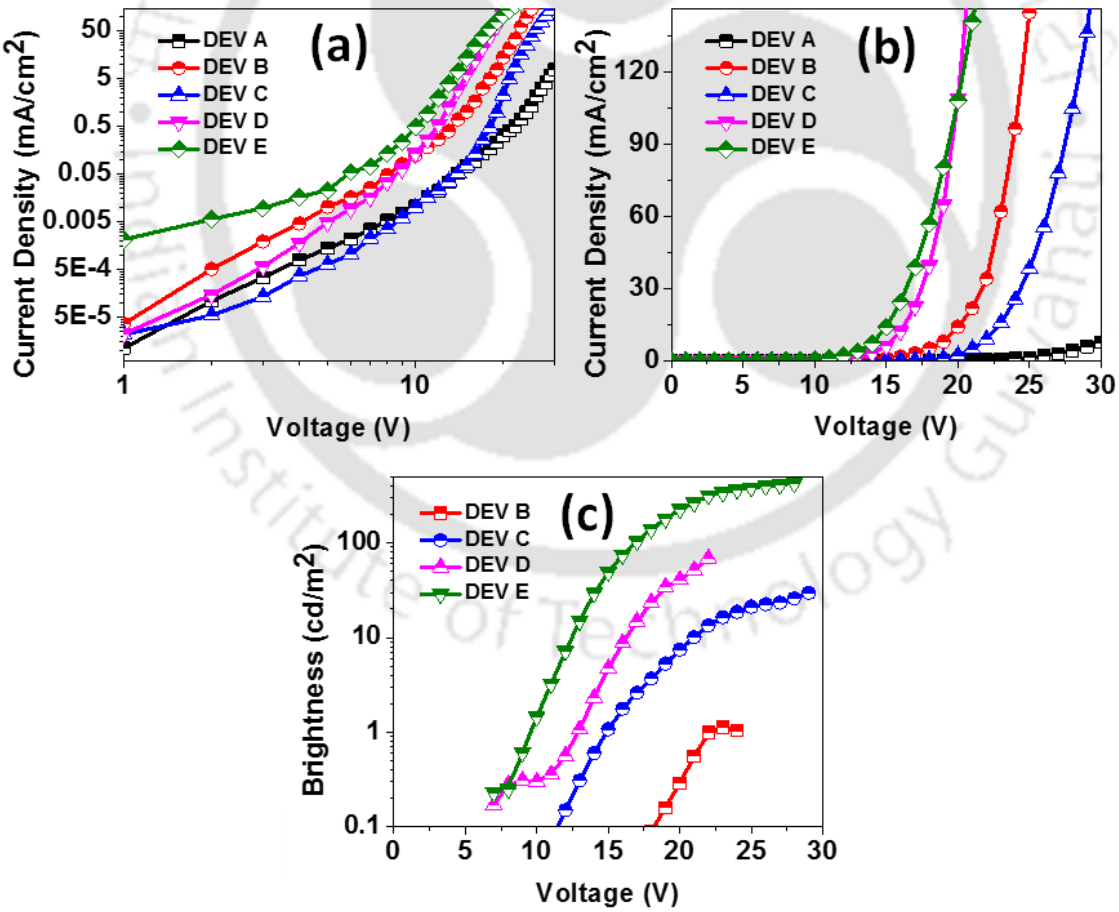


**Fig. 3.4** The current density vs. voltage characteristics of the fabricated PLEDs in logarithmic (a) and linear scales (b), and brightness vs. voltage characteristics of the fabricated PLEDs (c).

Fig. 3.4 (a) and (b) shows the current density v/s voltage characteristics of the fabricated PLEDs in logarithmic and linear scale respectively whereas Fig. 3.4 (c) shows its brightness v/s voltage characteristics. Fig. 3.4 (a) and (b) clearly suggests that the current flowing through all the devices is injection limited (ILC) at lower voltages and space charge limited (SCLC) at higher voltages. Also, the energy barrier for electrons in the cathode side is found to play a crucial role in defining the charge transport and brightness property of the devices. The energy band diagrams of the different devices with varying configurations are shown in Fig. 3.5.

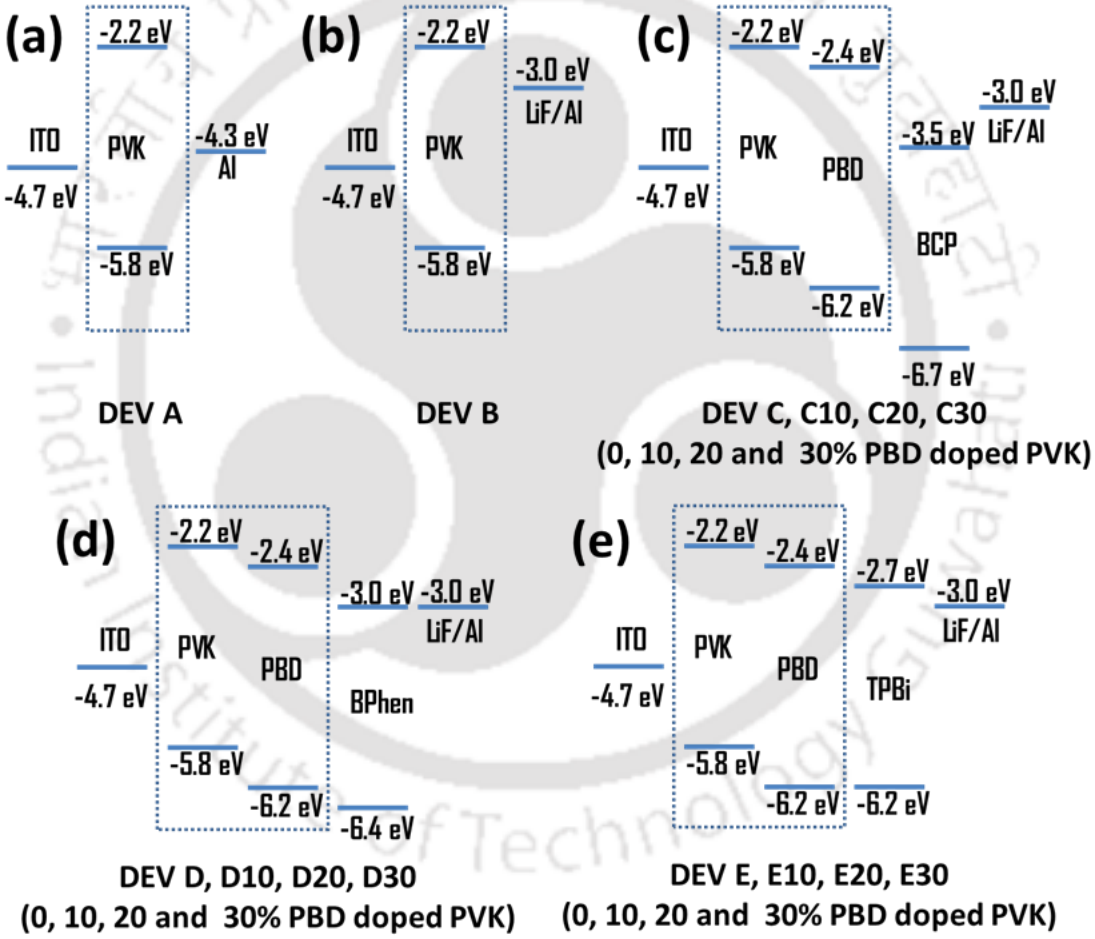


**Fig. 3.5** Energy band diagram of the devices with the different structures.

In case of Device A, since the hole barrier is less as compared to electron barrier, injection of hole starts at a lower voltage than the corresponding electrons. Further, as the hole mobility of PVK is high as compared to its electron mobility, the

electron-hole recombination takes place in the vicinity of the cathode material and the emission from the device is quenched.

**Table 3.1** Key device properties of the fabricated PLEDs (ITO is used as anode in all the devices).

| Device Name | EML | ETL | Cathode | Turn on Voltage, Von (V) | Brightness ($cd/m^2$) | CIE @20V |
|---|---|---|---|---|---|---|
| **DEV A** | PVK | - | Al | - | - | - |
| **DEV B** | PVK | - | LiF/Al | 22.64 | 1.13 | 0.36, 0.25 |
| **DEV C** | PVK | BCP | LiF/Al | 14.80 | 29.60 | 0.30, 0.30 |
| **DEV C10** | PVK:PBD (90:10) | BCP | LiF/Al | 15.75 | 39.45 | 0.28, 0.27 |
| **DEV C20** | PVK:PBD (90:20) | BCP | LiF/Al | 14.54 | 64.65 | 0.28, 0.26 |
| **DEV C30** | PVK:PBD (90:30) | BCP | LiF/Al | 14.10 | 107.53 | 0.26, 0.26 |
| **DEV D** | PVK | BPhen | LiF/Al | 12.94 | 68.87 | 0.25, 0.23 |
| **DEV D10** | PVK:PBD (90:10) | BPhen | LiF/Al | 9.13 | 103.95 | 0.23, 0.19 |
| **DEV D20** | PVK:PBD (90:20) | BPhen | LiF/Al | 8.88 | 147.79 | 0.22, 0.19 |
| **DEV D30** | PVK:PBD (90:30) | BPhen | LiF/Al | 8.75 | 190.16 | 0.19, 0.16 |
| **DEV E** | PVK | TPBi | LiF/Al | 9.55 | 426.24 | 0.20, 0.13 |
| **DEV E10** | PVK:PBD (90:10) | TPBi | LiF/Al | 8.65 | 251.06 | 0.18, 0.13 |
| **DEV E20** | PVK:PBD (90:20) | TPBi | LiF/Al | 8.41 | 195.64 | 0.18, 0.12 |
| **DEV E30** | PVK:PBD (90:30) | TPBi | LiF/Al | 8.25 | 122.87 | 0.18, 0.11 |

The high operating voltage in this device is distinctly due to the large injection barrier in the cathode side. The introduction of LiF interfacial layer in Device B significantly reduces the electron energy barrier of the device by modifying the fermi level of Al from -4.3 eV to -3.0 eV resulting in a reduction in the operating voltage. The light emitted from the device is however very less (1.13 cd/$m^2$), which can be attributed to the imbalanced charge transport property of PVK that results in the formation of recombination zone near the cathode. In Device C, the addition of BCP as electron transport layer creates an energy barrier for the holes, causing them to accumulate at the EML-ETL interface and thus shifting the recombination zone away from the cathode. As a result of this consequence, Device C shows a much-improved device brightness of 29.60 cd/$m^2$ as compared to Device B (1.13 cd/$m^2$). However, the deeper LUMO level of BCP (-3.5 eV) creates a large energy barrier at the EML-ETL interface for the electrons. In this event, the operating voltage of Device C is found to be higher than that of Device B. The energy barrier for electron at the ETL-EML interface is however reduced in Device D and Device E on using BPhen and TPBi with a LUMO level of -3.0 eV and -2.7 eV respectively, as ETL. This facilitates more electron injection into the EML and reduces the operating voltage of Device D and Device E. As more electrons are injected, the brightness value of the devices increased further to 68.87 cd/$m^2$ and 426.24 cd/$m^2$ in Device D and Device E respectively.

Fig. 3.6 (a-c) and Fig. 3.6 (d-f) depicts the current density v/s voltage (J-V) characteristics and the brightness v/s voltage (B-V) characteristics of undoped and PBD doped PVK based PLEDs. In all the device configurations, it has been observed that the current density in the device increases with the increase in the PBD doping ratio. This implies that with the increase in doping ratio of PBD, the electron transport property of PVK also increases. Suitably, the electrons flowing through the device increases and hence the total current increases. An interesting result is however observed in the case of brightness of these devices. As shown in Fig. 3.6 (d-f), the brightness of the PLEDs in device structures ITO/ doped PVK/BCP/LiF/Al and ITO/doped PVK/BPhen/LiF/Al have been found to increase with the increase in the PBD doping ratio. However, the brightness of the PLEDs in device structures ITO/doped PVK/TPBi/LiF/Al has found to increase with the increase in the PBD doping ratio till 12 V, however, it reduces as the doping ratio is increased further.

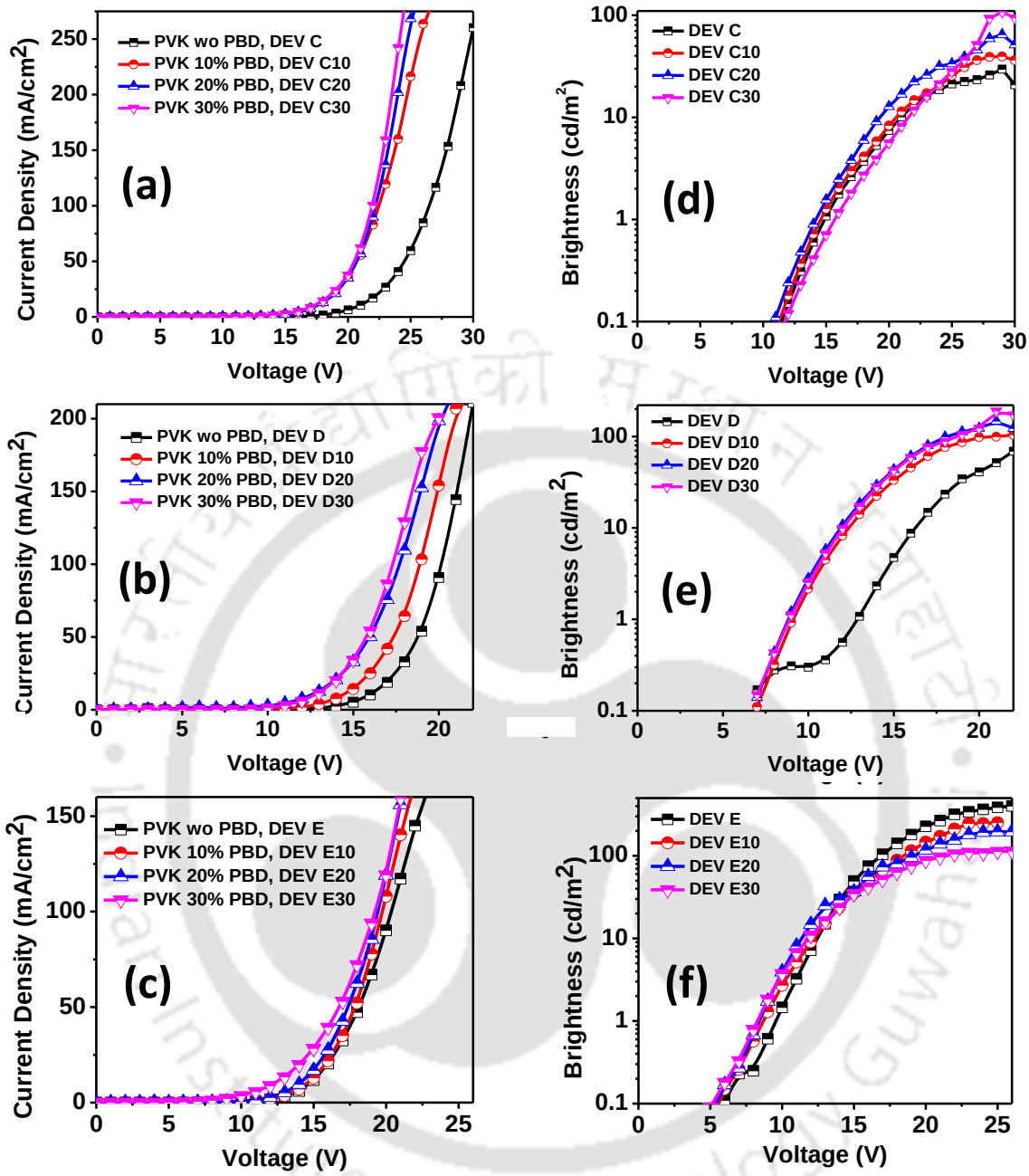


**Fig. 3.6** Current density vs. voltage (J–V) and brightness vs. voltage (B–V) characteristics of PLEDs using device structures ITO/undoped and doped PVK/BCP/LiF/Al (a and d); ITO/undoped and doped PVK/BPhen/LiF/Al (b and e) and ITO/undoped and doped PVK/TPBi/LiF/Al (c and f).

To understand the effect of PBD doping on the brightness, the energy band diagram of the devices (Fig. 3.5) were studied which conferred that with the addition of PBD in PVK, an additional energy levels for holes at -6.2 eV was created. Further, since the HOMO level of BCP and BPhen are deeper as compared to that of PBD

(-6.7 eV and -6.4 eV respectively); the holes have to overcome an energy barrier to jump from the HOMO level of PBD to the HOMO level of either BCP or BPhen. Consequently, the holes accumulate at the EML-ETL interface. However, as there is no such energy barrier in the case of TPBi (as both have same HOMO level), holes can easily move from the HOMO level of PBD to the HOMO level of TPBi at higher voltages. Thus, it could be established that, the recombination is less in case of PBD doped device in ITO/doped PVK/TPBi/LiF/Al based structure because of negligible amount of hole accumulation which results in a decrease in brightness at higher voltages.

Fig. 3.7 (a) and (b) shows the EL spectra and the CIE coordinates of the undoped PVK based PLEDs without or with different ETL (Device B, Device C, Device D and Device E). The EL spectra of the Devices B, C and D shows two peaks centred around 430 nm and 605 nm and emission approaching near white with CIE coordinates of (0.36, 0.27), (0.30, 0.30) and (0.25, 0.23), obtained from Devices B, C and D respectively. The EL spectra of Device E shows only a single peak centred around 430 nm and a deep blue emission with CIE coordinate of (0.18, 0.12). From the above-mentioned observations, it is evident that the peak at 430 nm in case of all the devices originated from PVK which has a characteristic emission peak at 420 nm. But the peak at 605 nm added to the curiosity as it was different from the emission characteristics of any of the materials used in this study and therefore can be assumed to be due to the formation of some new excited species/charge transfer complexes such as exciplex or electroplex. In order to analyze the origin of this emission peak, normalized photoluminescence (PL) spectra of PVK, BCP, BPhen, TPBi and PVK blended with BCP, BPhen and TPBi in 1:1 weight ratio was measured in thin film mode and shown in Fig. 3.7 (c). Since no such peak around 605 nm was observed in the PL spectra of the thin films, it can be assumed that the emission around 605 nm is not due to the exciplex formation but due to the electroplex formation. It was also observed that irrespective of the device structure, the emission was red shifted which is consistent with the mechanism of electroplex formation and arises due to the modification of the energy band gap at the EML-ETL interface due to the strong interfacial dipole.[25]

The effect of different applied voltages on the EL spectra of the fabricated PLEDs were further studied. Fig. 3.8 (a-d) shows the EL spectra, whereas, Fig. 3.8 (e-h) shows the normalized EL spectra of Devices B, C, D and E respectively at different applied voltages. The intensity of the both the peaks in Devices B, C and

D and the blue peak in Device E was found to increase with an increase in the applied voltage. From the normalized EL spectra, it was observed that with increasing voltage, the increase in the intensity of the 605 nm peak is more as compared to that of 430 nm peak suggesting more electroplex emission at higher voltages. However, since no electroplex emission was observed from Device E even at higher voltages, we predict that the formation of electroplex in PVK based PLEDs are ascribed to the poor electron injection in the PVK LUMO level from the cathode side and also the poor electron transport property of PVK.

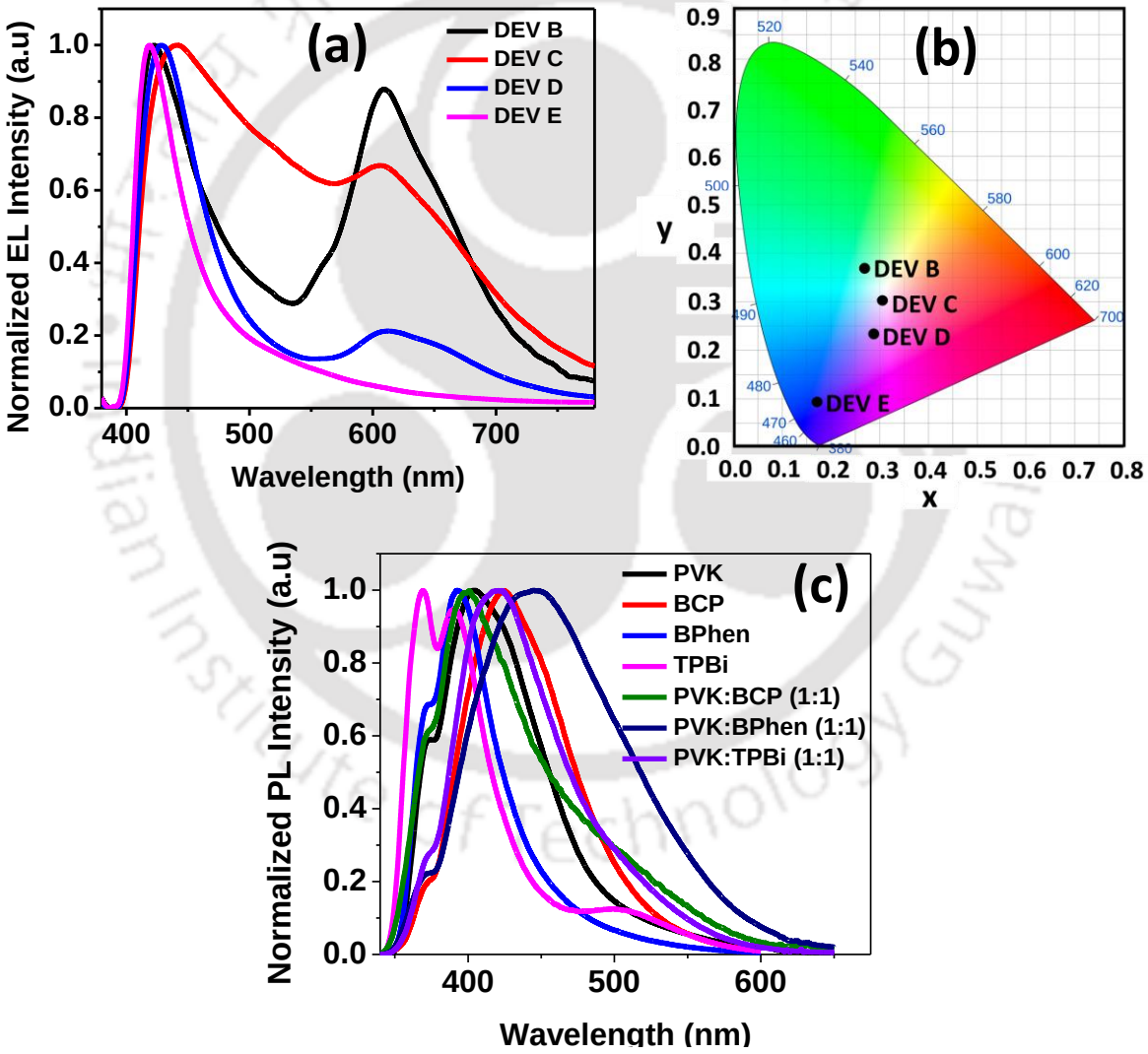


**Fig. 3.7** The EL spectra (a) and the CIE coordinates (b) of the undoped PVK based PLEDs without or with different ETLs and normalized photoluminescence (PL) spectra (c) of thin films of PVK, BCP, BPhen, TPBi and PVK blended with BCP, Bphen and TPBi in 1:1 weight ratio.

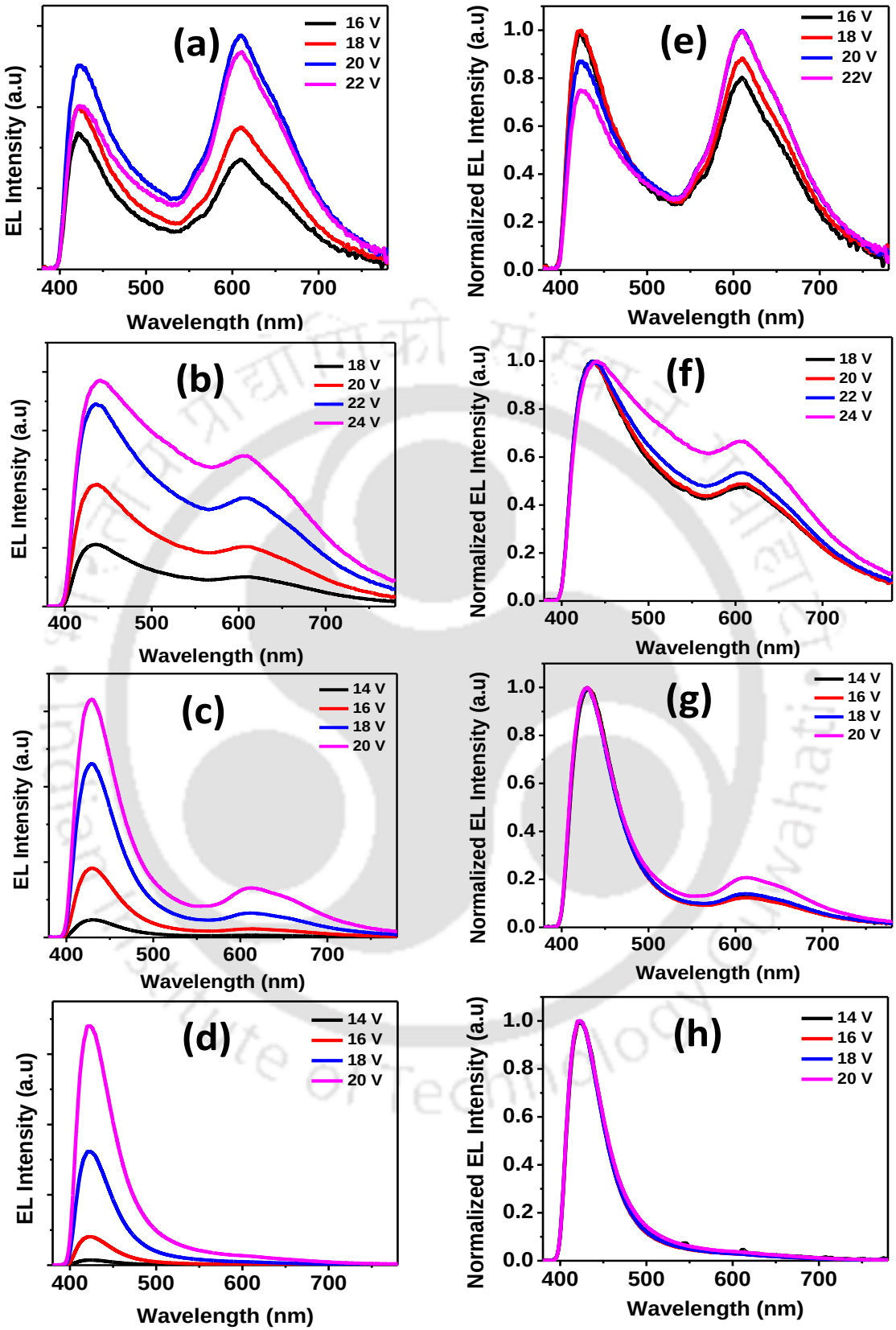


**Fig. 3.8** The EL spectra (a–d) and the normalized EL spectra (e–h) of devices B, C, D and E, respectively, at different applied voltages.

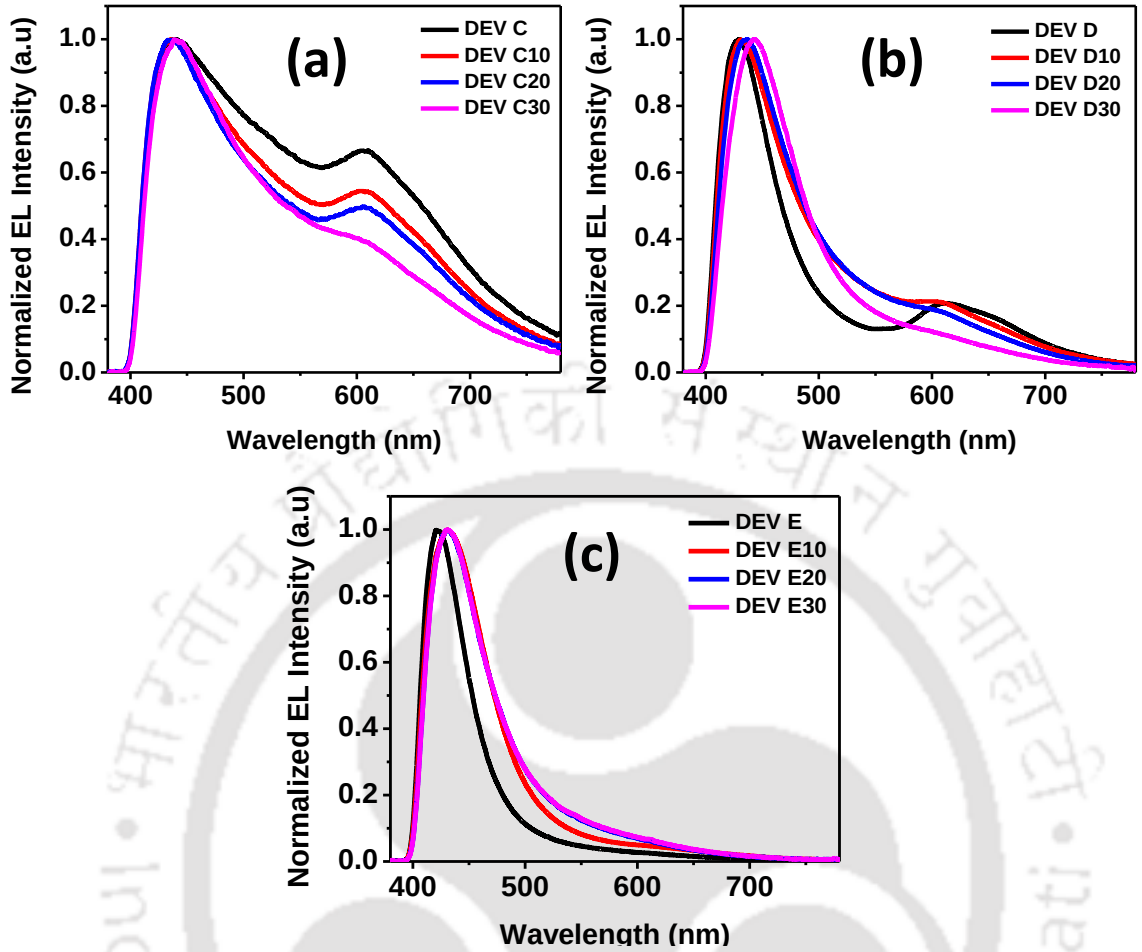


**Fig. 3.9** The normalized EL spectra of the PBD doped PVK devices.

As mentioned previously, the hole mobility of PVK is quite high as compared to its electron mobility, hence, holes can be transported easily in PVK. Therefore, in case of Device B, where no ETL is used, the recombination takes place near the cathode and electrons from cathode can directly recombine with the holes in the HOMO of PVK giving a strong electroplex emission. The use of BCP as ETL in Device C shifts the recombination zone away from cathode and facilitates more electron injection to the LUMO of PVK. However, with the addition of BCP layer a barrier of 0.9 eV for holes is created at the PVK–BCP interface making it difficult for holes to get injected into this layer. Similarly, it also creates a barrier of 1.3 eV for electrons at the BCP-PVK interface making it difficult for electrons to get injected into PVK. This results in an electroplex formation at the PVK-BCP interface due to the recombination of electrons at the LUMO of BCP with the holes at HOMO of the PVK. Again, BCP being an electron transport material, injects more electrons

into PVK as compared to that of Device B, as in Device C and therefore the electroplex emission is comparatively less. The energy barrier for holes and electrons at the EML-ETL interface is further reduced to 0.6 eV and 0.8 eV in Device D by using BPhen as ETL and to 0.4 eV and 0.5 eV in Device E by using TPBi as ETL respectively. This shows that the electroplex emission is significantly less in Device D with none forming in case of Device E.

To study the effect of electron transport property of PVK on electroplex formation the EL spectra of the PBD doped PVK based devices was also analyzed. Fig. 3.9 (a-c) shows the normalized EL spectra of the PBD doped PVK devices. From Fig. 3.9 (a-c), it was observed that the electroplex emission was reduced with increasing PBD doping. The doping of PBD enhanced the electron transport property of PVK. Therefore, less number of electrons accumulated at the ETL-EML interface in case of PBD doped PVK based PLEDs resulting in a reduction in the electroplex emission.

## 3.4 Conclusions

In summary, the key effects of electron injection barrier and the electron transport property of PVK on the charge transport, brightness and electroplex formation in PVK based PLEDs has been demonstrated. Single as well as multilayer PLEDs were fabricated using PVK and PBD doped PVK as emissive layers. In multilayer devices, three different ETLs viz. BCP, BPhen and TPBi that possess different electron injection barrier were examined. The energy barrier for electrons in the cathode side is found to play a crucial role in defining the charge transport, brightness and the electroluminescence property of the devices. Lowering the electron injection barrier improves the electrons flowing through the devices and thereby increases the current flowing through the devices and the recombination. Devices with TPBi that possess the lowest energy barrier for electrons (0.5 eV) were found to give the maximum brightness of 426.24 cd/m$^2$. To study the effect of electron transport property of PVK on the as-mentioned parameters, PVK was doped with PBD at varying doping ratios. The doping of PBD with PVK enhances the electron transport property of PVK and an improved current density and brightness of the devices were achieved with increased PBD doping. In EL studies, a near white emission with CIE coordinates of (0.30, 0.30) and (0.25, 0.23) at 20 V was obtained

from devices with BCP and BPhen as ETL respectively, due to an additional peak in the EL spectrum at ~605 nm, attributed to the electroplex formation in the EML-ETL interface, whereas the deep blue emission with a CIE coordinates of (0.18, 0.12) was obtained in case of devices using TPBi as ETL. The electroplex emission intensity was found to be voltage dependent and more electroplex emission was obtained at higher voltage. The electroplex formation was found to be controlled by the energy barrier for electrons at the ETL-EML interface and the electron transport property of PVK. Electroplex formation was found to reduce on reducing the electron injection barrier and almost no such emission was observed in case of devices with TPBi that possesses the lowest energy barrier for electrons (0.5 eV). The poor electron transport property of PVK was also found to be one of the main causes of electroplex formation in PVK based PLEDs. The doping of PBD in PVK improves the electron transport property of PVK whereas the electroplex formation is found to reduce with increasing PBD doping ratio. This metal free approach to generate WPLED presents a promising alternate and a cost-effective tuning of the devices using solution processed technique.

## 3.5 References


1. C. W. Tang and S. A. Vanslyke, *Appl. Phys. Lett.*, 1987, **51**, 913-915.
2. J. H. Burroughes, D. D. C. Bradley, A. R. Brown, R. N. Marks, K. Mackay, R. H. Friend, P. L. Burn and A. B. Holmes, *Nature*, 1990, **347**, 539-541.
3. A. Kraft, A. C. Grimsdale and A. B. Holmes, *Angew. Chem. Int. Edit.*, 1998, **37**, 402-428.
4. R. H. Friend, R. W. Gymer, A. B. Holmes, J. H. Burroughes, R. N. Marks, C. Taliani, D. D. C. Bradley, D. A. Dos Santos, J. L. Bredas, M. Logdlund and W. R. Salaneck, *Nature*, 1999, **397**, 121-128.
5. U. Mitschke and P. Bauerle, *J. Mater. Chem.*, 2000, **10**, 1471-1507.
6. M. T. Bernius, M. Inbasekaran, J. O'Brien and W. S. Wu, *Adv. Mater.*, 2000, **12**, 1737-1750.
7. G. Schwartz, S. Reineke, T. C. Rosenow, K. Walzer and K. Leo, *Adv. Funct. Mater.*, 2009, **19**, 1319-1333.
8. F. So, J. Kido and P. Burrows, *Mrs Bull*, 2008, **33**, 663-669.
9. S. Kim, H. J. Kwon, S. Lee, H. Shim, Y. Chun, W. Choi, J. Kwack, D. Han, M. Song, S. Kim, S. Mohammadi, I. Kee and S. Y. Lee, *Adv. Mater.*, 2011, **23**, 3511-3516.
10. Y. Fan, H. M. Zhang, J. S. Chen and D. G. Ma, *Org. Electron.*, 2013, **14**, 1898-1902.
11. A. C. Grimsdale, K. L. Chan, R. E. Martin, P. G. Jokisz and A. B. Holmes, *Chem. Rev.*, 2009, **109**, 897-1091.
12. P. Gopikrishna, D. Das and P. K. Iyer, *J. Mater. Chem. C* 2015, **3,** 9318-9326.
13. D. Das, P. Gopikrishna, A. Singh, A. Dey and P. K. Iyer, *Phys. Chem. Chem. Phys.*, 2016, **18**, 7389-7394.
14. T. Mori, T. Shinnai and M. Kijima, *Polym. Chem-Uk.*, 2011, **2,** 2830-2834.
15. T. Granlund, L. A. A. Pettersson, M. R. Anderson and O. Inganas, *J. Appl. Phys.* 1997, **81**, 8097-8104.
16. S. Y. Yang and M. X. Jiang, *Chem. Phys. Lett.*, 2009, **484**, 54-58.
17. Y. H. Yin, Z. B. Deng, Z. Y. Lu, X. Li, M. Li, B. G. Liu, Y. S. Wang and F. Teng, *Displays* 2015, **38,** 32-37.
18. D. Chen, Z. Wang, D. Wang, Y. C. Wu, C. C. Lo, A. Lien, Y. Cao and S. J. Su, *Org. Electron.*, 2015, **25,** 79-84.

19. E. Angioni, M. Chapran, K. Ivaniuk, N. Kostiv, V. Cherpak, P. Stakhira, A. Lazauskas, S. Tamulevicius, D. Volyniuk, N. J. Findlay, T. Tuttle, J. V. Grazulevicius and P. J. Skabara, *J. Mater. Chem. C* 2016, **4,** 3851-3856.
20. D. G. Georgiadou, L. C. Palilis, M. Vasilopoulou, G. Pistolis, D. Dimotikali and P. Argitis, *Rsc. Adv.*, 2012, **2,** 11786-11792.
21. J. Kalinowski, G. Giro, M. Cocchi and V. Fattori, R. Zamboni, *Chem. Phys.*, 2002, **277**, 387-396.
22. Z. R. Hong, O. Lengyel, C. S. Lee and S. T. Lee, *Org. Electron.*, 2003, **4**, 149-154.
23. J. F. Liang, S. Zhao, X. F. Jiang, T. Guo, H. L. Yip, L. Ying, F. Huang, W. Yang and Y. Cao, *Acs. Appl. Mater. Inter.*, 2016, **8,** 6164-6173.
24. Y. Nishikitani, N. Inokuchi, H. Nishide, S. Uchida, T. Shibanuma and S. Nishimura, *J. Phys. Chem. C* 2016, **120**, 13976-13986.
25. L. Wen, F. S. Li, J. X. Xie, C. X. Wu, Y. Zheng, D. L. Chen, S. Xu, T. L. Guo, B. Qu, Z. J. Chen and Q. H. Gong, *J. Lumin.*, 2011, **131,** 2252-2254.
26. M. Y. Wei, G. Gui, Y. H. Chung, L. X. Xiao, B. Qu and Z. J. Chen, *Phys. Status. Solidi. B* 2015, **252,** 1711-1716.
27. M. X. Zhang, Z. J. Chen, L. X. Xiao, B. Qu and Q. H. Gong, *Appl. Phys. Express.*, 2011, 4 (8).
28. Y. Y. Hao, W. X. Meng, H. X. Xu, H. Wang, X. G. Liu and B. S. Xu, *Org. Electron.*, 2011, **12,** 136-142.
29. Z. Y. Lu, Y. H. Yin and J. Xiao, *J. Lumin.*, 2016, **179,** 469-473.
30. J. Y. Park and R. C. Advincula, *Phys. Chem. Chem. Phys.*, 2014, **16**, 8589-8593.
31. J. Kido, K. Hongawa, K. Okuyama and K. Nagai, *Appl. Phys. Lett.*, 1994, **64,** 815-817.
32. C. Zhang, H. Vonseggern, B. Kraabel, H. W. Schmidt and A. J. Heeger, *Synthetic. Met.*, 1995, **72**, 185-188.
33. E. Gautier-Thianche, C. Sentein, A. Lorin, C. Denis, P. Raimond and J. M. Nunzi, *J. Appl. Phys.*, 1998, **83**, 4236-4241.
34. K. D'Almeida, J. C. Bernede, F. Ragot, A. Godoy, F. R. Diaz and S. Lefrant, *J. Appl. Polym. Sci.*, 2001, **82**, 2042-2055.
35. J. Kido, K. Hongawa, K. Okuyama and K. Nagai, *Appl. Phys. Lett.*, 1993, **63**, 2627-2629.

36. Y. M. Wang, F. Teng, Z. Xu, Y. B. Hou, S. Y. Yang, L. Qian, T. Zhang and D. A. Liu, *Appl. Surf. Sci.,* 2004, **236**, 251-255.
37. P. D'Angelo, M. Barra, A. CassineSe, M. G. Maglione, P. Vacca, C. Minarini and A. Rubino, *Solid. State. Electron.,* 2007, **51,** 123-129.
38. Y. S. Lai, C. H. Tu, D. L. Kwong and J. S. Chen, *Appl. Phys. Lett.,* 2005, **87**, 122101 (1-3).
39. M. Ben Khalifa, D. Vaufrey, A. Bouazizi, J. Tardy and H. Maaref, *Mat. Sci. Eng. C-Bio., S* 2002, **21**, 277-282.

# CHAPTER-4

## Highly efficient green phosphorescent organic light emitting diode based on $Ir(mppy)_3$ : effect of annealing temperature and mixed host

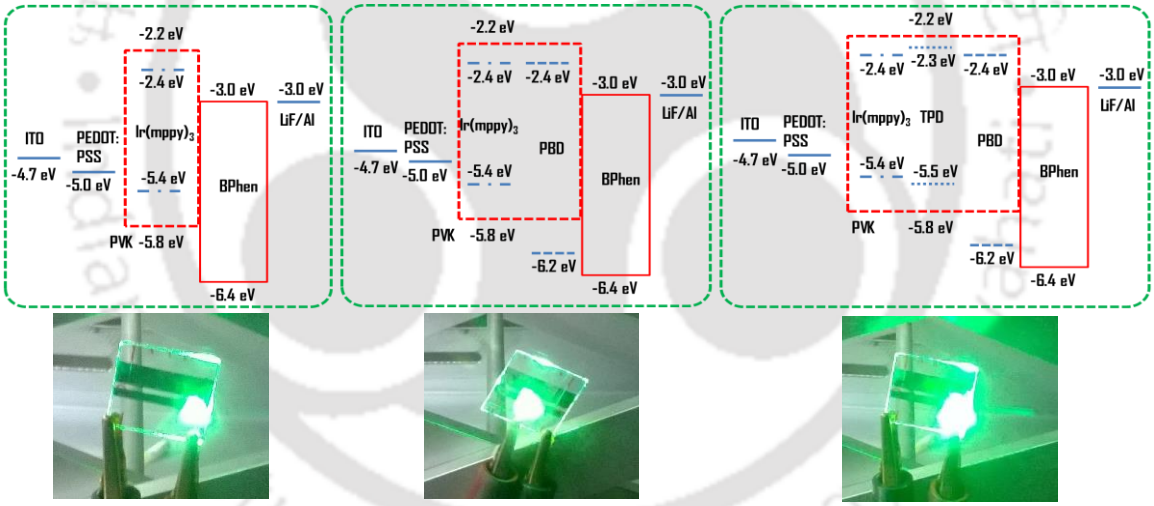

# Highly efficient green phosphorescent organic light emitting diode based on $Ir(mppy)_3$ : effect of annealing temperature and mixed host


## *Abstract*

*"Better charge balance and efficient charge injection in the emissive layer (EML) plays a vital role in defining the device performance of an organic light emitting diode (OLED) which in turn depends on the materials used and the processing condition such as solvent, thermal treatment etc. Herein, highly efficient, solution processed green phosphorescent organic light emitting diode (phOLED) based on $Ir(mppy)_3$ with single and mixed host namely PVK (Poly(9-vinylcarbazole)), PVK: PBD (2-(4-Biphenylyl)-5-(4-tert-butylphenyl)-1,3,4-oxadiazole), PVK: PBD: TPD (N, N'-Bis(3-methylphenyl)-N, N'-diphenylbenzidine) have been reported. Addition of electron and hole transporting material in appropriate ratio is found to improve the charge balance at the EML that results in improved device performance. The different host combinations have further been annealed at 80 °C, 100 °C, 120 °C, 140 °C and 160 °C and the effect of annealing temperature on the morphological, optical and electrical properties of the phOLEDs have been elucidated. At higher annealing temperature EML is found to form a compact structure with higher RMS roughness that leads to a strong interfacial adhesion and better charge injection. As a result, the device performance is found to increase with increasing annealing temperature and best result was observed for the devices annealed at 140 °C. Among all, PVK: PBD: TPD host based devices annealed at 140 °C is found to give best result with the maximum brightness of 17273 cd $m^{-2}$ and a maximum luminous efficiency of 61.21 cd $A^{-1}$."*

## 4.1 Introduction

Organic light emitting diodes (OLEDs) have aroused significant research interest worldwide in the past few decades due to its numerous advantages such as light weight, lower cost, easy processing for large area fabrication and also the flexibility.[1-5] In OLEDs, the organic molecules of the emissive layer are excited electrically in order to get light from the device. However, for an electrically excited organic molecule, the energy may be released radiatively through a fluorescence or phosphorescence process. According to quantum mechanics, the electronic state density ratio of singlet to triplet is 1:3. In fluorescent molecule, the triplet states are non-emissive, so only a quarter of the excitons generated (maximum) may contribute to light emission.[6,7] In phosphorescent molecule, the molecule is attached to a heavy metal atom such as Ir, Eu, Pt etc. which can induce spin orbit coupling effect, leading to a rapid exciton energy transfer from singlet to triplet states, as well as allowing for a spin flip that allows a triplet state to relax to ground state radiatively. Therefore, the major advantage of electro phosphorescent OLEDs (phOLEDs) is the high quantum and luminous efficiency (LE) because the heavy metal complex can harvest both singlet and triplet excitons, leading to nearly 100% internal quantum efficiency.[8,9] To achieve high efficiency electroluminescence (EL), phosphors are commonly doped into a host matrix to avoid concentration quenching and triplet–triplet annihilation.[10,11] To date, the most efficient phOLEDs [12-20] are fabricated using thermal deposition method in a finite vacuum chamber, making cost-effective manufacture and large area electronics impossible. To make this novel terminal electronics available for general applications the cost needed to be decreased, and thus new processing techniques were demanded. In this regard, solution processes, such as ink-jet printing and spin coating, can offer the advantage of cost-effective manufacturing of large area devices and solution processed OLEDs can have the potential to be printed in different designs and shapes thereby allowing enormous design possibilities and pave a way to create artistic applications with light. [21,22] But the performances of the OLEDs fabricated by the solution processing techniques are still relatively low compared to their thermally deposited counterparts. The efficiency of phOLEDs mainly depends on the efficient charge injection from the electrodes at a low drive voltage, good charge balance and high solid-state quantum yield of the emissive layer along with the confinement of the injected charge carriers within the emitting layers. [23, 24] It is therefore of utmost importance to carefully study the effect of processing conditions such as thermal treatment of the emissive layer as

they greatly influence the morphology of the films and their interfaces with the adjacent layers thereby influencing the electrical properties such as charge injection and charge transport in the device. [25-27] In solution processed phOLEDs, polymers have always been preferred as the host material due to their solution processing ability and among them, poly(N vinylcarbazole) (PVK) is a commonly used host material for phOLEDs because of its excellent film forming ability and high triplet energy level. [28-31] Yet, the offset between the hole and electron mobility of PVK is a major factor that limits the efficiency of such phOLEDs due to the lack of good charge balance. PVK is therefore doped with different electron transporting material (ETM) such as PBD (2-(4-Biphenylyl)-5-(4-tert-butylphenyl)-1,3,4-oxadiazole), OXD-7 1,3-bis[2-(4-tert-butylphenyl)-1,3,4-oxadiazo-5-yl]benzene etc. at a suitable ratio depending on the phosphorescent dopant used to achieve superior device performance. [32-35] It has also been reported that addition of a hole transport material (HTM) such as NPD (N,N′-Di-[(1-naphthyl)-N,N′-diphenyl]-1,1′-biphenyl)-4,4′-diamine), TPD(N,N′-Bis(3-methylphenyl)-N,N′-diphenylbenzidine) etc. into the host of PVK: ETM in small quantity can further improve the device performance of an phOLED. [36-38]

Considering the aforesaid factors, highly efficient, solution processed green phosphorescent organic light emitting diode (phOLED) based on $Ir(mppy)_3$ with single and mixed host namely PVK, PVK: PBD, PVK: PBD: TPD have been fabricated. Addition of electron and hole transporting layer in appropriate ratio is found to improve the charge balance of the emissive layer that results in improved device performance. The reported processing parameters of the PVK based phOLEDs varies widely. Therefore, apart from the charge balance in the emissive layer, in order to study the effect of processing conditions, different host combinations were annealed at 80 $^{o}$C, 100 $^{o}$C, 120 $^{o}$C, 140 $^{o}$C and 160 $^{o}$C and the effect of annealing temperature on the morphological, optical and electrical properties of the phOLEDs have been elucidated. The device performance is found to increase with increasing annealing temperature and best result was observed for the devices annealed at 140 $^{o}$C. Among all, PVK: PBD: TPD host based devices annealed at 140 $^{o}$C is found to give the maximum brightness of 17273 cd $m^{-2}$ and a maximum luminous efficiency of 61.21 cd $A^{-1}$. The results obtained in this study reported herein provide important information about the processing of emissive layer of an OLED and of significant importance to the researchers working in the field of OLED and other organic based electronic devices.

## 4.2 Experimental

Fig. 4.1 shows the chemical structures of the materials used in this study and the energy level diagram of the phOLEDs with different configuration. The materials were commercially purchased from Sigma Aldrich and Poly (ethylendioxythiophene): poly (styrene sulfonic acid) (PEDOT: PSS) was purchased from Clevios. All the materials were used as received. Atomic force microscopy (AFM) images were taken using an Agilent5500-STM instrument and the photoluminescence (PL) emission spectra were recorded on a Varian-Cary Eclipse spectrophotometer.

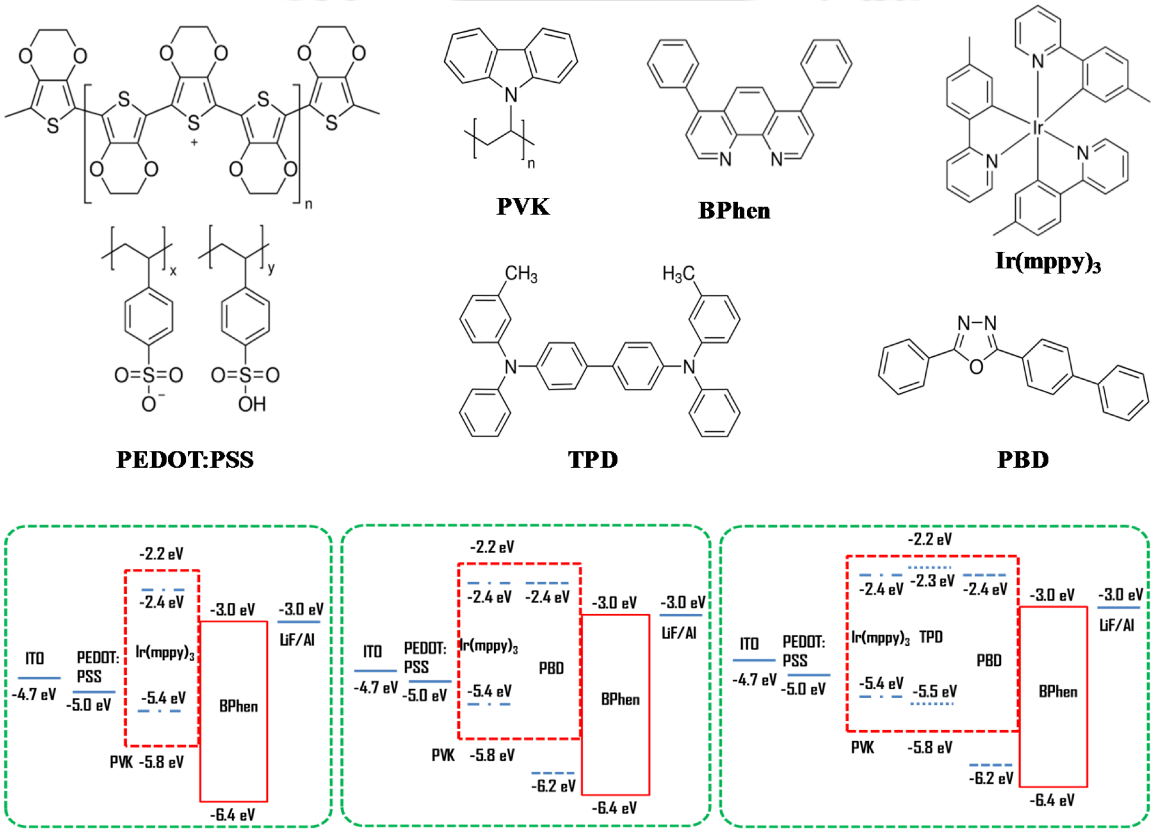


**Fig. 4.1** Chemical structures of the materials along with their energy level diagram as used in the phOLED fabrication.

In phOLEDs, ITO coated glass substrates were patterned and used as transparent anodes. The patterned ITO substrates were cleaned thoroughly by ultrasonication in soap solution, Millipore water, acetone and isopropanol, each for ten minutes at room temperature and dried by blowing Argon gas. The dried substrates were then treated under UV- Ozone for 30 mins. A 40-nm thick film of

PEDOT: PSS used as the hole injection/ transport layer in all the phOLEDs was spin coated onto the ITO substrates immediately after UV-Ozone treatment at 3000 rpm for 60 sec and annealed at 120 °C for 1 hour. Three different types of host namely PVK, PVK: PBD and PVK: PBD: TPD were used for the emissive layer and $Ir(mppy)_3$ was used as the dopant. The solutions of PVK:Ir(mppy)3 (94:6), PVK:PBD:$Ir(mppy)_3$ (70:24:6) and PVK:PBD:TPD:$Ir(mppy)_3$ (61:24:9:6) were made in chlorobenzene solution and were stirred for 30 min to ensure efficient doping. The solutions were then filtered using 0.45µm filter and coated above PEDOT: PSS layer. The EML with different host were then baked at different annealing temperature (80 $^oC$, 100 $^oC$, 120 $^oC$, 140 $^oC$ and 160 $^oC$) to analyse the effect of annealing temperature on the device performance. For all the phOLEDs, BPhen was used as electron transport and hole blocking layer. BPhen, LiF and Al were thermally evaporated at a rate 2 Å/s.0.1 Å/s and 10 Å/s at a base pressure of $10^{-6}$ mbar to complete the phOLED fabrication. The active area of the phOLEDs was 24 $mm^2$. The current density vs. voltage (J-V) characteristics of the WPLEDs were measured using a Keithley 2400 source meter, whereas the brightness vs. voltage (B-V) characteristics and the EL spectra were recorded using Konica Minolta CS 2000 Spectroradiometer. All characterizations were done inside glove box under argon atmosphere.

## 4.3 Results and discussion

To investigate the effect of annealing temperature on the performance of phOLEDs, first and foremost four different set of phOLEDs with PVK: $Ir(mppy)_3$ as emissive layer were fabricated where the emissive layers were annealed at 80 $^oC$, 100 $^oC$, 120 $^oC$, 140 $^oC$ and 160 $^oC$ respectively. The current density vs. voltage (J-V), brightness vs. voltage (B-V) and the luminous efficiency vs. Brightness curve of the as fabricated phOLEDs are shown in Fig 4.2 (a), (b) and (c) respectively and their normalized EL spectra are shown in Fig. 4.2 (d). The key device properties of these devices are summarized in Table 4.1.

As it can be seen from Fig 4.2 (a) and (b), the annealing temperature of the emissive layer effects the current density and brightness of the phOLEDs significantly. It was observed that the current density of the phOLEDs increases with increasing the annealing temperature, which may be due to an increase in the bulk conductivity of the emissive layer that may arise due to the increased film density of the emissive layer probably due to the increased interchain interaction at higher annealing temperature.[25,26]

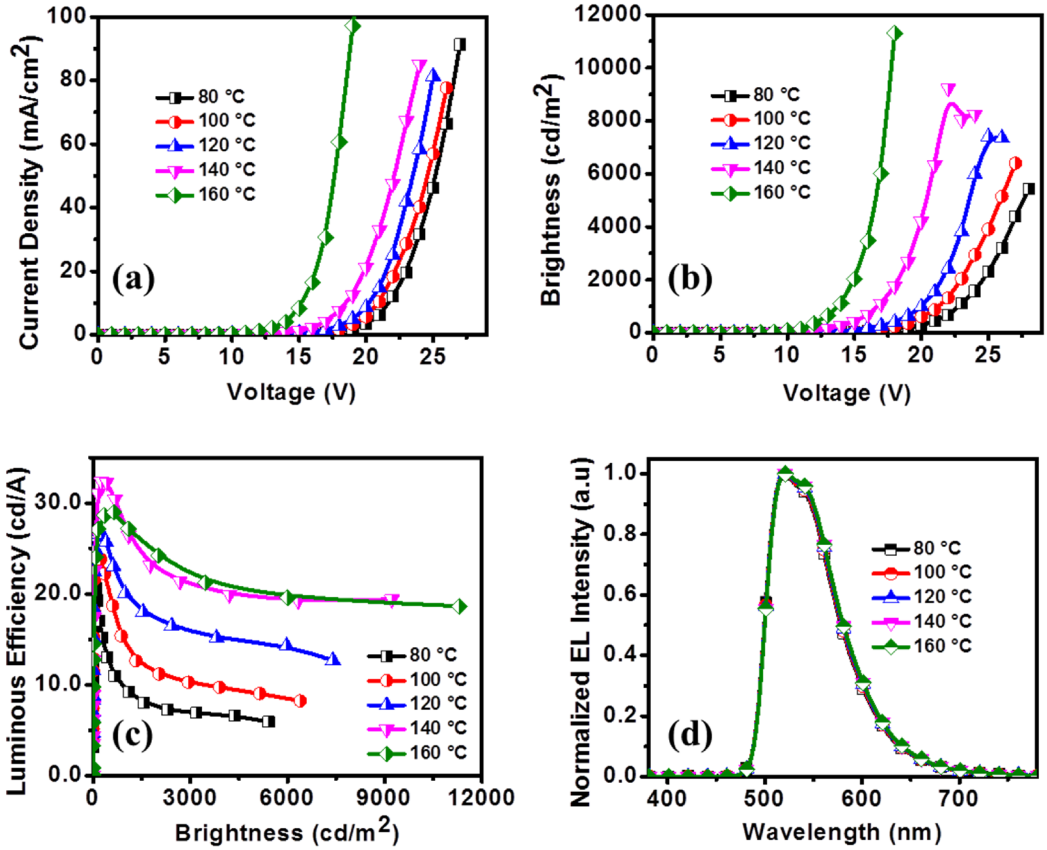


**Fig. 4.2** The current density vs. voltage (J-V) characteristics (a), brightness vs. voltage (B-V) characteristics (b), luminous efficiency vs. brightness characteristics (LE-B) (c) and the normalized EL spectra (d) of the PVK: $Ir(mppy)_3$ based phOLEDs with emissive layers annealed at different temperature.

**Table 4.1** Key device parameters of PVK: $Ir(mppy)_3$ based PLEDs.

| Annealing Temperature | Turn on voltage (V) | Maximum brightness ($cd/m^2$) | Power Efficiency[a] (lm/W) | Luminous Efficiency[a] LE (cd/A) |
|---|---|---|---|---|
| **80** | 7.60 (7.67, 0.10) | 5423 (5275, 178) | 3.24 (3.10, 0.12) | 20.65 (19.77, 1.78) |
| **100** | 7.01 (7.05, 0.05) | 6394 (6201, 157) | 3.96 (3.52, 0.23) | 23.95 (21.98, 1.44) |
| **120** | 6.32 (6.37, 0.06) | 7407 (7225, 227) | 4.65 (4.32, 0.17) | 26.61 (25.34, 1.23) |
| **140** | 4.91 (4.99, 0.11) | 9225 (8978, 294) | 6.77 (6.47, 0.21) | 32.33 (31.03, 1.29) |
| **160** | 4.68 (4.75, 0.08) | 11306 (10732, 247) | 6.61 (6.41, 0.18) | 27.37 (27.68, 1.17) |

[a]Maximum value. Values in the bracket are average value of 10 devices and standard deviation.

The brightness of the phOLEDs were also found to follow a similar trend as that of current density and the maximum brightness value is found to improve from 5423 cd $m^{-2}$ to 11306 cd $m^{-2}$ as the annealing temperature was varied from 80 $^{o}$C to 160 $^{o}$C. Most importantly, the turn on voltages of the phOLEDs were found to reduce with increase in the annealing temperature and changes from 7.60V to 4.68V as the annealing temperature was varied from 80 $^{o}$C to 160 $^{o}$C. The improvement in brightness and the reduction in the turn on voltages of the phOLEDs with increased annealing temperature is in agreement with the fact that the interchain interaction increases with increasing the annealing temperature.

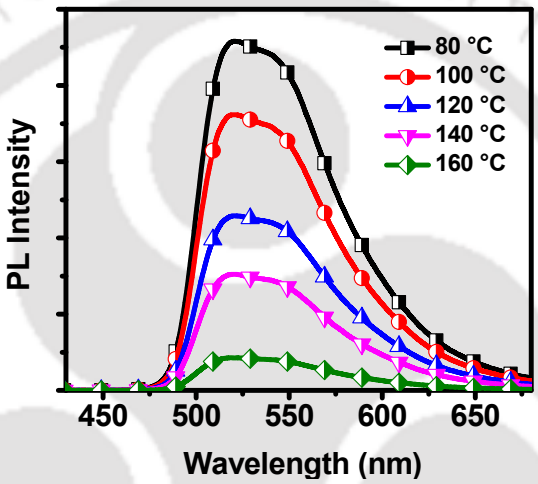


**Fig. 4.3** The PL spectra of the PVK: $Ir(mppy)_3$ thin film at different annealing spectra.

The photoluminescence (PL) spectra of the PVK: $Ir(mppy)_3$ thin film at different annealing spectra is shown in Fig. 4.3. No shift in the PL spectra was observed with temperature. However, it was observed that an increased interchain interaction at higher annealing temperature leads to a decreased photoluminescence efficiency (Fig 4.3). It is therefore expected that the devices with EML annealed at higher annealing temperature should show lower LE. Interestingly, the opposite results were observed in this case. From Fig. 4.2 (c), it can be seen that the LE of the phOLEDs increase from 20.65 cd $A^{-1}$ to 32.33 cd $A^{-1}$ with increasing the annealing temperature from 80 $^{o}$C to 140 $^{o}$C. However the LE of the phOLEDs decrease to 27.37 cd $A^{-1}$ for the annealing temperature from 160 $^{o}$C. Therefore, it is evident that apart from interchain interaction, annealing temperature may also effect the morphology and the interface with the electrode. To observe the effect of annealing temperature on the morphology of the EML, AFM images of the EML were

taken after annealing them at different temperature. The AFM images of the EML annealed at different temperature is shown in Fig. 4.4.

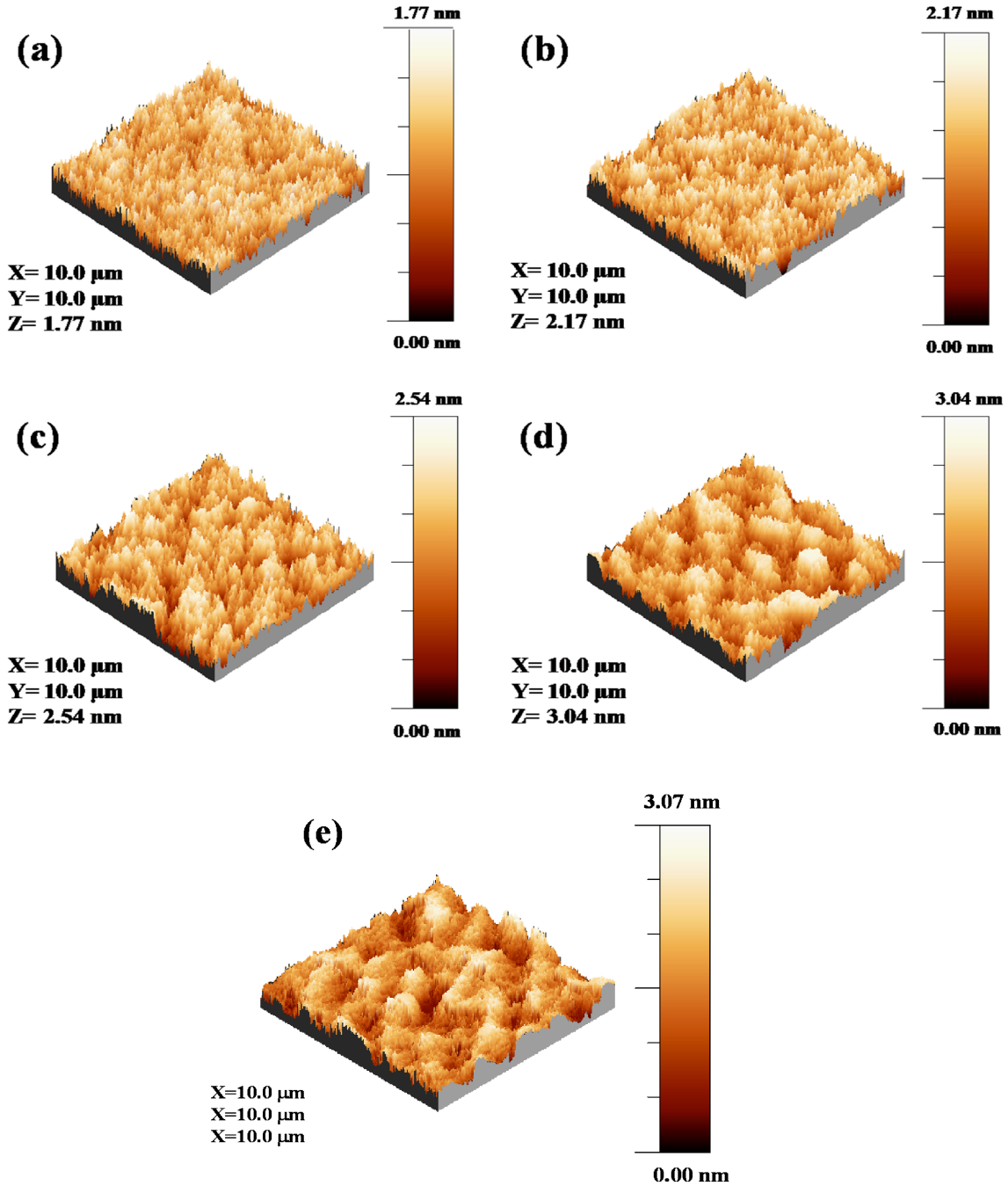


**Fig. 4.4** The AFM images of the PVK: $Ir(mppy)_3$ EML annealed at 80 °C (a), 100 °C (b), 120 °C (c), 140 °C (d) and 160 °C (e).

The RMS roughness value of the EML was found to be 0.328nm, 0. 408 nm, 0.489 nm, 0.532 nm and 0.549 nm for annealing temperature of 80 °C, 100 °C, 120 °C, 140 °C and

160 °C respectively. It was observed that the RMS roughness of the EML increases with increasing annealing temperature due to the formation of a compact structure that results from the surface shrinking of the polymer host. This compact structure and the rough surface of the EML annealed at higher temperature makes its interfacial adhesion with adjacent layers stronger and lead to the formation of a better interfacial contact with ETL and the cathode. Due to the strong interfacial adhesion, the effective area for electron injection becomes larger that facilitate more electron injection into the EML, thereby improving the charge balance in the EML, which is reflected by an increase in the LE upto 140 °C .[39-41] However, at annealing temperature 160 °C, the drop in the PL quantum yield is significantly less which may be the reason for the decrease in LE. Annealing temperature, however, was not found to affect the electroluminescence of the phOLEDs as no visible influence was observed in the normalized EL spectra of the devices (Fig. 4.2 (d)).

PVK usually have higher hole mobility as compared to its electron mobility. It is therefore often doped with an electron transporting material to improve charge balance. Considering the HOMO and LUMO position of $Ir(mppy)_3$ used as dopant in this study, PVK was replaced with binary host of PVK doped with PBD and ternary host of PVK doped with PBD and TPD to further improve the efficiency of the phOLEDs. Like the previous study, four different set of phOLEDs with PVK:PBD:$Ir(mppy)_3$ as emissive layer were fabricated and the emissive layers were annealed at 80 °C, 100 °C, 120 °C, 140 °C and 160 °C respectively and the effect of annealing temperature in case of mixed host was investigated. The current density vs. voltage (J-V), brightness vs. voltage (B-V) and the luminous efficiency vs. Brightness curve of the as fabricated phOLEDs with binary and ternary host are shown in Fig. 4.5 (a), (b) and (c) and Fig 4.6 (a), (b) and (c) respectively and their normalized EL spectra are shown in Fig. 4.5 (d) and Fig. 4.6 (d) respectively. The key device properties of these devices are summarized in Table 4.2 and Table 4.3 respectively.

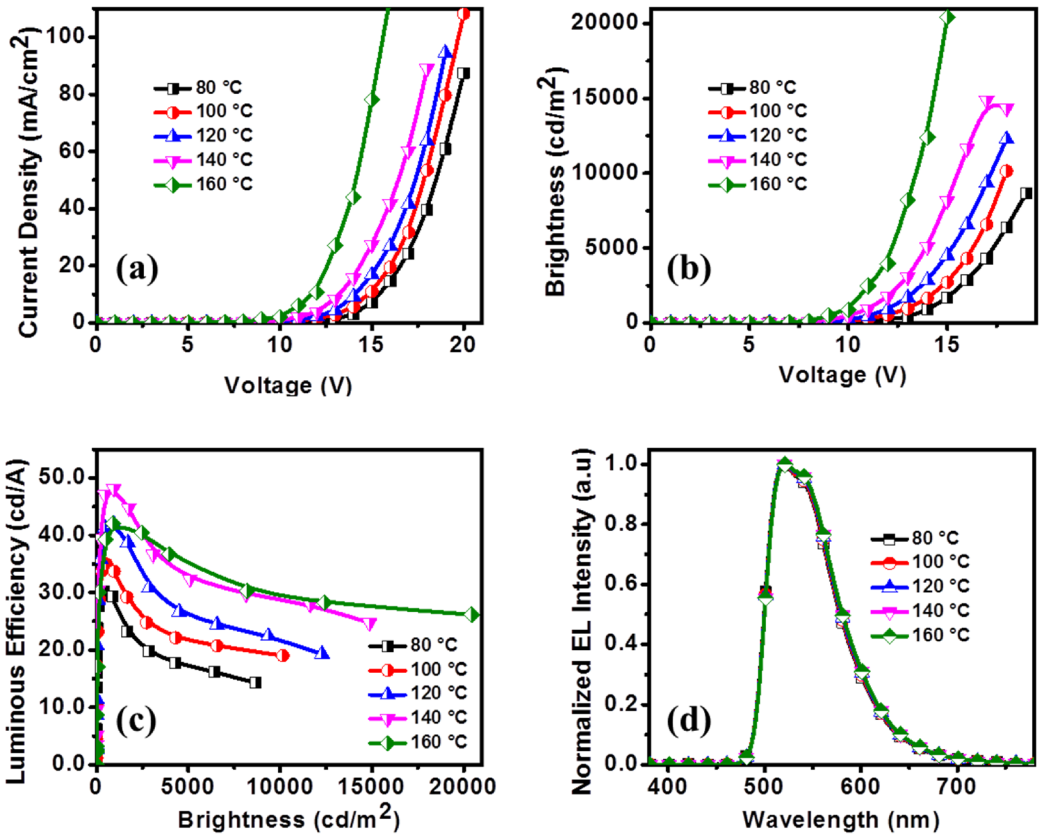


**Fig. 4.5** The current density vs. voltage (J-V) characteristics (a), brightness vs. voltage (B-V) characteristics (b), luminous efficiency vs. brightness characteristics (LE-B) (c) and the normalized EL spectra (d) of the PVK: PBD: $Ir(mppy)_3$ based phOLEDs with emissive layers annealed at different temperature.

**Table 4.2** Key device parameters of PVK: PBD: $Ir(mppy)_3$ based PLEDs.

| Annealing Temperature | Turn on voltage (V) | Maximum brightness ($cd/m^2$) | Power Efficiency[a] (lm/W) | Luminous Efficiency[a] LE (cd/A) |
|---|---|---|---|---|
| **80** | 5.81 (5.92, 0.12) | 8677 (8344, 149) | 6.49 (6.24, 0.18) | 30.20 (28.45, 0.97) |
| **100** | 4.89 (5.01, 0.09) | 10148 (9636, 173) | 7.85 (7.23, 0.21) | 34.98 (31.63, 1.22) |
| **120** | 4.61 (4.74, 0.14) | 12285 (11390, 274) | 10.23 (9.78, 0.19) | 42.01 (38.82, 1.38) |
| **140** | 4.16 (4.24, 0.06) | 14873 (14127, 288) | 12.49 (11.83, 0.17) | 48.12 (44.12, 1.56) |
| **160** | 3.97 (4.09, 0.09) | 20432 (19788, 148) | 12.47 (11.48, 0.19) | 42.16 (40.73, 1.27) |

[a]Maximum value. Values in the bracket are average value of 10 devices and standard deviation.

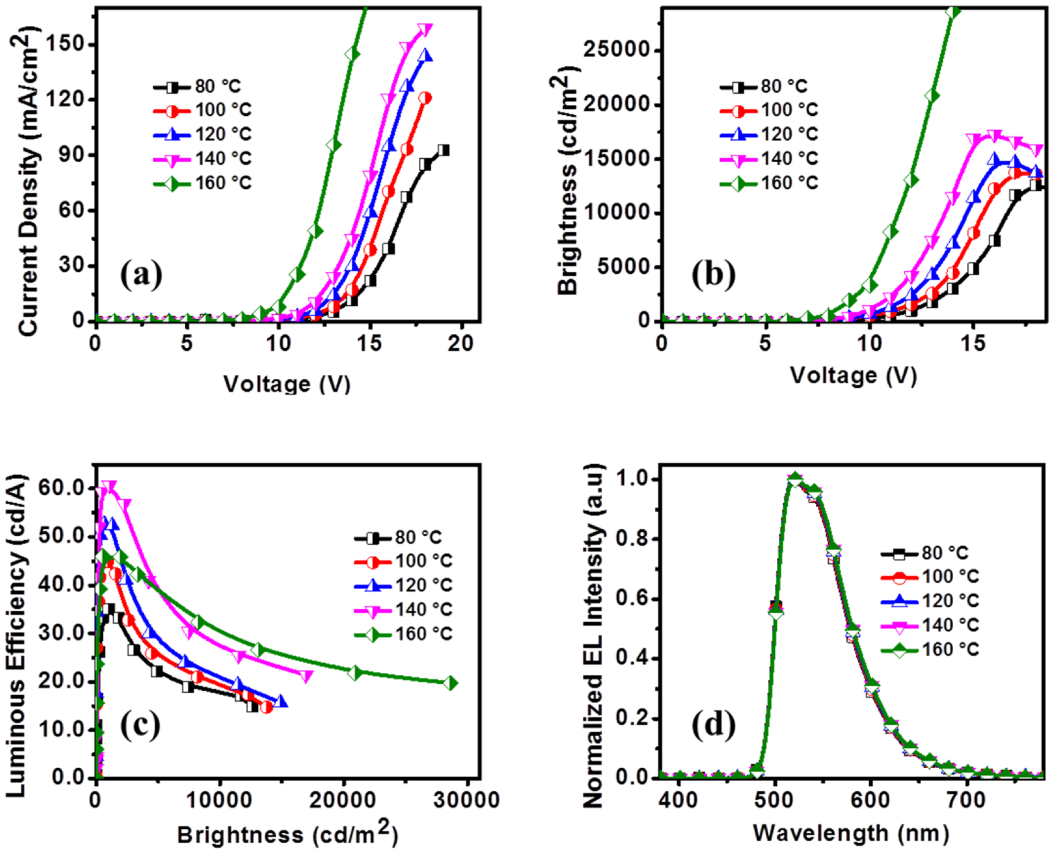


**Fig. 4.6** The current density vs. voltage (J-V) characteristics (a), brightness vs. voltage (B-V) characteristics (b), luminous efficiency vs. brightness characteristics (LE-B) (c) and the normalized EL spectra (d) of the PVK: PBD: TPD: $Ir(mppy)_3$ based phOLEDs with emissive layers annealed at different temperature.

**Table 4.3** Key device parameters of PVK: PBD: TPD: $Ir(mppy)_3$ based PLEDs.

| Annealing Temperature | Turn on voltage (V) | Maximum brightness ($cd/m^2$) | PE (lm/W) | LE (cd/A) |
|---|---|---|---|---|
| **80** | 4.94 (5.09, 0.13) | 12618 (11668, 234) | 8.62 (8.01, 0.35) | 35.15 (33.30, 1.62) |
| **100** | 4.77 (4.87, 0.08) | 13768 (12456, 188) | 11.40 (10.27, 0.42) | 44.95 (42.05, 1.77) |
| **120** | 4.59 (4.68, 0.10) | 14891 (13980, 341) | 14.78 (13.41, 0.29) | 52.69 (49.92, 1.84) |
| **140** | 4.41 (4.49, 0.05) | 17273 (16238, 248) | 18.14 (17.67, 0.23) | 61.21 (58.85, 2.24) |
| **160** | 3.78 (3.83, 0.03) | 28621 (27643, 287) | 16.47 (15.84, 0.21) | 46.14 (44.58, 1.42) |

[a]Maximum value. Values in the bracket are average value of 10 devices and standard deviation.

Fig. 4.7 shows the AFM images of PVK: PBD: $Ir(mppy)_3$ and PVK: PBD: TPD: $Ir(mppy)_3$ thin films annealed at 80 °C. No significant difference in the RMS roughness value of the thin films were observed on addition of PBD and TPD into the host and the films are found to show a RMS roughness value of 0.306 nm and 0.322 nm respectively which is similar to the rms roughness value of 0.328 nm for the PVK: $Ir(mppy)_3$ thin film annealed at 80 °C. Therefore, the improvement in device performance in mixed host based devices is expected to be due to the better charge balance of the emissive layer that facilitates improved recombination.

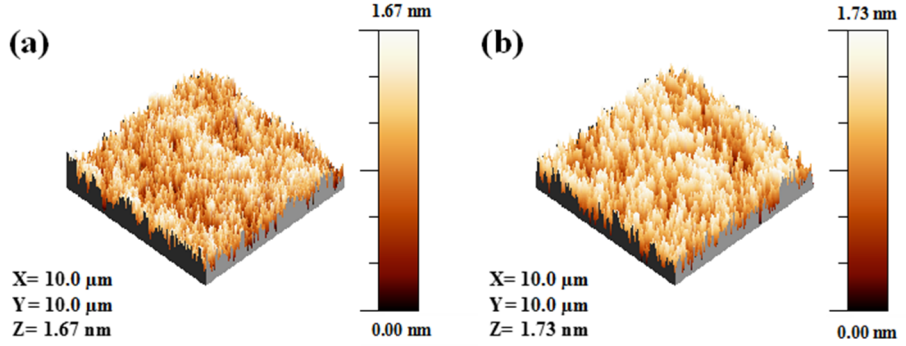


**Fig. 4.7** The AFM images of PVK: PBD: $Ir(mppy)_3$ (a) and PVK: PBD: TPD: $Ir(mppy)_3$ (b) thin films annealed at 80 °C.

In case of the devices with sole PVK as host material, the significantly low electron mobility of electron as compared to that of hole can lead to the formation of space charge in the EML thereby reducing the device efficiency. Due to its high electron mobility, the addition of PBD improves the electron transport ability of PVK and therefore the build-up of space charge in such devices is less. It is therefore observed from that the current density, brightness and the LE of the phOLEDs for a particular voltage at a constant annealing temperature is more in case of the devices with PVK: PBD host as compared to that of PVK host. For example, the maximum brightness and the maximum luminous efficiency of the devices with PVK: PBD host was found to improve to 8677 cd $m^{-2}$ and 30.20 cd $A^{-1}$ from 5423 cd $m^{-2}$ and 20.65 cd $A^{-1}$ with PVK as host for an annealing temperature of 80 °C. Also, similar to the case of PVK based devices, all the key device parameters of the phOLEDs were found to improve with an increase in the annealing temperature. The maximum brightness and the maximum luminous efficiency of the device with PVK: PBD host was found to improve from 8677 cd $m^{-2}$ and 30.20 cd $A^{-1}$ to 14873 cd $m^{-2}$ and 48.12 cd $A^{-1}$ respectively with increasing the annealing temperature from 80 °C to 140 °C. However,

although the maximum brightness value has improved from 14873 cd $m^{-2}$ to 20432 cd $m^{-2}$ for the annealing temperature from 160 °C, the LE of the phOLEDs was found to decrease to decrease to 42.16 cd $A^{-1}$ as compared to that of 48.12 cd $A^{-1}$ at 140 °C. Annealing temperature, however, was not found to affect the electroluminescence of the phOLEDs as no visible influence was observed in the normalized EL spectra of the devices (Fig.4.5 (d)).

The use of ternary host of PVK: PBD: TPD was found to further improve the device performance. Although PVK is considered as a hole transporting material, still the hole mobility of the PVK is of the order of $10^{-9}$. PBD however has an electron mobility of the order of $10^{-5}$. Therefore, addition of TPD in small quantity is expected to improve the hole mobility of PVK and the charge balance of the emissive layer. As a result the maximum brightness and the maximum luminous efficiency of the devices with PVK: PBD: TPD host was found to improve to 12618 cd $m^{-2}$ and 35.15 cd $A^{-1}$ as compared to that of 8677 cd $m^{-2}$ and 30.20 cd $A^{-1}$ for PVK:PBD host and 5423 cd $m^{-2}$ and 20.65 cd $A^{-1}$ for PVK host for an annealing temperature of 80 °C. Also in case of PVK: PBD: TPD host based devices, the maximum brightness and the maximum luminous efficiency of the device was found to improve from 12618 cd $m^{-2}$ and 35.15 cd $A^{-1}$ to 17273 cd $m^{-2}$ and 61.21 cd $A^{-1}$ respectively with increasing the annealing temperature from 80 °C to 140 °C. However, although the maximum brightness value has improved from 17273 cd $m^{-2}$ to 28621 cd $m^{-2}$ for the annealing temperature from 160 °C, the LE of the phOLEDs was found to decrease to decrease to 46.14 cd $A^{-1}$ as compared to that of 61.21 cd $A^{-1}$ at 140 °C. Annealing temperature, however, was not found to affect the electroluminescence of the phOLEDs as no visible influence was observed in the normalized EL spectra of the devices (Fig.4.6 (d))

## 4.4 Conclusions

In summary, Highly efficient, solution processed green phosphorescent organic light emitting diode (phOLED) based on $Ir(mppy)_3$ with single and mixed host namely PVK (Poly(9-vinylcarbazole)), PVK: PBD (2-(4-Biphenylyl)-5-(4-tert-butylphenyl)-1,3,4-oxadiazole), PVK: PBD: TPD (N,N′-Bis(3-methylphenyl)-N,N′-diphenylbenzidine) have been reported. The annealing temperature of the emissive layer is found to play a significant role in defining the device performance of an phOLED. The different host combinations were annealed at 80 °C, 100 °C, 120 °C, 140 °C and 160 °C and the effect of annealing temperature on the morphological, optical and electrical properties of the phOLEDs have been elucidated. Higher annealing temperature is found to increase the interchain

interaction in the emissive layer that leads to increased conductivity and higher current density in the device. It was also observed that the RMS roughness of the EML increases with increasing annealing temperature due to the formation of a compact structure that leads to strong interfacial adhesion with adjacent layers and facilitate more electron injection into the EML, thereby improving the charge balance in the EML. The device performance is found to increase with increasing annealing temperature and best result was observed for the devices annealed at 140 $^{o}$C. However, the EL spectra of the phOLEDs was not influenced by the different annealing temperature of the EML. Further, addition of electron and hole transporting material in appropriate ratio is found to improve the charge balance of the emissive layer that results in improved device performance. Among all, PVK: PBD: TPD host based devices annealed at 140 $^{o}$C is found to give the maximum brightness of 17273 cd $m^{-2}$ and a maximum luminous efficiency of 61.21 cd $A^{-1}$.

## 4.5 References


1. C. W. Tang and S. A. Vanslyke, *Appl. Phys. Lett.*, 1987, **51**, 913-915.
2. C. W. Tang, S. A. Vanslyke and C. H. Chen, *J. Appl. Phys.*, 1989, **65**, 3610-3616.
3. J. H. Burroughes, D. D. C. Bradley, A. R. Brown, R. N. Marks, K. Mackay, R. H. Friend, P. L. Burn and A. B. Holmes, *Nature*, 1990, **347**, 539-541.
4. M. A. Baldo, D. F. O'Brien, Y. You, A. Shoustikov, S. Sibley, M. E. Thompson and S. R. Forrest, *Nature*, 1998, **395**, 151-154.
5. V. Bulovic, P. E. Burrows and S. R. Forrest, *Semiconduct. Semimet.*, 2000, **64**, 255-306.
6. W. Helfrich and W. G. Schneider, *J. Chem. Phys.*, 1966, **44**, 2902-2909.
7. T. Tsutsui, M. J. Yang, M. Yahiro, K. Nakamura, T. Watanabe, T. Tsuji, Y. Fukuda, T. Wakimoto and S. Miyaguchi, *Jpn. J. Appl. Phys. 2*, 1999, **38**, L1502-L1504.
8. C. Adachi, M. A. Baldo, M. E. Thompson and S. R. Forrest, *J. Appl. Phys.*, 2001, **90**, 5048-5051.
9. S. Reineke, F. Lindner, G. Schwartz, N. Seidler, K. Walzer, B. Lussem and K. Leo, *Nature*, 2009, **459**, 234-U116.
10. M. A. Baldo, C. Adachi and S. R. Forrest, *Phys. Rev. B*, 2000, **62**, 10967-10977.
11. L. Li, T. Q. Hu, C. R. Yin, L. H. Xie, Y. Yang, C. Wang, J. Y. Lin, M. D. Yi, S. H. Ye and W. Huang, *Polym. Chem.-Uk*, 2015, **6**, 983-988.
12. C. W. Lee and J. Y. Lee, *Adv. Mater.*, 2013, **25**, 596-600.
13. H. Liu, G. Cheng, D. H. Hu, F. Z. Shen, Y. Lv, G. N. Sun, B. Yang, P. Lu and Y. G. Ma, *Adv. Funct. Mater.*, 2012, **22**, 2830-2836.
14. C. J. Zheng, J. Ye, M. F. Lo, M. K. Fung, X. M. Ou, X. H. Zhang and C. S. Lee, *Chem. Mater.*, 2012, **24**, 643-650.
15. H. Fukagawa, N. Yokoyama, S. Irisa and S. Tokito, *Adv. Mater.*, 2010, **22**, 4775-4778.
16. P. Schrogel, M. Hoping, W. Kowalsky, A. Hunze, G. Wagenblast, C. Lennartz and P. Strohriegl, *Chem. Mater.*, 2011, **23**, 4947-4953.
17. D. Wagner, S. T. Hoffmann, U. Heinemeyer, I. Munster, A. Kohler and P. Strohriegl, *Chem. Mater.*, 2013, **25**, 3758-3765.
18. J. Q. Ding, Q. Wang, L. Zhao, D. G. Ma, L. X. Wang, X. B. Jing and F. S. Wang, *J. Mater. Chem.*, 2010, **20**, 8126-8133.
19. D. Kim, L. Y. Zhu and J. L. Bredas, *Chem. Mater.*, 2012, **24**, 2604-2610.

20. C. H. Yang, M. Mauro, F. Polo, S. Watanabe, I. Muenster, R. Frohlich and L. De Cola, *Chem. Mater.*, 2012, **24**, 3684-3695.
21. M. Cai, T. Xiao, E. Hellerich, Y. Chen, R. Shinar and J. Shinar, *Adv. Mater.*, 2011, **23**, 3590-3596.
22. A. C. Arias, J. D. MacKenzie, I. McCulloch, J. Rivnay and A. Salleo, *Chem. Rev.*, 2010, **110**, 3-24.
23. W. Brutting, S. Berleb, A. G. Muckl, *Org. Electron.*,2002, **2**,1-36.
24. J. S. Huang, G. Li, E. Wu, Q. F. Xu and Y. Yang, *Adv. Mater.*, 2006, **18**, 114-117.
25. M. C. Gather, S. Köber, S. Heun andK. Meerholz, *J. Appl. Phys.*, 2009, **106**, 024506-024506(10).
26. S. Burns, J. MacLeod, T. T. Do, P. Sonar and S. D. Yambem, *Sci. Rep.*, 2017, **7**, 40805 (1-8).
27. T. O. Nguyen, R. C. Kwong, M. E. Thompson and B. J. Schwartz, *Appl. Phys. Lett.*, 2000, **76**, 2454-2456.
28. J. Y. Park and R. C. Advincula, *Phys. Chem. Chem. Phys.*, 2014, **16**, 8589-8593.
29. J. Kido, K. Hongawa, K. Okuyama and K. Nagai, *Appl. Phys. Lett.*, 1994, **64**, 815-817.
30. C. Zhang, H. Vonseggern, B. Kraabel, H. W. Schmidt and A. J. Heeger, *Synthetic Met.*, 1995, **72**, 185-188.
31. E. Gautier-Thianche, C. Sentein, A. Lorin, C. Denis, P. Raimond and J. M. Nunzi, *J. Appl. Phys.*, 1998, **83**, 4236-4241.
32. T. Earmme and S. A. Jenekhe, *J. Mater. Chem.*, 2012, **22**, 4660-4668.
33. H. B. Wu, G. J. Zhou, J. H. Zou, C. L. Ho, W. Y. Wong, W. Yang, J. B. Peng and Y. Cao, *Adv. Mater.*, 2009, **21**, 4181-4184.
34. K. M. Vaeth and C. W. Tang, *J. Appl. Phys.*, 2002, **92**, 3447-3453.
35. X. H. Yang, D. Neher, D. Hertel and T. K. Daubler, *Adv. Mater.*, 2004, **16**, 161-166.
36. J. J. Park, T. J. Park, W. S. Jeon, R. Pode, J. Jang, J. H. Kwon, E. S. Yu and M. Y. Chae, *Org. Electron.*, 2009, **10**, 189-193.
37. D. H. Lee, J. S. Choi, H. Chae, C. H. Chung and S. M. Cho, *Displays*, 2008, **29**, 436-439.
38. S. A. Choulis, V. E. Choong, M. K. Mathai and F. So, *Appl. Phys. Lett.*, 2005, **87**, 113503-113503(3).

39. K. Wei, G. Wen, Y. Zhao, Z. Lin, X. Mei, L. Huangb and Q. Ling, *J. Mater. Chem. C*, 2016, **4**, 9804-9812.

40. T. W. Lee and O. O. Park, *Adv. Mater.*, 2000, **12**, 801-804.

41. J. Luo, X. Li, Q. Hou, J. Peng, W. Yang, and Y. Cao, *Adv. Mater.*, 2007, **19**, 1113-1117.

# CHAPTER-5

## Solution processed WPLEDs with good color stability and high color rendering index via a phosphor-sensitized system

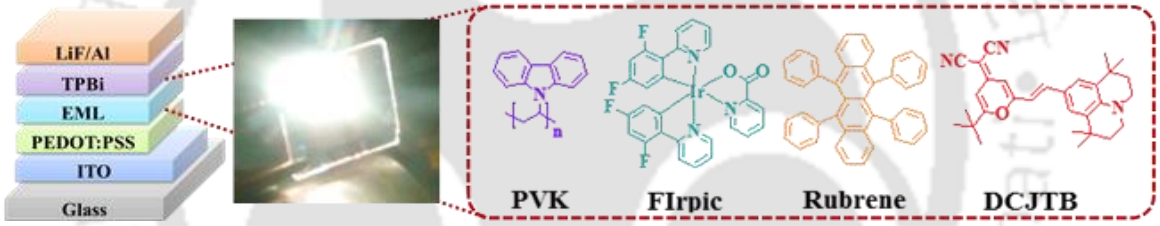


*Chemistry Select, 2017, 2, 3184-3190*

# Solution processed WPLEDs with good color stability and high color rendering index via a phosphor-sensitized system


## ***Abstract***

*"In this chapter, we present efficient, solution processed white polymer light emitting diodes (WPLEDs) with good color stability and high color rendering index (CRI) via a phosphor-sensitized system using blue phosphorescent dye Bis[2-(4,6-difluorophenyl)pyridinato-C2,N](picolinato)iridium(III) (FIrpic) as emitter and sensitizer, and the fluorescent dye Rubrene and 4-(dicyanomethylene)-2-t-butyl-6-(1,1,7,7-tetramethyljulolidyl-9-enyl)-4H-pyran (DCJTB) as yellow and orange/red emitter respectively. Two different fluorophores, Rubrene and DCJTB, were chosen due to their different emission zone and different charge trapping ability. WPLEDs, in which FIrpic with Rubrene or DCJTB is doped at different feed ratios into poly (N-vinylcarbazole) (PVK) host, were fabricated and the effect of their concentration on the current density vs. voltage (J-V) characteristics and the electroluminescence (EL) spectra were studied. WPLEDs made with FIrpic:Rubrene (10:1) and FIrpic:DCJTB (80:1) were found to give CIE coordinates of (0.30, 0.42) and (0.34, 0.40) with CRI value of 58 and 76 at luminous efficiencies of 4.91 cd $A^{-1}$ and 2.79 cd $A^{-1}$ respectively. Finally, FIrpic, Rubrene and DCJTB were doped into PVK to get high quality white light and CIE coordinates of (0.41, 0.43) with a CRI value of 78 at luminous efficiency of 4.73 cd $A^{-1}$ was achieved for FIrpic : Rubrene : DCJTB feed ratio of (100:8:1)."*

## 5.1 Introduction

White organic light emitting diodes (WOLEDs) are one of the most vital developments in the arena of optoelectronic devices due to their potential applications in the field of flat panel displays and new generation solid-state lighting sources[1-7]. Among them, white polymer light emitting diodes (WPLEDs) have attracted great attention as they can be solution processed leading to a low-cost manufacturing process to fabricate large area and flexible devices [8-14]. Usually white light is obtained by simultaneous emission from two complementary colors or the three primary colors. To achieve this, the most common and easy way is doping small molecule of different emission region in appropriate ratio in a polymer matrix. The polymer is either used as host material if there is complete energy transfer or both as blue emitter and host material in case of partial energy transfer. This generally gives rise to all fluorescent, all phosphorescent, fluorescent-phosphorescent and phosphorescent-fluorescent systems for realizing white light. The large availability of room temperature fluorescent materials makes the all fluorescent system attractive but due to its inability to harvest triplet excitons, the internal quantum efficiency of such WPLEDs is limited to 25% [15,16]. An all phosphorescent system is of particular interest in this regard due to their ability to harvest both singlet and triplet excitons and therefore such a system can achieve higher quantum efficiency of approximately 100% [17,18]. However, they suffer from the disadvantage of efficiency roll off at high current density owing to triplet-triplet annihilation due to the high dopant concentration of the phosphorescent dyes [19-21]. In case of fluorescent-phosphorescent system, a blue fluorescent emitter together with either a yellow or a combination of green and red phosphor dopants is used [22-24]. It is a well-known fact that any fluorescent material has lower triplet energy levels compared to that of the phosphorescent materials. Therefore, the sole purpose of achieving a high quantum efficiency is not satisfied in this system due to the possibility of energy transfer from the phosphorescent emitters to the fluorescent emitter resulting in a decrease in the luminous efficiency. A solution to this problem is introduction of a phosphorescent dye as a sensitizer in fluorescence-based devices [25-29]. In this approach, a blue phosphorescent material is used as blue emitter and sensitizer in a fluorescence-contained host and energy from both the singlet and triplet excitons of the blue phosphor transfers on the fluorophore via long range

dipole-dipole Förster process finally leading to the internal efficiency of fluorescence as high as 100% [29]. It solves the efficiency role off problem of the all phosphorescence system by reducing the triplet density at high current density. Yet, the charge trapping ability and the concentration quenching effect of the fluorescent dopant molecule plays an important role in controlling the efficiency of above fore said system and is considered as the main cause for energy loss [30]. Therefore, to realize efficient phosphor-sensitized WPLEDs, one should consider the charge trapping ability of the fluorescent dopant molecule and its concentration should be kept as low as possible. Here, we present efficient, solution processed WPLEDs with good color stability and high CRI via a phosphor-sensitized system using blue phosphorescent dye FIrpic as emitter and sensitizer, and the fluorescent dye Rubrene and DCJTB as yellow and orange/red emitter respectively. Two different fluorophores, Rubrene and DCJTB, were chosen due to their different emission zone and different charge trapping ability. WPLEDs, in which FIrpic with Rubrene or DCJTB is doped at different feed ratios into PVK host, were fabricated and the effect of their concentration on the current density vs. voltage (J-V) characteristics and the EL spectra were studied. WPLEDs made with FIrpic : Rubrene (10:1) and FIrpic : DCJTB (80:1) were found to give CIE coordinates of (0.30, 0.42) and (0.34, 0.40) with CRI value of 58 and 76 at luminous efficiency of 4.91 cd $A^{-1}$ and 2.79 cd $A^{-1}$ respectively. Finally, FIrpic, Rubrene and DCJTB were doped into PVK to get high quality white light and CIE coordinates of (0.41, 0.43) with a CRI value of 78 at luminous efficiency of 4.73 cd $A^{-1}$ was achieved for FIrpic: Rubrene: DCJTB feed ratio of (100:8:1).

## 5.2 Experimental

Fig. 5.1 shows the chemical structures of the materials along with their energy level diagram as used in the WPLED fabrication. Poly (ethylendioxythiophene): poly (styrene sulfonic acid) (PEDOT: PSS) was purchased from Clevios and all other materials were purchased from Sigma Aldrich and used as received.

ITO substrates after patterning were used as transparent anodes and cleaned thoroughly by ultrasonication in soap solution, Millipore water, acetone and isopropanol, each for ten minutes at room temperature followed by 30 min of UV-Ozone treatment. PEDOT: PSS was spin coated immediately after UV-Ozone

treatment at 3000 rpm for 60 sec and annealed at 120 °C for 1 hr to give a film thickness of 40 nm.

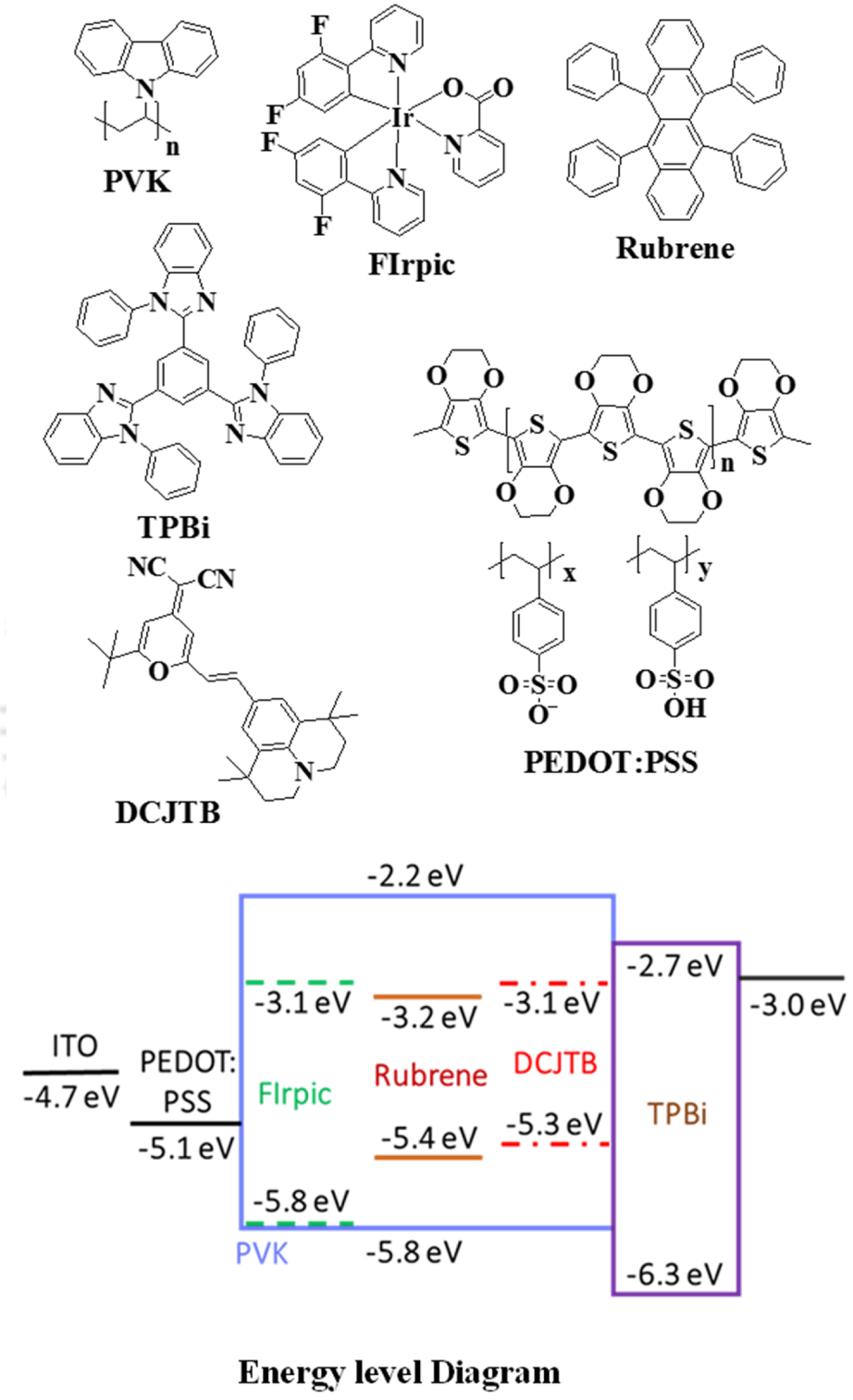


**Fig. 5.1** Chemical structures of the materials along with their energy level diagram as used in the WPLED fabrication.

Separate solutions were made containing PVK: FIrpic: Rubrene, PVK: Firpic: DCJTB and PVK: FIrpic: Rubrene: DCJTB in chlorobenzene solution and were then spin coated above PEDOT: PSS layer to give the EML and were baked at 140 °C for 1 hour to remove the residual solvent. Prior to spin coating the solutions were stirred for 30 min to ensure efficient doping and filtered using 0.45µm filter. The substrates were then transferred to the evaporation chamber and TPBi, interfacial layer LiF and Cathode material Al were thermally evaporated at a base pressure of $10^{-6}$ mbar at a rate of 2 Å/s, 0.1 Å/s and 10 Å/s respectively. The active area of the PLEDs was 24 $mm^2$. The current density vs. voltage (J-V) characteristics of the WPLEDs were measured using a Keithley 2400 source meter, whereas the brightness vs. voltage (B-V) characteristics and the EL spectra were recorded using Konica Minolta CS 2000 Spectroradiometer. All characterizations were done inside glove box under argon atmosphere.

.

## 5.3 Results and discussion

### 5.3.1 Photophysical studies

Fig. 5.2 (a) shows the photoluminescence (PL) spectrum of PVK and the PL and UV-Vis absorption (UV) spectra of FIrpic, Rubrene, and DCJTB. The PL spectrum of FIrpic shows a peak at 467 nm with a shoulder peak at 495 nm whereas the emission peak of Rubrene and DCJTB are at 570 nm and 630 nm respectively, making them suitable for realizing white light while combining at the right proportions.

The small spectral overlap between the UV spectra of Rubrene and DCJTB and the PL spectrum of PVK suggests that the energy transfer should not occur efficiently from PVK to Rubrene or DCJTB. However, due to the excellent overlap between the PL spectrum of FIrpic and the absorption of Rubrene and DCJTB, FIrpic can be used as an energy transfer bridge between PVK and Rubrene or DCJTB so that energy can transfer easily from PVK to Rubrene or DCJTB.

Fig. 5.2 (b) shows the probable energy transfer mechanism. Under applied voltage, excitons are generated in PVK which then moves from singlet state of PVK to singlet state of FIrpic due to energy transfer and then to the triplet state of FIrpic through ISC. As a result we get the blue emission from FIrpic. Due to the overlap of the UV spectra of DCJTB and Rubrene with the emission spectra of FIrpic, some of the excitons moves from the triplet state of the FIrpic to the singlet state of the DCJTB or Rubrene and gives yellow or red emission.

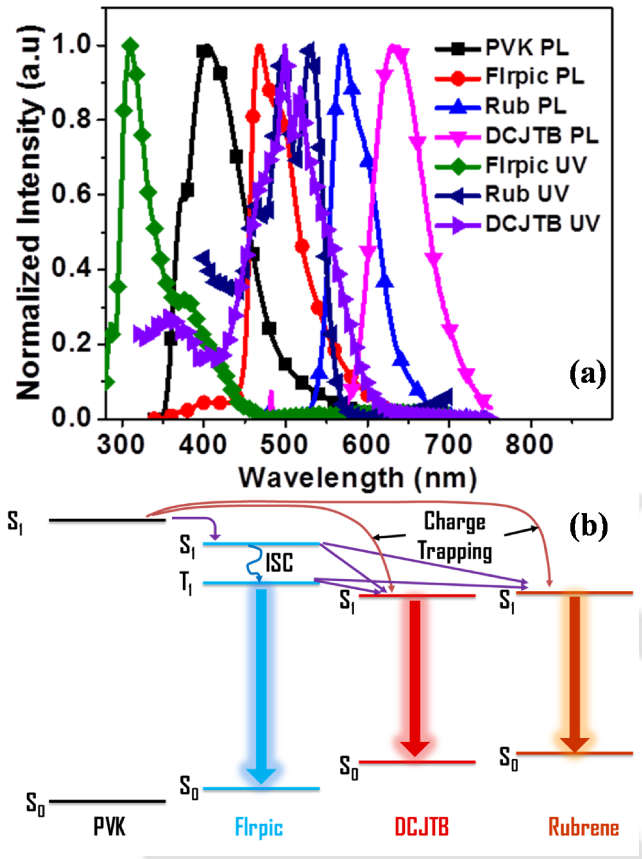


**Fig. 5.2** PL spectrum of PVK and the PL and absorption spectra of FIrpic, Rubrene, and DCJTB.

### 5.3.2 FIrpic: Rubrene based WPLEDs

WPLEDs using FIrpic as blue emitter and sensitizer with Rubrene as yellow dopant have been fabricated in ITO/PEDOT: PSS (40 nm)/emissive layer (EML) (110 nm)/TPBi (30 nm)/LiF (1 nm)/Al (100 nm) structure. PVK was used as the host material in the EML and the EML composition is thus PVK: FIrpic: Rubrene. The doping concentration of FIrpic was fixed at 10 wt% of the blend, whereas, FIrpic: Rubrene weight ratio was varied to tune the electroluminescent properties of the devices. The devices with FIrpic is referred to as Device B (10 wt % FIrpic) whereas devices with different FIrpic: Rubrene weight ratio are referred to as Device R1 (5: 1), Device R2 (8: 1), Device R3 (10: 1) and Device R4 (15: 1). The key device parameters of the as fabricated WPLEDs are listed in Table 5.1. Fig. 5.3 (a) shows the normalized EL spectra of Devices R1-R4 at 12.0 V. The EL spectra of all the devices cover almost the wavelength range of 450-650 nm and exhibit three clear peaks at 475 nm, 500 nm and 540 nm. The first two peaks of the EL spectra centered at 475 nm and 500 nm is clearly due to the emission from FIrpic whereas the peak at 540 nm is due to the emission from Rubrene. The slight blue shift of the Rubrene peak can be due to

the low concentration of the Rubrene molecule in the EML. Although the EML contains PVK as host material no emission was observed in the wavelength range of 400-450 suggesting complete energy transfer from the host material to the dopant dyes. From the EL spectra, it was also observed that the emission intensity is altered with the FIrpic: Rubrene weight ratio. The intensity of the yellow emission is found to increase as the FIrpic: Rubrene weight ratio is decreased from (15:1) in device R4 to (5:1) in device R1. As a result, the CIE coordinates (at 12.0 V) of the devices R1-R4 also varied from (0.33, 0.45) to (0.29, 0.42), emitting almost in the white range. Device R3 with a CIE coordinate of (0.30, 0.42) is found to be the closest to white light and the EL spectra of device R3 at different applied voltage is shown in Fig. 5.3 (b). From Fig. 5.3 (b), it was found that the emission color of device R3 is almost insensitive to the applied voltage. However, it can be seen that the relative intensity of the blue component of the emission increases slightly with the applied voltage which may be due to the different roles of Rubrene and FIrpic molecules in the trapping and transport of electrons in EL processes.

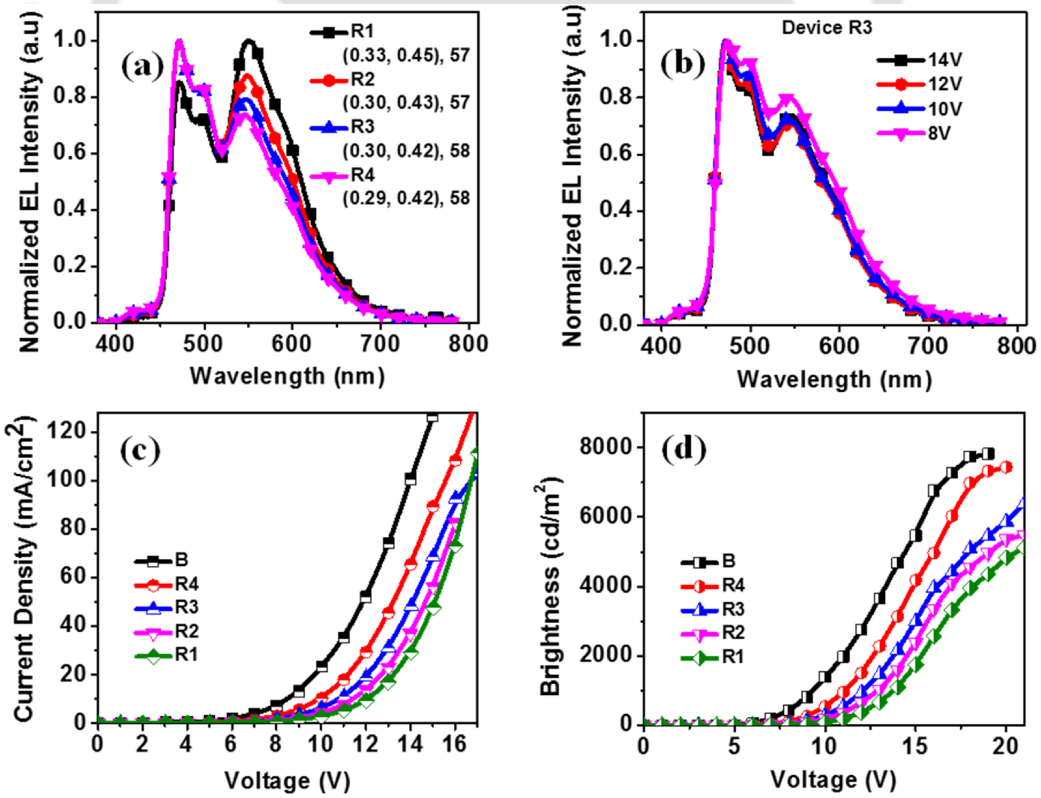


**Fig. 5.3** The EL spectra of device R1-R4 (a), EL spectrum of device R3 at different applied voltage (b), current density vs. voltage (J-V) characteristics (c) of device B and R1-R4 and brightness vs. voltage (B-V) characteristics of device B and R1-R4 (d).

**Table 5.1** Key device parameters of FIrpic: Rubrene based WPLEDs.

| Device Name | Turn on voltage (V) | Maximum brightness ($cd/m^2$) | CIE at 12.0 V | CRI | Power Efficiency[a] (lm/W) | Luminous Efficiency[a] LE (cd/A) |
|---|---|---|---|---|---|---|
| **B** | 4.06 (4.17, 0.11) | 7823 (7585, 179) | - | - | 6.11 (5.97, 0.10) | 2.59 (2.41, 0.15) |
| **R1** | 6.29 (6.39, 0.09) | 5129 (4942, 156) | 0.33, 0.45 | 57 | 3.88 (3.65, 0.19) | 1.19 (1.01, 0.11) |
| **R2** | 5.50 (5.62, 0.13) | 5490 (5285, 185) | 0.30, 0.43 | 57 | 4.72 (4.66, 0.07) | 1.34 (1.08, 0.14) |
| **R3** | 5.23 (5.39, 0.20) | 6398 (6186, 199) | 0.30, 0.42 | 58 | 4.91 (4.82, 0.11) | 1.37 (1.11, 0.13) |
| **R4** | 4.84 (4.94, 0.09) | 7443 (7168, 322) | 0.29, 0.43 | 58 | 5.29 (5.13, 0.02) | 1.42 (1.23, 0.09) |

[a]Maximum value. Values in the bracket are average value of 10 devices and standard deviation.

Owing to the excitons formation due to the charge trapping on Rubrene molecules, more yellow emission is mainly observed at lower voltage. However, at high bias more excitons are formed on both Firpic and Rubrene due to large injection of electrons and holes and as a result emission from FIrpic molecule appears. The variation of EL spectra with voltage is less owing to the energy level alignment between FIrpic and Rubrene molecule. Fig. 5.3 (c) shows the current density vs. voltage curves of the as fabricated WPLEDs. From Fig. 5.3 (c) it can be seen that on increasing the Rubrene concentration, the current density at the same applied voltage decreases. This can be due to the charge trapping at the Rubrene molecule. The LUMO and HOMO energy levels of the Rubrene molecule acts as traps for both electrons and holes resulting in a direct recombination of holes and electrons. This lowers the electron and hole transport in the emissive layer thereby increasing the driving voltage with increased Rubrene concentration. The Brightness vs. voltage curve of the FIrpic: Rubrene based WPLEDs are shown in Fig. 5.3 (d). The brightness of the devices is found to reduce with increasing Rubrene concentration in the EML.

### 5.3.3 FIrpic: DCJTB based WPLEDs

WPLEDs using FIrpic as blue emitter and sensitizer with DCJTB as orange/red dopant have been fabricated in ITO/PEDOT: PSS (40 nm)/emissive layer (EML) (110 nm)/TPBi (30 nm)/LiF (1 nm)/ Al (100 nm) structure. Since Rubrene emits in the 540 nm range in FIrpic: Rubrene based devices, they cover only the 450-650 nm range of the visible spectrum thereby reducing its color quality (CRI< 60). DCJTB was used mainly for two

reasons: 1) It emits in the range of 450-750 nm, thus covering more region of the visible range. 2) Its different charge trapping ability allows us to study the effect of charge trapping on various device parameters. Similar to the FIrpic system, in this case also PVK was used as the host material in the EML and the EML composition is thus PVK: FIrpic: DCJTB. The doping concentration of FIrpic was fixed at 10 wt% of the blend whereas FIrpic: DCJTB weight ratio was varied and devices with different FIrpic: DCJTB weight ratio are referred as Device D1 (40: 1), Device D2 (60: 1), Device D3 (80: 1) and Device D4 (100: 1). The key device parameters of the as fabricated WPLEDs are listed in Table 5.2. Fig. 5.4 (a) shows the normalized EL spectra of Devices D1-D4 at 12.0 V. Due to DCJTB the EL spectra of all the devices cover a much broader wavelength range of 450-750 nm and exhibit two peaks at 475 nm and 500 nm due to the emission from FIrpic and a third peak at 600 nm due to the emission from DCJTB.

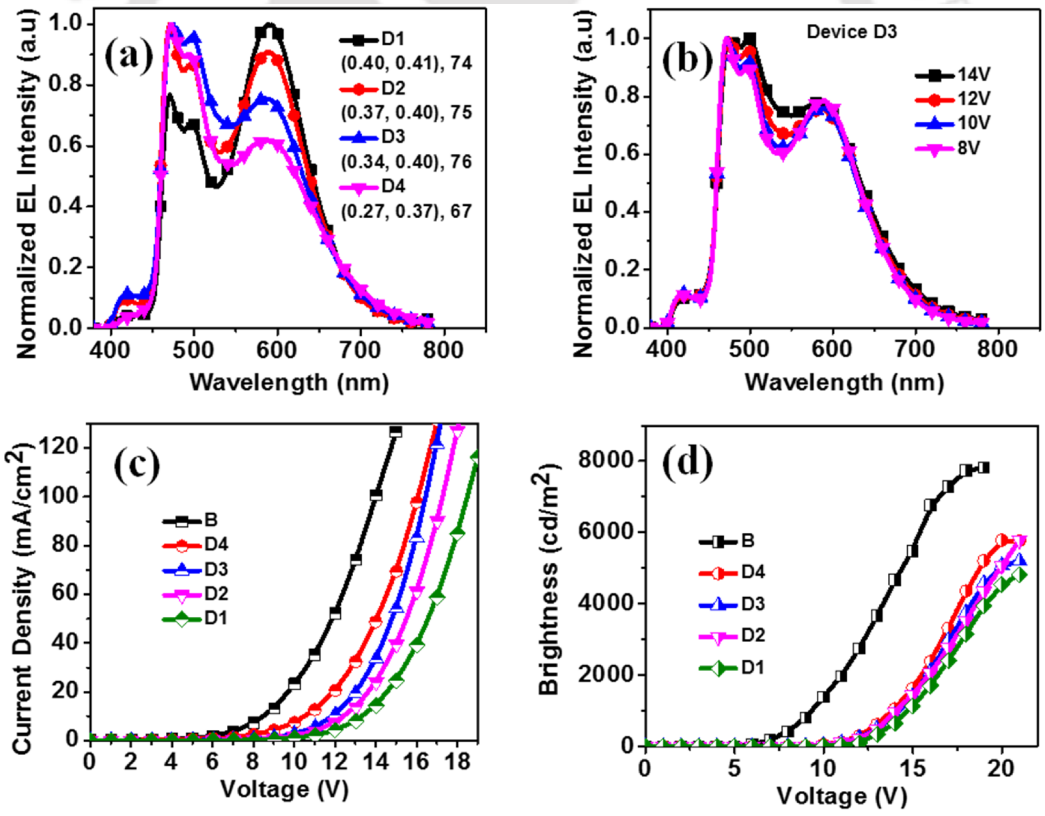


**Fig. 5.4** The EL spectra of device D1-D4 (a), EL Spectrum of device D3 at different applied voltage (b), current density vs. voltage (J-V) characteristics of device B and D1-D4 (c) and brightness vs. voltage (B-V) characteristics of device B and D1-D4 (d).

**Table 5.2** Key device parameters of FIrpic: DCJTB based WPLEDs.

| Device Name | Turn on voltage (V) | Maximum brightness ($cd/m^2$) | CIE at 12.0 V | CRI | Power Efficiency[a] (lm/W) | Luminous Efficiency[a] LE (cd/A) |
|---|---|---|---|---|---|---|
| **B** | 4.06 (4.17, 0.11) | 7823 (7585, 179) | - | - | 6.11 (5.97, 0.10) | 2.59 (2.41, 0.15) |
| **D1** | 6.89 (6.98, 0.12) | 4129 (4004, 159) | 0.40, 0.41 | 74 | 2.41 (2.28, 0.17) | 0.56 (0.48, 0.09) |
| **D2** | 6.03 (6.14, 0.08) | 5189 (5044, 114) | 0.37, 0.40 | 75 | 2.57 (2.48, 0.06) | 0.60 (0.55, 0.08) |
| **D3** | 5.86 (5.93, 0.06) | 5198 (5093, 88) | 0.34, 0.40 | 76 | 2.79 (2.67, 0.14) | 0.65 (0.61, 0.06) |
| **D4** | 5.77 (5.85, 0.06) | 5786 (5609, 144) | 0.27, 0.37 | 67 | 3.23 (3.11, 0.11) | 0.75 (0.67, 0.10) |

[a]Maximum value. Values in the bracket are average value of 10 devices and standard deviation.

The intensity of the orange emission is found to increase as the FIrpic: DCJTB weight ratio is increased from (100:1) in device D4 to (40:1) in device D1. All the devices are found to emit in the white range with CIE coordinates (at 12.0 V) of the devices D1–D4 varying from (0.40, 0.41) to (0.27, 0.37). Devices D3 with a CIE coordinate of (0.34, 0.40) is found to be the closest to white light and the EL spectra of device D3 at different applied voltage is shown in Fig. 5.4 (b). From Fig. 5.4 (b), it was found that the emission spectra of device D3 is almost stable at different applied voltage. However, there is a slight increase in blue emission at higher applied voltage which may be due to the strong charge trapping nature of the DCJTB molecule. The variation of the EL spectra with respect to voltage in case of FIrpic: DCJTB system is slightly more as compared to that of FIrpic: Rubrene system due to the strong charge trapping nature of the DCJTB molecule as compared to that of Rubrene molecule. This becomes evident once we study the current density vs. voltage curves (J-V) of the FIrpic: DCJTB based WPLEDs as shown in 5.4 (c). From 5.4 (c), it can be seen that on increasing the DCJTB concentration, the current density at the same applied voltage decreases. In other words, the device operating voltage increases with increasing DCJTB concentration. Similar type of results was also obtained in FIrpic: Rubrene based WPLEDs. However, the shift in device operating voltage is more in FIrpic: DCJTB based WPLEDs as compared to that of FIrpic: Rubrene based WPLEDs which supports the earlier assumption that DCJTB molecule has a strong charge trapping nature as compared to that of Rubrene. The Brightness vs. voltage curve of the FIrpic:

DCJTB based WPLEDs are shown in 5.4 (d). The brightness of the devices is found to reduce with increasing DCJTB concentration in the EML.

### 5.3.4 FIrpic: Rubrene: DCJTB based WPLEDs

To further improve the color quality, PVK was doped with FIrpic, Rubrene and DCJTB together, and WPLEDs were fabricated in the ITO/PEDOT: PSS (40 nm)/emissive layer (EML) (110 nm)/TPBi (30 nm)/LiF (1 nm)/ Al (100 nm) architecture. From the earlier results, the weight ratio of Rubrene:DCJTB was fixed at (8:1) and the FIrpic: Rubrene: DCJTB weight ratio was varied and devices with different FIrpic: Rubrene: DCJTB weight ratio are referred as Device W1 (40: 8: 1), Device W2 (60: 8: 1), Device W3 (80: 8: 1) and Device W4 (100: 8: 1). The key device parameters of the as fabricated WPLEDs are listed in Table 5.3. Fig. 5.5 (a) shows the normalized EL spectra of Devices W1-W4 at 12.0 V. The EL spectra of all the devices are found to cover the wavelength range of 450-750 nm and exhibit four clear peaks at 475 nm, 500 nm, 540 nm and 580 nm. The peaks at 475 nm and 500 nm are clearly due to the emission from FIrpic and the peaks at 540 nm and 580 nm are due to the emission from Rubrene and DCJTB molecule respectively.

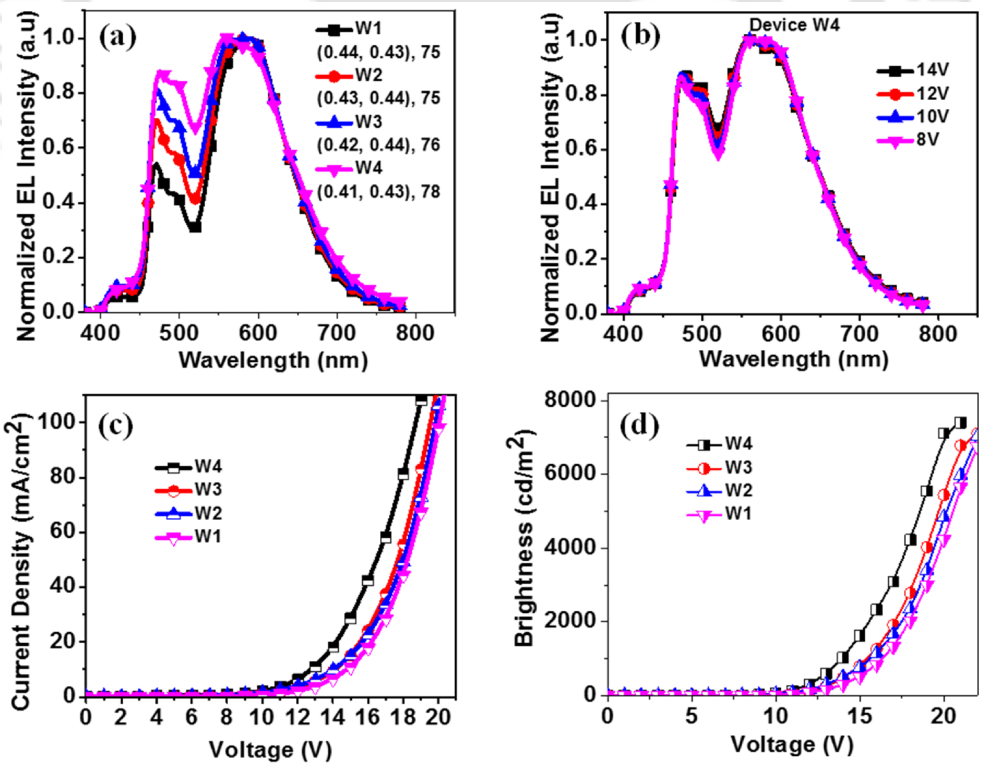


**Fig. 5.5** The EL spectra of device W1-W4 (a), EL Spectrum of device W4 at different applied voltage (b), current density vs. voltage (J-V) characteristics of device W1-W4 (c) and brightness vs. voltage (B-V) characteristics of device W1-W4 (d).

**Table 5.3.** Key device parameters of FIrpic: Rubrene: DCJTB based WPLEDs.

| Device Name | Turn on voltage (V) | Maximum brightness ($cd/m^2$) | CIE at 12.0 V | CRI | Power Efficiency[a] (lm/W) | Luminous Efficiency[a] LE (cd/A) |
|---|---|---|---|---|---|---|
| **W1** | 6.58 (6.63, 0.04) | 6746 (6645, 108) | 0.44, 0.43 | 75 | 3.94 (3.86, 0.07) | 0.80 (0.72, 0.11) |
| **W2** | 6.45 (6.54, 0.06) | 7024 (6847, 129) | 0.43, 0.44 | 75 | 4.24 (4.11, 0.10) | 0.86 (0.77, 0.13) |
| **W3** | 6.31 (6.44, 0.09) | 7103 (7023, 56) | 0.42, 0.44 | 76 | 4.40 (4.32, 0.06) | 0.90 (0.84, 0.11) |
| **W4** | 5.90 (6.06, 0.07) | 7395 (7195, 142) | 0.41, 0.43 | 78 | 4.73 (4.64, 0.08) | 1.06 (0.98, 0.09) |

[a]Maximum value. Values in the bracket are average value of 10 devices and standard deviation.

The intensity of the blue emission is found to increase as the FIrpic content was increased from (40:8:1) in device W1 to (100:8:1) in device W4. All the devices are found to emit in the yellowish-white range with CIE coordinates (at 12.0 V) of the devices W1–W4 varying from (0.44, 0.43) to (0.41, 0.43). Devices W4 with a CIE coordinate of (0.41, 0.43) is found to be the closest to white light among the FIrpic: Rubrene: DCJTB based WPLEDs and the EL spectra of device W4 at different applied voltage is shown in Fig. 5.5 (b). The EL spectra of device W4 is found to be highly stable at different applied voltages. The device is also found to exhibit a very good CRI value of 76. The current density vs. voltage (J-V) and brightness vs. voltage curve (B-V) of the WPLEDs are shown in Fig. 5.5 (c) and Fig. 5.5 (d) respectively. The presence of Rubrene and DCJTB shifts the operating voltage of the devices to a higher value which is due to the charge trapping phenomenon.

## 5.4 Conclusions

In conclusion, we have fabricated solution-processed WPLEDs which are highly efficient, good color stability and high color rendering index via a phosphor-sensitized system using blue phosphorescent dye FIrpic as emitter and sensitizer, and the fluorescent dye Rubrene and DCJTB as yellow and orange/red emitter respectively. Two different fluorophores, Rubrene and DCJTB, were chosen due to their different emission zone and different charge trapping ability. WPLEDs with only Rubrene or DCJTB as fluorescent dopant in which FIrpic and Rubrene or DCJTB are doped into PVK were fabricated and the effect of their concentration on the current density vs. voltage (J-V) characteristics and

the EL spectra were studied. It was observed that the stability of the EL spectra as well as the operating voltage of the devices is related to the charge trapping ability of the fluorophore used in a phosphor sensitized system. The brightness of the devices is also found to reduce on increasing the fluorophore dopant concentration in the EML. WPLEDs made with FIrpic : Rubrene (10:1) and FIrpic : DCJTB (80:1) were found to give CIE coordinates of (0.30, 0.42) and (0.34, 0.40) with CRI value of 58 and 76 at luminous efficiency of 4.91 cd $A^{-1}$ and 2.79 cd $A^{-1}$ respectively. Finally, FIrpic, Rubrene and DCJTB were doped into PVK to get high quality white light and CIE coordinates of (0.41, 0.43) with a CRI value of 78 at luminous efficiency of 4.73 cd $A^{-1}$ was achieved for FIrpic : Rubrene : DCJTB feed ratio of (100:8:1).

## 5.5 References


1. J. Kido, K. Hongawa, K. Okuyama, K. Nagai, *Appl. Phys. Lett.* 1994, **64**, 815-817.
2. B. W. D'Andrade, S. R. Forrest, *Adv. Mater.* 2004, **16**, 1585-1595.
3. M. C. Gather, A. Kohnen, K. Meerholz, *Adv. Mater.* 2011, **23**, 233-248.
4. Y. L. Chang, Z. H. Lu, *J. Disp. Technol.* 2013, **9**, 459-468.
5. J. F. Liang, S. Zhao, X. F. Jiang, T. Guo, H. L. Yip, L. Ying, F. Huang, W. Yang, Y. Cao, *ACS Appl. Mater. Inter.* 2016, **8**, 6164-6173.
6. G. Zhou, W. Y. Wong, S. Suo, *J. Photochem. Photobio. C: Photochem. Rev.* 2010, **11**, 133-156.
7. X. Yang, G. Zhou, W. Y. Wong, *J. Mater. Chem. C* 2014, **2**, 1760-1778.
8. L. Ying, C. L. Ho, H. B. Wu, Y. Cao, W. Y. Wong, *Adv. Mater.* 2014, **26**, 2459-2473.
9. D. Das, P. Gopikrishna, A. Singh, A. Dey, P. K. Iyer, *Phys. Chem. Chem. Phys.* 2016, **18**, 7389-7394.
10. L. Li, Z. B. Yu, W. L. Hu, C. H. Chang, Q. Chen, Q. B. Pei, *Adv. Mater.* 2011, **23**, 5563-5567.
11. H. Wu, G. Zhou, J. Zou, C. L. Ho, W. Y. Wong, W. Yang, J. Peng, Y.Cao, *Adv. Mater.* 2009, **21**, 4181-4184.
12. J. Zou, H. Wu, C. S. Lam, C. Wang, J. Zhu, C. Zhong, S. Hu, C. L. Ho, G. J. Zhou, H. Wu, W. C. H. Choy, J. Peng, Y. Cao, W. Y. Wong, *Adv. Mater.* 2011, **23**, 2976-2980.
13. B. Zhang, G. Tan, C. S. Lam, B. Yao, C. L. Ho, L. Liu, Z. Xie, W.Y. Wong, J. Ding, L. Wang. *Adv. Mater.* 2012, **24**, 1873-1877.
14. C. L. Ho, L. C. Chi, W. Y. Hung, W. J. Chen, Y. C. Lin, H. Wu, E. Mondal, G. J. Zhou, K. T. Wong W. Y. Wong, *J. Mater. Chem.* 2012, **22**, 215-224.
15. A. R. Brown, K. Pichler, N. C. Greenham, D. D. C. Bradley, R. H. Friend, A. B. Holmes, *Chem. Phys. Lett.* 1993, **210**, 61-66.
16. M. A. Baldo, D. F. O'Brien, M. E. Thompson, S. R. Forrest, *Phys. Rev. B* 1999, **60**, 14422-14428.
17. C. Adachi, M. A. Baldo, M. E. Thompson, S. R. Forrest, *J. Appl. Phys.* 2001, **90**, 5048-5051.
18. S. Reineke, F. Lindner, G. Schwartz, N. Seidler, K. Walzer, B. Lussem, K. Leo, *Nature* 2009, **459**, 234-U116.

19. M. A. Baldo, M. E. Thompson, S. R. Forrest, *Nature* 2000, **403**, 750-753.
20. B. W. D'Andrade, J. Brooks, V. Adamovich, M. E. Thompson, S. R. Forrest, *Adv. Mater.* 2002, **14** (15), 1032-1036.
21. G. J. Zhou, W. Y. Wong, B. Yao, Z. Xie, L. Wang, *J. Mater. Chem.* 2008, **18**, 1799-1809.
22. H. A. Al Attar, A. P. Monkman, M. Tavasli, S. Bettington, M. R. Bryce, *Appl. Phys. Lett.* 2005, **86** (12).
23. T. H. Kim, H. K. Lee, O. O. Park, B. D. Chin, S. H. Lee, J. K. Kim, *Adv. Funct. Mater.* 2006, **16**, 611-617.
24. M. E. Kondakova, J. C. Deaton, T. D. Pawlik, D. J. Giesen, D. Y. Kondakov, R. H. Young, T. L. Royster, D. L. Comfort, J. D. Shore, *J. Appl. Phys.* 2010, **107** (1).
25. G. F. He, S. C. Chang, F. C. Chen, Y. F. Li, Y. Yang, *Appl. Phys. Lett.* 2002, **81**, 1509-1511.
26. S. D. Kan, X. D. Liu, F. Z. Shen, J. Y. Zhang, Y. G. Ma, G. Zhang, Y. Wang, B. C. Shen, *Adv. Funct. Mater.* 2003, **13**, 603-608.
27. H. Kanno, Y. R. Sun, S. R. Forrest, *Appl. Phys. Lett.* 2006, **89** (14).
28. X. R. Wang, H. You, H. Tang, G. H. Ding, D. G. Ma, H. Tian, R. G. Sun, *J. Lumin.* 2008, **128**, 27-30.
29. L. D. Hou, L. A. Duan, J. A. Qiao, D. Q. Zhang, L. D. Wang, Y. Cao, Y. Qiu, *J. Mater. Chem.* 2011, **21**, 5312-5318.
30. T. L. Ye, S. Y. Shao, J. S. Chen, Z. Y. Chen, L. X. Wang, D. G. Ma, *J. Appl. Phys.* 2010, **107** (5).

# CHAPTER-6

## Summary and conclusions

# Summary and conclusions

White organic light emitting diodes (WOLEDs) are one of the prominent research topic in the field of optoelectronic devices and has potential applications in the field of flat panel displays and new generation solid state lighting sources. Especially, WOLEDs that are fabricated using solution process technique solution processes, such as inkjet printing and spin coating, can offer the advantage of cost effective manufacturing of large area devices and solution processed OLEDs can have the potential to be printed in different designs and shapes thereby allowing enormous design possibilities and pave a way to create artistic applications with light. Therefore, the fabrication of highly efficient polymer based light emitting diode that can emit light has been the prime motive of the work carried out in this thesis.

Firstly, fabrication of efficient blue and white light emitting diodes based on a core modified polyfluorene derivative has been discussed in this thesis. Polyfluorenes are well known emissive materials for blue PLEDs and serve well for light emission and charge transfer due to their high luminescence efficiency, thermal stability, good processability and excellent film forming properties. Unfortunately, they suffer from poor electron transport as compared to hole transport due to the presence of high density electron traps within the polymer. However, the addition of a strong electron accepting moiety can significantly enhance the electron transport property of polyfluorene. Using a well charge balanced, core modified copolymer of polyfluorene, poly[2,7-(9,90-dioctylfluorene)-co-N-phenyl-1,8-naphthalimide (99:01)] (PFONPN01), efficient blue PLEDs were successfully fabricated. In this study, $Alq_3$ was used as electron transport layer (ETL) and the e□ect of ETL thickness on the device performance was studied by varying the $Alq_3$ thickness. The high brightness and wide electroluminescence spectra of PFONPN01 in the blue-green region (400–550 nm) make a suitable host material for realizing white light. Therefore, it was further utilized for fabrication of WPLEDs by doping it with a narrow band gap yellow dopant DBT.

Secondly, white polymer light emitting diodes based on another widely used polymer poly(9-vinylcarbazole) (PVK) were fabricated using the concept of

electroplax formation and discussed herein. The effect of the electron injection barrier on charge transport properties, electroluminescence and controlling the electroplex formation has also been elucidated in this chapter. Further, the electron transport of PVK was modified by doping it with an electron transporting material 2-phenyl-5-(4-biphenylyl)-1,3,4-oxadiazole (PBD) and it was found to had remarkable influence on the aforesaid properties, especially on the electroplex formation.

Thirdly, highly efficient, solution processed green phosphorescent organic light emitting diode based on $Ir(mppy)_3$ has been discussed. Better charge balance and efficient charge injection in the emissive layer (EML) plays a vital role in defining the device performance of an organic light emitting diode (OLED) which in turn depends on the materials used and the processing condition such as solvent, thermal treatment etc.The effect of annealing temperature and mixed host on the device performance has been carefully studied in this chapter. The device performance is found to increase with increasing annealing temperature and best result was observed for the devices annealed at 140 $^{o}$C. However, the EL spectra of the phOLEDs was not influenced by the different annealing temperature of the EML. Further, addition of electron and hole transporting layer in appropriate ratio is found to improve the charge balance of the emissive layer that results in improved device performance.

Finally, solution processed WPLEDs with good color stability and high color rendering index via a phosphor-sensitized system has been discussed in this thesis. In this work, blue phosphorescent dye Bis[2-(4,6-difluorophenyl)pyridinato-C2,N](picolinato)iridium(III) (FIrpic) was used as emitter and sensitizer, and the fluorescent dye Rubrene and 4-(dicyanomethylene)-2-t-butyl-6-(1,1,7,7-tetramethyljulolidyl-9-enyl)-4H-pyran (DCJTB) as yellow and orange/red emitter respectively. Two different fluorophores, Rubrene and DCJTB, were chosen due to their different emission zone and different charge trapping ability. It was observed that the stability of the EL spectra as well as the operating voltage of the devices is related to the charge trapping ability of the fluorophore used in a phosphor sensitized system. The brightness of the devices is also found to reduce on increasing the fluorophore dopant concentration in the EML.

Overall, design and development of efficient, solution processed polymer based light emitting diodes has been the main topic of this thesis. To be an efficient lighting source, OLEDs should produce high quality white light with higher efficiency and better stability. This mainly depends on the efficient charge injection from the electrodes at a low drive voltage, good charge balance and high solid-state quantum yield of the emissive layer along with the confinement of the injected charge carriers within the emitting layers. Utilization of the triplet states of excitons in the emission also plays an important role in defining the efficiency of an OLED. Traditional fluorescent emitters can harvest only singlet excitons and have limited e□ciency. Metal-based organometallic phosphors however can harvest both singlet and triplet excitons by heavy atom enhanced intersystem crossing (ISC). They show higher efficiency but are rare and costly. Another type of molecules that have gained attention in recent years is the thermally activated delayed fluorescence (TADF) molecules. TADF emitters could utilize all singlet and triplet excitons and realize high e□ciency without assistance of noble metal, there is high potentiality to fabricate much lower cost but more promising OLED devices. My future research goal is to fabricate and characterize high performance blue, green and red OLEDs utilizing fluorescent, phosphorescent as well as TADF molecules as emitter; optimize different layers of the OLED to gain higher efficiency and finally to develop high quality white light emitting OLEDs with higher efficiency and better stability. Significant effort will also be given to fabricate these devices on flexible substrates.

**Future Challenges, Opportunities and Perspectives**

White organic light emitting devices (WOLEDs) are receiving much research attention because of their promise for applications in solid state lighting sources, back lighting for liquid crystal displays as well as full color flat panel displays due to their unique advantages of light weight, high solid state quantum efficiency as well as great potential for the mass production of large area flexible devices. According to the standard colorimetric system set up by Commission Internationale de L'Eclairage (CIE) in 1931, all colors are correlated to two coordinates in the system, and ideal white light emission is situated at the equal energy point with CIE coordinates of (0.33, 0.33). Generally, to realize the white light emission, one can mix the three primary colors (red, green and blue, RGB)

in a certain proportion or two complementary lights (orange or yellow and blue) as long as the connection line of their coordinates lies across the white light region. To address this point, various systems including inorganic phosphors, nanocrystals, organic small molecules, polymers and inorganic/organic hybrids are utilized to generate white light emission. In comparison to the white light emitting device systems which relied on inorganic phosphors or nanocrystals, white polymer light emitting devices (WPLEDs) can offer more versatile and advanced properties in terms of broadened electroluminescent (EL) spectra, unlimited choices of chemical modifications as well as the employment of low cost solution processing techniques. In addition, the efficiencies of WPLEDs can potentially be enhanced by tailoring spectral radiation with a high luminous efficacy, which is associated with the spectral power distribution of a white light source. It should also be noted that for solid state lighting, all the photons should be taken into account for illumination since they can be redirected to the forward viewing direction by engineering the lighting fixtures. The champion power efficiency (PE), which is defined as the output light power from a device per electrical power input, has been reported up to 100 lm $W^{-1}$ by using organometallic phosphorescent materials, which is much higher than that achieved with typical incandescent light bulb of ca. 15 lm $W^{-1}$, indicating a bright future of organic semiconductors for solid state lighting.

Additionally, color quality comprising appropriate color temperature (CT) and high color rendering index (CRI) is also needed to be considered for solid state lighting based on WPLEDs. The CT is preferred to range within 2500–6000 K for solid state lighting, which can be determined by comparing the chromaticity of the light source with that of the ideal black body radiator. By considering that organic materials normally present relatively broad EL spectra, the light of WPLEDs generally exhibits high CRI of over 80 and can be perceived as natural white light by the human eye. One of the key issues of applying WPLEDs for solid state lighting is on the stability, which embraces both color stability and long term operation stability. The color stability in terms of the bias dependent color shift for WPLEDs is essentially more challenging than their monochromatic counterparts, as the individual color emitters are spatially distributed within the emissive layer. The proposed explanations include the shift of the recombination zones, saturation of the long wavelength emitters, the competition between charge trapping and unperturbed charge transport, or the different voltage dependencies of trap assisted and bimolecular recombination. On the other hand, the long term operation stability is always associated with the organic

semiconductors. However, this can be circumvented through developing more efficient polymeric emitters, reducing device resistance by rationally matching the energy levels of emitters with the host materials and electrodes, controlling the fi lm morphology of each individual layer, or incorporating advanced encapsulating techniques to avoid ambient corrosion by moisture and oxygen.

Efforts devoted to develop novel highly efficient polymer systems and their device engineering have led to enormous progress in white polymer light emitting devices, which have significantly narrowed the gap with their inorganic and vacuum processed small molecule counterparts. From materials point of view, developing novel polymers with appropriate energy levels that can match with the electrodes and maintain charge balance at high current density while simultaneously avoid the negative concentration quenching effects, are highly desirable. In contrast, the device engineering aspects including tandem and inverted structures that can lead to more rational device geometry so that all electrically generated excitons can be well controlled and utilized are also of pivotal importance. Specific attention should also be paid on the collection of all generated photons since they can be redirected to the forward viewing direction by engineering the lighting fixtures. In addition, by considering that the majority of the light generated in the organic materials is confined due to the factors including the total internal reflection, surface plasmon coupling, as well as metal absorption, out coupling efficiency (η out) of only approximately 20% was obtained according to the Snell's law. Consequently, future attention should be focused on developing advanced out coupling technologies toward highly efficient WPLEDs by reducing wastage of the generated light. Of particular challenge for the commercialization of WPLEDs in the solid state lighting market is the useful lifetime, which is typically defined as the working time of the device efficiency to be decayed to 95%, 90% or 50% with respect to its initial value under a continuous operation period. However, the lifetime tests at normal operation conditions is really time consuming, while accelerating testing conditions such as enhanced driving voltages or elevated operational temperatures may suffer from spectral stability issue which may lead to less reliable results. Principally, developing highly efficient and stable monochromatic polymeric blue, green and red emitters with high glass transition temperatures is highly favored, since the device degradation starts from the components with shortest lifetime and any changes of monochromatic color may have great influence on the white emission. In addition, optimizing device architectures to reduce resistance such as introducing multi layered

devices to align the energy levels of each layer may effectively reduce the driving voltage, which can in turn lead to extension of the device lifetime. More to these issues, as reported by Gather et al., the underlying process determining the relation between thermal annealing during fabrication and device lifetime, and hence the rational choice of device fabrication process, would potentially pave a way to attain long lived devices exploiting commercially available polymeric light emitting materials. In addition to the pursuit of high efficiency and long term operational stability, the environmental issue should also be evaluated during the polymer synthesis, device manufacturing, operation and disposal. To address this point, more efforts should also be put on reducing the amount of organic solvents and developing novel polymers using environment friendly solvents.